Government of **Western Australia**
Department of **Mines and Petroleum**

RECORD 2010/20

YILGARN–SUPERIOR WORKSHOP — ABSTRACTS
Fifth International Archean Symposium
10 September 2010

compiled by
S Wyche

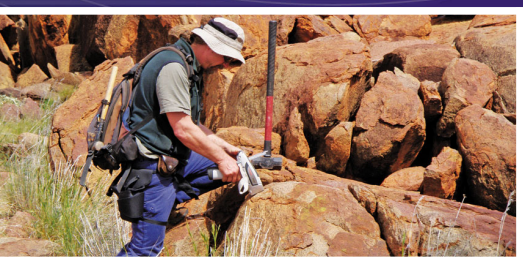

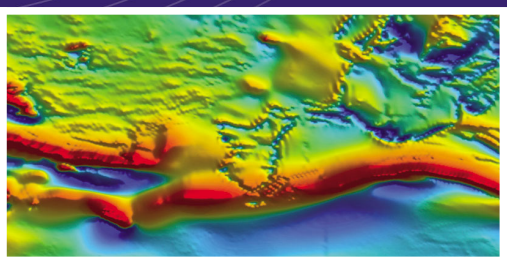

Geological Survey of Western Australia

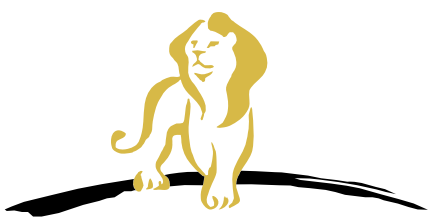

ANGLOGOLD ASHANTI

Government of Western Australia
Department of Mines and Petroleum

RECORD 2010/20

YILGARN–SUPERIOR WORKSHOP — ABSTRACTS

Fifth International Archean Symposium

10 September 2010

compiled by
S Wyche

Perth 2010

Geological Survey of
Western Australia

MINISTER FOR MINES AND PETROLEUM
Hon. Norman Moore MLC

DIRECTOR GENERAL, DEPARTMENT OF MINES AND PETROLEUM
Richard Sellers

ACTING EXECUTIVE DIRECTOR, GEOLOGICAL SURVEY OF WESTERN AUSTRALIA
Rick Rogerson

REFERENCE
The recommended reference for this publication is:

(a) For reference to an individual contribution:
Cassidy, KF 2010, Gold systems in the eastern Yilgarn Craton: scale-integrated signatures and targeting criteria, *in* Yilgarn–Superior Workshop — Abstracts, Fifth International Archean Symposium, 10 September 2010: Geological Survey of Western Australia, Record 2010/20, p. 51–56.

(b) For reference to the publication:
Geological Survey of Western Australia 2010, Yilgarn–Superior Workshop — Abstracts, Fifth International Archean Symposium, 10 September 2010: Geological Survey of Western Australia, Record 2010/20, 60p.

National Library of Australia Card Number and ISBN 978-1-74168-324-0 (Print); 978-1-74168-323-3 (PDF)

Published 2010 by Geological Survey of Western Australia
This Record is published in digital format (PDF) and is available online at www.dmp.wa.gov.au/GSWApublications.
Laser-printed copies can be ordered from the Information Centre for the cost of printing and binding.

Further details of geological publications and maps produced by the Geological Survey of Western Australia are available from:
Information Centre
Department of Mines and Petroleum
100 Plain Street
EAST PERTH, WESTERN AUSTRALIA 6004
Telephone: +61 8 9222 3459 Facsimile: +61 8 9222 3444
www.dmp.wa.gov.au/GSWApublications

Contents

Preface

The Superior Province and Yilgarn Craton share many common elements including similar lithological associations and apparently similar tectonic histories. However, there are significant differences between them in terms of the distribution and endowments of various metals, including gold, nickel, and the base metals. Do these differences reflect more fundamental differences between the two regions, and what do they tell us about crustal architecture and tectonic processes in the Meso- to Neoarchean?

The Fifth International Archean Symposium provides a timely opportunity to review the large amount of work that has been carried out in the Superior Province and Yilgarn Craton in the past ten years. In the Superior Province, new data and interpretations have been generated through the Discover Abitibi Initiative, and the Lithoprobe and NATMAP projects. In the Yilgarn Craton, the pmd*CRC, and various AMIRA, MERIWA, and ARC-supported projects, have substantially increased the understanding of the tectonic framework and the context of mineral systems, particularly in the eastern part of the craton.

This workshop has been organized to take advantage of the fact that many of the key researchers associated with the Superior Province and Yilgarn Craton are gathered in Perth for the decennial Archean Symposium. During the course of the day, there will be a range of talks touching on the metallogenic implications of the crustal architecture within the Superior and Yilgarn, and particularly the Abitibi greenstone belt and Eastern Goldfields Superterrane. Other talks will focus on the occurrence of particular commodities. At the end of the program, there will be a debate about what Meso- to Neoarchean crustal architecture and minerals systems are telling us about tectonic processes at that time. You are strongly encouraged to join in.

I would like to thank the Geological Survey of Canada, the Ontario Geological Survey, Géologie Québec, CSIRO, and Geoscience Australia for supporting speakers to attend this meeting. I would also like to thank our sponsors, AngloGold Ashanti.

Stephen Wyche
Manager, Yilgarn Mapping
Geological Survey of Western Australia

Yilgarn–Superior Workshop program — 10 September 2010

Fifth International Archean Symposium

8.30	**Introduction**	
	Yilgarn–Superior overview	
8.35	Archean cratonic architecture: implications for the Yilgarn and Superior Provinces	*Graham Begg*
9.00	Superior Province: overview, update and reflections	*John Percival*
9.25	Abitibi–Wawa Subprovince tectonic and metallogenic evolution	*John Ayer*
9.50	Granitic magmatism in the Yilgarn Craton: implications for crustal growth and metallogeny	*David Champion*
10.15	Eastern Goldfields structural evolution	*Richard Blewett*

Morning Tea 10.40 – 11.05

	Magmatic Ni–Cu–PGE metallogeny	
11.05	Eastern Goldfields and Abitibi: comparisons and implications for NiS deposits	*Steve Barnes*
11.35	Stratigraphic and volcanological controls on Ni–Cu–(PGE) mineralization in the Abitibi greenstone belt	*Mike Lesher*

Lunch 12.05 –1.05

	VMS metallogeny and context	
1.05	What happens when there is no volcanism: BIFs and how greenstones have developed in the Superior and elsewhere	*Phil Thurston*
1.30	The Abitibi Subprovince: its evolution and its VMS deposits — an overview	*Jean Goutier*
1.55	Stratigraphy of the 2720–2710 Ma Kidd–Munro volcanic episode in the Abitibi greenstone belt: implications for base metal mineralization	*Ben Berger*
2.20	Yilgarn volcanogenic massive sulphides	*Susan Vearncombe*

Afternoon Tea 2.45 – 3.10

	Gold metallogeny	
3.10	Gold systems in the eastern Yilgarn Craton: scale-integrated signatures and targeting	*Kevin Cassidy*
3.35	Timmins–Porcupine Archaean gold deposits and parallels with the Golden Mile	*Roger Bateman*
4.00 – 5.00	**DEBATE:** Meso- to Neoarchean crustal architecture and mineral systems demonstrate that tectonic processes at that time were different from those operating today Chairman: John Hronsky For: *Jean Bedard; Martin Van Kranendonk* Against: *Rob Kerrich*; *Derek Wyman* 10 minutes for each speaker	
5.00 – 5.15	**Closing statement**	

Archean cratonic architecture: implications for the Yilgarn and Superior Provinces

by

GC Begg[1,2], WL Griffin[1], Suzanne Y O'Reilly[1], LM Natapov[1]

Introduction

Utilising a multi-disciplinary approach, we have undertaken an exercise to systematically map the global continental lithosphere, with particular emphasis on the Sub-Continental Lithospheric Mantle (SCLM). Results indicate that about 70% of the SCLM may be of Archean origin, having mostly formed between 3.5-3.0 Ga (Griffin et al., 5IAS conference volume) as the residue of hot mantle plumes (see Arndt et al., 2009 for a review of SCLM origin). This is similar to the amount (about 60%) of the continental crust that is inferred (by analysis of zircon based Hf isotopes and U-Pb ages) to have formed by the end of the Archean (global compilation by Belousova et al., in review). Characterised by stiff, buoyant properties, this durable SCLM forced a new organisational structure on plate tectonics (which appears to have been operational since at least the Eoarchean; e.g. Dilek & Polat, 2008), leading to the development of cratons and the supercontinent cycles typical of the post-3.0 Ga Earth. In this context, an exploration of the lithospheric and geodynamic controls on ore deposits in the early Earth prior to the Mesoproterozoic (Begg et al., 5IAS conference volume), has concluded that:- 1) It is likely that prior to the appearance of buoyant, stiff SCLM, (tectonic) environments existed that were favourable for the formation of certain ores, but not for ore deposit preservation; 2) The appearance of buoyant, stiff SCLM and associated cratonic lithosphere, coupled with plate tectonics, provided suitable lithospheric and geodynamic settings (e.g. craton margins, continental shelves, intracratonic basins, and backarc basins) for ore-forming processes and the preservation of the resultant deposits; 3) A durable SCLM provided the possibility of captive ore metal source regions.

Despite a thick, robust lithosphere, plate tectonic processes such as rifting, convergence, accretion and collision, have conspired to destroy most Archean ore deposits via crustal detachment, reworking, or erosion. Surviving well-preserved Archean cratons are those lucky enough not to have been subjected to significant post-Archean subduction-related magmatism and major collision-related crustal thickening. Among this number, why are the Yilgarn and Superior cratons so well endowed with Late Archean orogenic gold deposits and nickel sulphide deposits in particular? Are these two cratons more alike than different? How do our findings about the SCLM shape our understanding of these two cratons?

[1] GEMOC Key Centre, Macquarie University, Sydney
[2] Minerals Targeting International PL, West Perth, Australia

Yilgarn late Archean history case study

Nd isotope model ages of Neoarchean granitoids in the Yilgarn (Cassidy, 2006) have given us a stunning definition of the ancient Western Yilgarn backstop to the Neoarchean Eastern Goldfields Superterrane (EGS). Giant nickel sulphide camps (Kambalda and Agnew-Wiluna) lie along the eastern edge of the Western Yilgarn. These ca 2.71-2.70 Ga deposits and associated mafic-ultramafic magmatism may be explained by a model whereby plume impact beneath the thick lithosphere of the Western Yilgarn has resulted in focussed plume melting at specific points of this margin. Support for plume-SCLM interaction is seen in the geochemistry of ultramafic dykes within the Kambalda Sequence (Said and Kerrich, 2010). The above is consistent with a plume-driven craton margin model for nickel sulphide deposit genesis that can equally explain post-Archean deposits elsewhere (Begg et al., in press). Importantly, post-Archean examples of this model did not form adjacent to major oceans or close to zones of active subduction.

Post-Archean orogenic gold deposits predominantly form in inverted pericratonic basins that have been affected by subduction (e.g. Hronsky and Groves, 2009). Generally these basins have experienced a backarc/retro-arc setting prior to inversion. The Eastern Goldfields Superterrane displays a broad organisation of volcanic units that is suggestive of an arc (2715-2704 Ma) and rifted arc (2692-2680 Ma) in the east (Kurnalpi and Gindalbie terranes; Barley et al., 2008), and a plume-influenced pericratonic (backarc) basin (>2715-ca 2692 Ma) overprinted by a backarc basin (ca 2.69-2.67 Ga) in the west (Kalgoorlie terrane). To the east of the

EGS is a cratonic block, herein called the Burtville Craton, where greenstone belts are considerably older (ca 2.82-2.77 Ga). Therefore if a ca 2.72-2.68 Ga paleosubduction zone suture exists, it is buried somewhere beneath the intervening Linden and Edjudina terranes, and is possibly evidenced by the Hootanui Shear Zone. Evidence for this suture from a single seismic reflection line is equivocal.

Pre- 2.72 Ga rocks, inherited zircons and slightly enriched Nd isotopic signatures are evidence of an older basement to the EGS. Only the Gindalbie terrane in the central-eastern part of the EGS appears to host dominantly juvenile magmatism between about 2.68-2.65 Ga. Seismic reflection lines indicate a complex mid- to lower- crust, and metamorphic patterns are consistent with late extension synchronous with the the development of Late Basins (Goscombe et al., 2009). Preservation of deposits and volcanic belts with low to medium metamorphic grade is testament to limited overall crustal thickening during amalgamation of the EGS.

We have developed a geodynamic model of evolution for the Late Archean EGS that embraces the concept of a thick, durable, buoyant and relatively stiff pre-existing proto-EGS SCLM, and its behaviour during subduction and accretion events. This proto-EGS SCLM may have contained extensive zones of metasomatism from earlier (subduction-related?) mantle magmatism. West-dipping subduction on the eastern edge of the Yilgarn resulted in the Burtville Craton rifting away from the proto-EGS (still attached to the Western Yilgarn), opening a moderate width intervening ocean basin by ca 2.73 Ga. Facilitated by a hot weak lower crust, some detachment of proto-EGS crust is likely to have occurred during this rifting. At ca 2.72 Ga west-dipping subduction initiated on the east edge of the proto-EGS, followed by subduction hinge rollback. This facilitated fragmentation of the proto-EGS SCLM, and established an arc and incipient backarc magmatic architecture (Kurnalpi and Kalgoorlie terranes, respectively). Ca 2.71-2.70 Ga plume impact beneath the east flank of the Western Yilgarn craton led to focussed melting at the craton margin, with melt transfer into crustal backarc basins via active translithospheric faults. This mafic-ultramafic magmatism was responsible for nickel sulphide deposit genesis.

Rollback, SCLM fragmentation, arc and backarc magmatism continued until re-accretion of the Burtville Craton at ca 2.67 Ga led to east-dipping subduction initiation on the southwest edge of the Western Yilgarn. Successive accretion of EGS SCLM fragments proceeded diachronously from east to west in the period 2.67-2.66 Ga. Each closure involved modest crustal thickening, intracrustal ponding of magmas, forced removal of intervening zones of chilled dense asthenospheric mantle from between SCLM blocks, (and subsequent) crustal extensional collapse and significant vertical tectonics as granitoid domes attempted to re-order the crustal density structure. As the accretion process matured, continued shortening caused SCLM blocks to translate laterally with respect to each other, propagating regional translithospheric faults through the overlying crust, forming and inverting more late basins, and possibly triggering delamination of any remaining "orogenic roots" beneath SCLM block boundaries. Strike-slip motion ±delamination favored the low-degree partial melting of discrete zones of metasomatised SCLM, providing potentially Au-rich alkaline melts for introduction into (±mixing with) the crust. Intrusives such as lamprophyres, sanukitoids, and syenites may be outcomes of this process. Ultimately Au-rich fluids were focussed into upper crustal deposits. Termination of subduction by accretion at the southwest edge of the Yilgarn at ca 2.65 Ga may have triggered the late bloom of low-Ca granites.

Comparison to Superior?

Detailed comparison between the Yilgarn and Superior cratons is not attempted here, but we invite an analysis of the latter that embraces a similar SCLM-centric, geodynamically-linked approach. Is the distinctive trait of these two strongly mineralised cratons the appearance of Late Neoarchean pericratonic backarc basins, and the interaction between mantle melts and SCLM? Was the southern Abitibi a backarc, at least at some stage of its evolution? Can the metallogenic difference in the Abitibi (more VMS base metal endowment, but less nickel sulphides) be explained by perhaps wider separation of SCLM blocks, less plume-focus, or different geodynamic histories?

Acknowledgements

We thank WMC Resources Ltd and BHP Billiton Ltd for their support and acknowledge the input of former colleagues within these companies. This work has been supported by Discovery, SPIRT, and Linkage grants from the Australian Research Council (S.Y. O'Reilly and W.L. Griffin).

References

Arndt, NT, Coltice, N, Helmstaedt, H and Gregoire, M 2009, Origin of Archean subcontinental lithospheric mantle: Some petrological constraints: Lithos, v. 109, p. 61-71.

Barley ME, Brown SJA, Krapez B and Kositcin N, 2008, Physical volcanology and geochemistry of a Late Archaean volcanic arc: Kurnalpi and Gindalbie Terranes, Eastern Goldfields Superterrane, Western Australia: Precambrian Research, v. 161, p. 53-76.

Begg GC, Griffin WL, O'Reilly SY and Natapov L, 2010, The Lithosphere, Geodynamics and Metallogeny of the Early Earth: 5IAS Conference Volume.

Begg GC, Hronsky JAM, Arndt NT, Griffin WL, O'Reilly SY and Hayward N, in press, Lithospheric, Cratonic, and Geodynamic Setting of Ni-Cu-PGE Sulfide Deposits: Economic Geology.

Belousova EA, Kostitsyn YA, Griffin WL, Begg GC, O'Reilly SY and Pearson, NJ, in review, The growth of the continental crust: Constraints from zircon Hf-isotope data: Lithos.

Cassidy KF, 2006, Geological Evolution of the eastern Yilgarn Craton (EYC), and terrane, domain and fault system nomenclature, *in* Final Report, 3D Geological models of the eastern Yilgarn Craton, Project Y2, September 2001 – December 2004 *edited by* RS Blewett and AP Hitchman: Geoscience Australia Record 2006/05, p. 1-38.

Dilek Y & Polat A 2008, Suprasubduction zone ophiolites and Archean tectonics: Geology, v. 36, p. 431-432.

Goscombe B, Blewett RS, Czarnota K, Groenewald PB and Maas R, 2009, Metamorphic evolution and integrated terrane analysis of the eastern Yilgarn Craton: rationale, methods, outcomes and interpretation. Geoscience Australia, Record 2009/23. 270p.

Griffin WL, O'Reilly SY, Afonso JC and Begg GC, 2010, The Evolution and Extent of Archean Continental Lithosphere: Implications for Tectonic Models: 5IAS Conference Volume.

Hronsky JAM and Groves DI, 2009, Towards a Unified Model for Magmatic-Hydrothermal Gold Metallogeny with Implications for Orogenic Gold, *in* Williams, P.J., ed., Smart Science for Exploration and Mining: Proceedings of the 10th Biennial SGA Meeting of The Society for Geology Applied to Mineral Deposits,Townsville, Australia, v. 1, p. 102-104.

Said N and Kerrich R, 2010, Magnesian dyke suites of the 2.7Ga Kambalda Sequence, Western Australia:Evidence for coeval melting of plume asthenosphere and metasomatised lithospheric mantle: Precambrian Research, v. 180, p.183-203.

Superior Province: overview, update and reflections

by

John A Percival[1] and Greg M Stott[2]

Introduction

Although the Superior holds the status of Earth's largest Archean craton, evidence from dyke swarms, rift margins and smaller cratons with common lineage (Bleeker, 2003) suggest that it is a remnant of a continent that was fragmented during the Paleoproterozoic. How the Superior and Yilgarn fit within a parental Superia reconstruction remains an open question, particularly as our understanding of the complex history and metallogenic diversity of the Superior continues to evolve. The tectonic framework of the Superior has come into sharp focus over the past three decades, guided by about 2000 U-Pb zircon ages constraining the timing of crystallization, inheritance, sediment deposition, deformation and metamorphism in both the developed and frontier parts of the craton, as well as geophysical images of the third dimension (e.g. White et al., 2003). As many as 15 independent tracts of Mesoarchean to Eoarchean sialic crust (3.9-2.8 Ga) (Figure 1) point to an earlier cycle of continental rifting and re-amalgamation prior to ca. 2.7 Ga.

Classic Mesoarchean rift sequences of the Superior comprise thin veneers of quartzite, komatiite and iron formation (Thurston and Chivers, 1990) on sialic basement. At the southern margin of the North Caribou terrane the rift package is tectonically juxtaposed against juvenile Neoarchean oceanic terranes (e.g. Percival et al., 2006). A different origin may be responsible for the mixed Mesoarchean – Neoarchean sequence that characterizes the "Ring of Fire" region of the James Bay Lowland, northern Ontario. Originally drilled for diamonds, this geophysically targeted area has yielded volcanogenic massive sulphide, intrusion-hosted Cu-Ni-PGE and chromite discoveries, as well as lode gold occurrences. An older suite of layered mafic – ultramafic intrusions (2808 Ma) may mark rifting at the northern margin of the North Caribou terrane, which gave rise to the largely juvenile, Neoarchean Oxford-Stull domain. The richly mineralized sequences include volcanic rocks (2737 Ma) hosting small, Cu-Zn-rich massive sulphide deposits, and layered intrusions of similar age containing stratigraphically lower Cu-Ni-PGE deposits and thick chromite-rich layers (up to 48 m of 51% Cr_2O_3) higher in the section. Map relationships are being defined through geophysical surveys and abundant drill intersections beneath a few tens of metres of Paleozoic cover. The Oxford-Stull domain extends several hundred kilometres west, into Manitoba, and has been projected eastward beneath James Bay into Québec: areas requiring re-evaluation of mineral potential on the basis of the recent Ring of Fire mineral discoveries.

A growing number of diamondiferous kimberlite occurrences (Attawapiskat, Renard, Kirkland Lake, Cobalt) support geophysical evidence for cold, refractory mantle lithosphere beneath the Superior Province. Furthermore, diamonds in breccias of Neoarchean age at Wawa suggest that a diamond stability field and corresponding cool geotherm existed prior to 2.7 Ga. This observation flies in the face of evidence for high crustal temperatures in the Superior between 2.70 and 2.65 Ga, including high-T, low-P regional metamorphism, widespread emplacement of crust-derived granites, and mineralization related to hydrothermal fluid circulation, including lode gold deposits. Other possible related events within this time window include deposition of "Timiskaming-type" conglomerates, transcurrent faulting, and initiation of post-orogenic cooling. Many of these features characterize the cratonization process in other cratons (e.g., Slave, Yilgarn), although event ages are offset. A simple model of lithosphere inversion (Percival and Pysklywec, 2007) explains the paradoxical cool mantle lithosphere - hot crust relationship. During arc magmatism (ca. 2750-2700 Ma), mantle lithosphere became more depleted, refractory and buoyant than at any time in subsequent Earth history through subduction-related hydrous fluxing and melt extraction from mantle convecting at temperatures 100-150°C warmer than today. Gravitationally unstable mafic-ultramafic residues in basal arc crust triggered roll-over of the stiff lithosphere, juxtaposing formerly basal lithosphere with basal crust and producing a crustal temperature spike. Thermomechanical models support the observed crustal thermal effects, as well as predicting transient shallow basin development in accord with the timing of Timiskaming conglomerate deposition. Although similar processes may underlie Yilgarn cratonization, no Superia connection is implied.

[1] Geological Survey of Canada
[2] Ontario Geological Survey

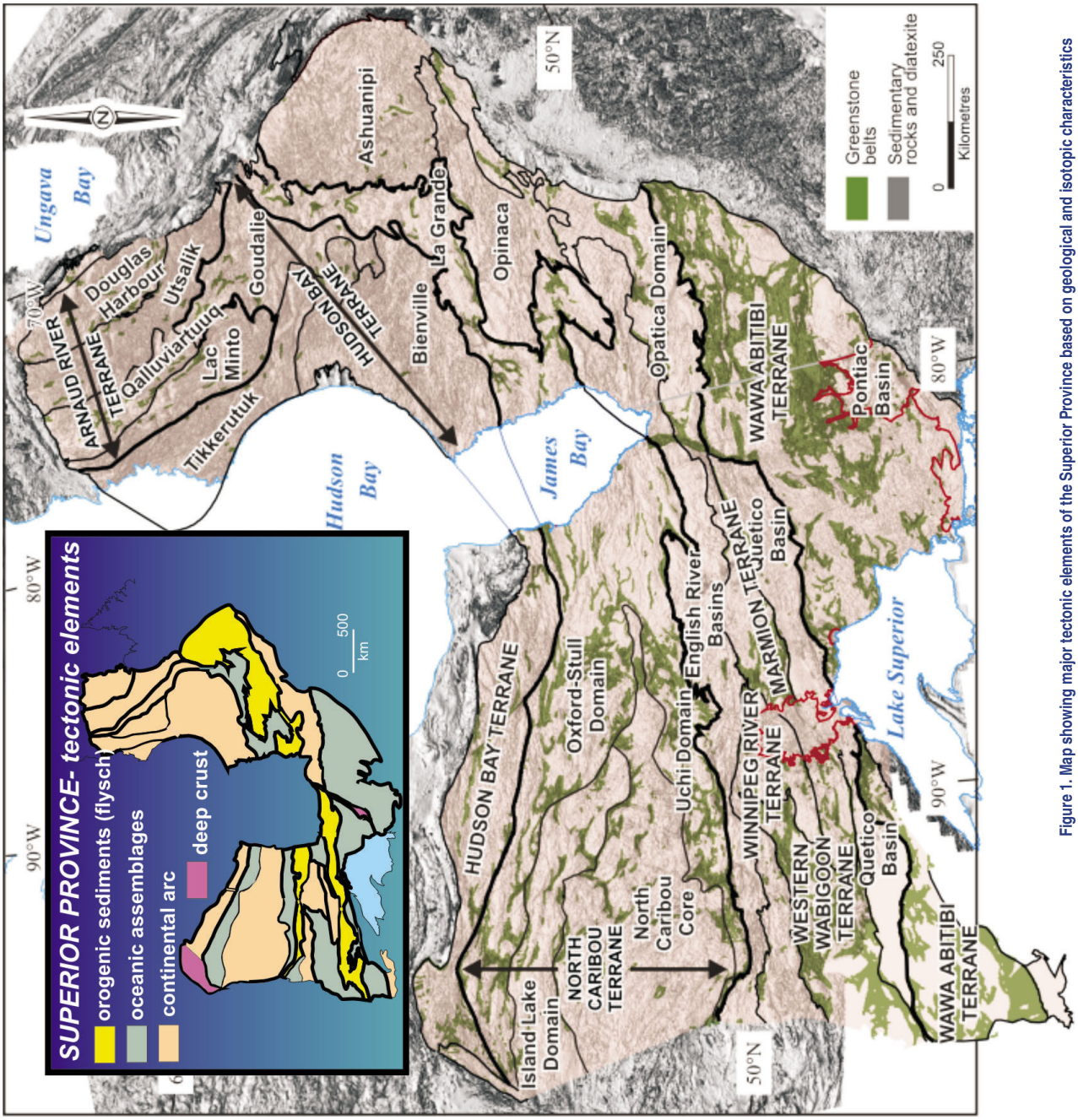

Figure 1. Map showing major tectonic elements of the Superior Province based on geological and isotopic characteristics

The geologically and geochronologically diverse Superior craton may have lost fragments during multiple rifting events in the Paleoproterozoic, based on the geographic distribution of numerous dyke swarms. Successful reconstruction of the supercontinent depends on matching Archean characteristics as well as dyke chronology and paleomagnetic positioning.

Acknowledgements

Data collection and synthesis activities have been supported by the Geological Survey of Canada through the NATMAP and Targeted Geoscience Initiative programs. Lithoprobe was jointly funded by the Natural Science and Engineering Research Council and Natural Resources Canada. The synthesis has benefited from numerous discussions with colleagues, collaborators and students.

References

Bleeker, W 2003, The late Archean record: A puzzle in ca. 35 pieces. Lithos, v. 71, p. 99-134.

Percival, JA and Pysklywec, R 2007, Are Archean lithospheric keels inverted? Earth and Planetary Science Letters, v. 254, p. 393-403.

Percival, JA, McNicoll, V and Bailes, AH 2006, Strike-slip juxtaposition of ca. 2.72 Ga juvenile arc and >2.98 Ga continent margin sequences and its implications for Archean terrane accretion, western Superior Province, Canada. Canadian Journal of Earth Sciences, v. 43, p. 895-927.

Thurston, PC and Chivers, KM 1990, Secular variation in greenstone sequence development emphasising Superior Province, Canada. Precambrian Research, v. 46, p. 21-58.

White, DJ, Musacchio, G, Helmstaedt, HH, Harrap, RM, Thurston, PC, van der Velden, A and Hall, K, 2003, Images of a lower-crustal oceanic slab: Direct evidence for tectonic accretion in the Archean western Superior province. Geology, v. 31, p. 997-1000.

Abitibi–Wawa Subprovince tectonic and metallogenic evolution

by

John Ayer[1], Jean Goutier[2], Phil Thurston[3], Benoît Dubé[4] and Balz Kamber[3]

Introduction

The Abitibi greenstone belt (AGB) has a coherent stratigraphy developed over a period of almost 100 million years (Figure 1). Autochthonous evolution is indicated by zircon xenocrysts with ages similar to those of underlying units in about 20% of the samples and in younger zircon ages for feeder dikes cutting the older units (Ayer et al., 2002). Early stratigraphic development consists of seven distinct volcanic episodes from 2765 to 2695 Ma, locally separated by submarine unconformities which are commonly marked by chemical sedimentation (Thurston et al., 2008). The volcanic episodes consist of tholeiites and komatiites, locally with coeval calc-alkalic intermediate to felsic volcanic rocks; the former derived by extension-related melting and successive plumes from mantle sources, and the latter either by melting of underplated mafic crust, or from subduction-related magmas. Volcanogenic Massive Sulphide (VMS) deposits have yielded about 700 million tons of Cu-Zn ore. The deposits are typically spatially associated with high silica (high temperature) rhyolites and are most abundant within the Deloro (2734-2724 Ma), Kidd-Munro (2720-2711 Ma) and Blake River (2703-2695 Ma) episodes. Komatiites are found in only 4 of the episodes (2765-2735 Ma Pacuad; 2723-2720 Ma Stoughton-Roquemaure; Kidd-Munro and Tisdale), but only the Kidd-Munro and Tisdale host komatiite-associated Ni-Cu-PGE deposits. These two assemblages are also distinctive in that geochemistry shows they were derived by shallower melting of the mantle plume sources than the older komatiites (Sproule et al., 2002). Magmatic deposits have yielded about 15 million tons of Ni-Cu-PGE ore in roughly equal amount from those associated with komatiites and those associated with mafic to ultramafic intrusions.

Early tectonic evolution and base metal mineralization

Most of the AGB has juvenile Nd and Hf isotopic compositions in both volcanic rocks and coeval syn-volcanic plutons. The southwestern part of the AGB however, has samples yielding >2.8 Ga xenocrystic zircons and evolved Nd and Hf isotopes in the Neoarchean units indicating localized contamination by Mesoarchean crust. This is somewhat similar to the Michipicoten greenstone belt (MGB) occurring within the Wawa subprovince, a continuation of the Wawa-Abitibi subprovince, west of the Kapuskasing Structural Zone. One distinction however is that the MGB has a preserved lower stratigrahic unit of 2.9 Ga volcanic rocks (the Hawk assemblage), as well as similarly evolved Hf isotopic values indicating Mesoarchean contamination in the overlying Neoarchean assemblages (Figure 2). On the other hand, galenas associated with the Winston Lake and Manitouwadge VMS deposits within the Neoarchen Terrace Bay-Manitouwadge assemblage (2723-2720 Ma), occurring along the northern margin of the Wawa subprovince, have primitive Pb isotope signatures (μ = 7.78 to 7.84) which are similar to the those of VMS deposits in the AGB (μ = 7.70 to 7.90) (Thorpe 1999). Collectively, the above data suggests that Neoarchean evolution of the Wawa-Abitibi subprovinces initiated by rifting of a Mesoarchean protocontinent, now only preserved intact at the base of MGB subprovince (Ketchum et al., 2008). The northern Wawa subprovince and all but the southwestern part of the AGB developed in a rifted oceanic basin without any preserved evidence of a Mesoarchean crustal substrate. The presence of numerous VMS mines, high temperature rhyolites, and komatiies in these uncontaminated areas suggests that the areas without a Mesoarchean crustal substrate experienced higher degrees of upper crustal heat flow thus promoting development of VMS deposits.

Hornblende geobarometry of tonalites coeval with the volcanic episodes in the central and southern AGB indicate emplacement as mid-crustal laccoliths (15-20 km depth) now preserved within the cores of batholithic domes. Younger granodiorite and granite plutons were intruded into the mid to upper crust (6-12 km depth) after 2695 Ma, coeval with the onset of D_1 regional compression, also resulting in uplift, folding, and unconformable deposition of turbiditic sediments and localized volcanism in submarine basins from the 2690-2685 Ma Porcupine episode. Subsequent deformation was episodic resulting in D_2 thrusts and folds, overprinted in turn by protracted D_3 sinistral, and D_4 dextral, transpressive to oblique-slip deformation (both folding and faulting). D_3 also resulted in deposition of shallow water to alluvial-fluvial clastic sediments and localized alkaline volcanism and plutonism from 2680 to 2670 Ma in pull-apart basins (the Timiskaming epoch).

[1] Ontario Geological Survey, Sudbury, Ontario
[2] Géologie Québec, Rouyn, Québec
[3] Laurentian University, Sudbury, Ontario
[4] Geological Survey of Canada, Québec City, Québec

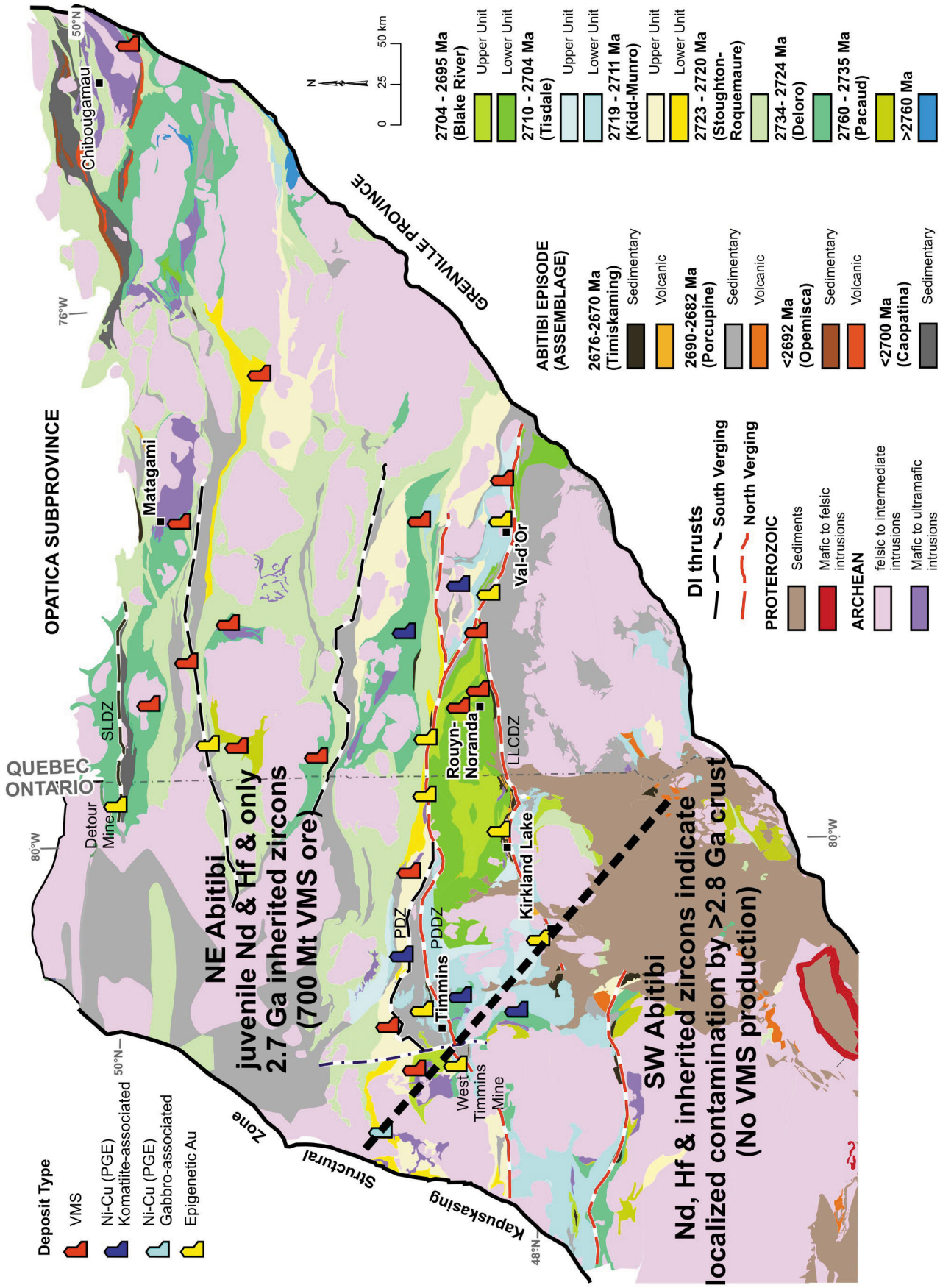

Figure 1. Abitibi Subprovince stratigraphy, mines/camps and isotopic characteristics

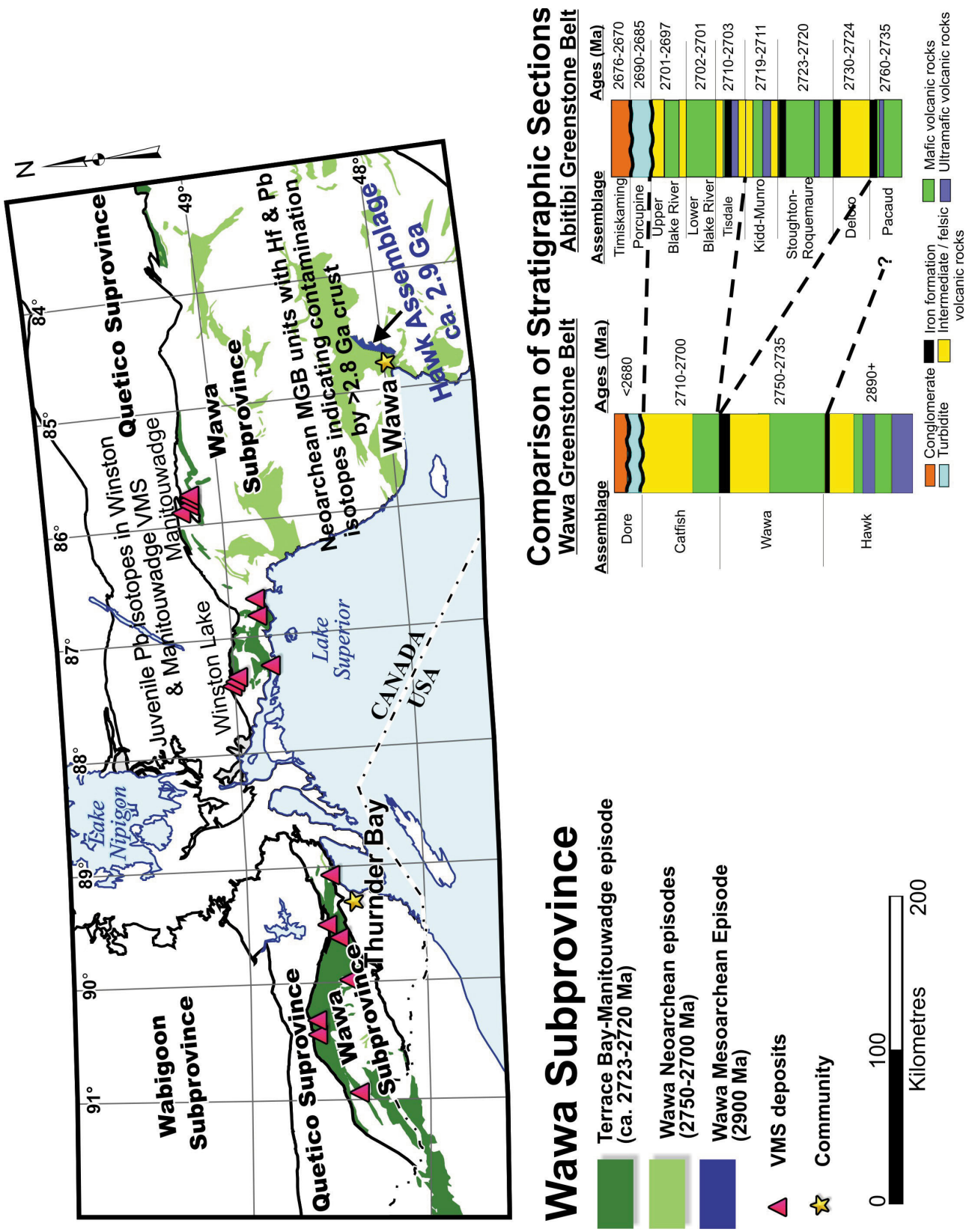

Figure 2. Wawa Subprovince stratigrapy, VMS deposits and isotopic chartacteristics

Post-tectonic, S-type granites ranging in age from 2665 to 2630 Ma were emplaced into the upper crust along the southern margin of the AGB.

Late tectonic evolution and epigenetic gold mineralization

Recent mapping, structural and geochronological work demonstrates that late tectonic events were diachronous, with somewhat older ages for similar events in the northern AGB. Here, D_1 deformation, syntectonic plutonism and sedimentation are all about 10 million years older than in the south. The Caopatina turbiditic episode was deposited after ca. 2700 Ma and the unconformably overlying conglomerates, sandstones and alklaic volcanic rocks of the Opemisca episode were deposited after ca. 2692 Ma, about the same time as plutons which stitched the tectonic contact between the AGB and the ca. 2.8 Ga Opatica subprovince to the north.

The 170 million ounces of epigenetic gold produced from the AGB developed in a number of episodic mineralization events. Gold mineralization events in the Timmins and Kirkland Lake camps range in age from about 2680 to 2665 Ma. However, the most economically significant mineralization event is post-Timiskaming and is associated with reverse-oblique-slip deformation overprinting early thrusting on north-verging regional faults ("breaks"). These deformation zones were the locus of repeated strain increments resulting in broad easterly-trending, ductile deformation zones with kinematics commonly indicating a complex deformation history. Typically these "breaks" occur at contacts between volcanic and younger sedimentary assemblages (including both the Porcupine and Timiskaming assemblages). Recent structural studies in these camps typically show early dip-slip displacement associated with north-south compression followed by sinistral and/or dextral displacement associated with various oblique-reverse "transpressive" events with gold commonly concentrated in higher order hangingwall faults in close proximity to the major breaks (e.g. Bateman et al., 2008; Ispolatov et al., 2008).

In the northeast AGB, early epigenetic gold mineralization has been precisely constrained at 2697 ± 1 Ma and is thought to be closely associated with D_1 deformation (Kitney et al 2009). Recent geochronological and structural studies in the northwest AGB at the Detour Lake Mine (Oliver et al submitted) show that the Sunday Lake deformation zone (SLDZ) represents a north-dipping D_1 fault in which Deloro–aged volcanic rocks were thrust southerly over clastic sedimentary rocks of the Caopatina assemblage. Subsequent oblique-slip deformation events overprint D_1 with both dextral and sinistral asymmetry. Gold mineralization occurs in the hangingwall to the SLDZ in both narrow high grade zones at the contact between ultramafic and mafic volcanic units and also as broad bulk tonnage lower grade zones in the mafic flows. Geochronology indicates that unmineralized albitite dikes cutting the gold zones are a late magmatic event containing inherited zircons indicating emplacement after ca. 2697 Ma. This indicates that epigenetic gold mineralization at Detour Lake is not synvolcanic as was previously interpreted. Albitite dikes in the southern AGB have magmatic ages ranging from 2676 to 2672 Ma and in the Timmins camp are cut by the main stage auriferous quartz-carbonate veins (Bateman et al., 2008). Thus Detour Lake gold mineralization is older than the main gold event in the southern AGB.

Large scale south-verging thrust faults can be found as far south as Timmins where the Pipestone deformation zone (PDZ) marks the southern contact between Kidd-Munro assemblage volcanic rocks and the Porcupine assemblage (Bleeker et al. 2008). Similar to the northern thrusts, epigenetic gold is commonly found in the hangingwall of the PDZ thrust. Recent geochronologic results show that the PDZ extends west of Timmins where the new West Timmins gold mine lies at the fault contact between the Kidd-Munro and Porcupine assemblages (Figure 1).

South of the PDZ, large scale breaks such as the Porcupine-Destor deformation zone (PDDZ) and Larder Lake-Cadillac deformation zone (LLCDZ) differ from the northern faults in that they have associated younger sedimentary units of the Timiskaming assemblage (2676-2670 Ma). The PPDZ also truncates the PDZ (Bleeker *et al.*, 2008) and has north-verging early displacement vectors (Bateman et al. 2008). Collectively, the above features indicate that younger gold episodes could account for the greater endowment of camps such as Timmins and Kirkland Lake which are proximal to the north-verging thrusts in the southern AGB. However, the northern thrusts should also be targetted for gold as they are less explored and generally covered by deep overburden.

Lead isotopes from leached feldspars from syn- and post-tectonic granitic rocks indicate progressively more radiogenic Pb values, specifically high $^{207}Pb/^{204}Pb$, towards the southern margin of the AGB. The common Pb-isotope array suggests mixing between relatively primitive mantle values for the 2685-2665 Ma syn-tectonic suite and highly enriched values in the 2660-2630 Ma post-tectonic suites, the latter indicating contamination via anatectic fluids from older crustal material (>3.0 Ga). Similar Pb isotope values (Carignan et al., 1993) also occur within granitic plutons intruding metasedimentary units along strike to the east in Québec (Pontiac subprovince) (Figure 1). New geochronologic results from numerous supracrustal enclaves along the southern margin of AGB in Ontario indicate these plutons intruded typical AGB stratigraphic units and not a distinct metasedimentary subprovince. This suggests that rather than identifying the metasedimentary rocks in Québec as a separate subprovince, it might be best to think of them as an extensive metasedimentary basin on the southeastern margin of the AGB, of similar age to less extensive Porcupine units evident throughout the AGB. From a metallogenic perspective, it is interesting to note that Pb values from the syntectonic granitic suite along the south margin of the AGB are very similar to those from galena and pyrite associated with gold-bearing veins in the Timmins, Kirkland Lake and Val d'Or camps (Canadian Pb isotope database, Geological Survey of Canada; Olivo et al 2007). The 2680-2665 Ma

timing, Pb-isotope values and emplacement depths of 6-12 km for these plutons may thus be in some way related to structural and hydrothermal events responsible for at least some of epigenetic gold mineralization emplaced into overlying greenstones in the southern AGB.

The south-younging of tectonic and epigenetic gold mineralization events across the AGB can be explained in two ways. First, by successive events of late tectonic accretion of terrains that show progressively more contamination from ancient non-AGB continental crust. Second, by the progressive closure of oceanic basins and accompanying sediment subduction, leading first to collision between the north verging Abitibi with the Opatica subprovinces in the north, and culminating in later collision with a north-verging Minnesotia River subprovince to the south.

References

Ayer, J., Amelin, Y., Corfu, F., Kamo, S., Ketchum, J. F., Kwok, K., and Trowell, N. F., 2002, Evolution of the Abitibi greenstone belt based on U-Pb geochronology: autochthonous volcanic construction followed by plutonism, regional deformation and sedimentation: Precambrian Research, v. 115, p. 63-95.

Bateman, R., Ayer, J.A., and Dubé, B., 2008, The Timmins-Porcupine gold camp, Ontario: anatomy of an Archean greenstone belt and ontogeny of gold mineralization: Economic Geology, v. 103, pp. 1285-1308.

Bleeker, W., van Breemen, O., and Berger, B., 2008, The Pipestone thrust and the fundamental terrane architecture of the south-central Abitibi greenstone belt, Superior craton, Canada: GAC Annual Meeting, Québec City, May 2008.

Carignan, J., Gariepy, C., Machado, N., and Rive, N., 1993, Pb isotope geochemistry of granitoids and gneisses from the late Archean Pontiac and Abitibi subprovinces of Canada: Chemical Geology, v.106, pp. 299-316.

Ispolatov, V., Lafrance, B., Dubé, B., Creaser, R., and Hamilton, M., 2008, Geological and structural setting of gold mineralization in the Kirkland Lake-Larder Lake gold belt, Ontario: Economic Geology, v.103, pp. 1309-1340.

Ketchum, J.W.F., Ayer, J.A., van Breemen, O., Pearson, N.J., Becker, J.K., 2008, Pericontinental crustal growth of the southwestern Abitibi Subprovince, Canada, - U-Pb, Hf and Nd isotopic evidence: Economic Geology, v. 103, pp. 1151-1184.

Kitney, K.E., Olivo, G.R., Davis, D.W., Desrochier, J-P., Tessier, A. 2009, Structural, Mineralogical, Geochemical and geochronological of the Barrie gold deposit, Abitibi subprovince, Canada: Proceedings of the Tenth Biennial SGA Meeting, pp. 288-290.

Oliver, J. Ayer, J. Dube, B., Aubertin, R. Bursen, M., Pennaton, G., and Friedman, R. submitted, Structural, chronologic, lithologic and alteration characteristics of gold mineralization: The Detour Lake Gold Deposit, Ontario, Canada. Exploration Mining Journal.

Olivo, G.R., Isnard, H., Williams-Jones, A.E., Gariepy, C., 2007, Pb isotope compositions from the C quartz-tourmaline vein of the Sisco Gold deposit, Val d'Or Québec: constraints on the origin and age of gold mineralization: Economic geology v. 102, pp. 137-146.

Sproule R.A., Lesher C.M., Ayer J.A., Thurston P.C., Herzberg C.T., 2002, Spatial and temporal variations in the geochemistry of komatiites and komatiitic basalts in the Abitibi greenstone belt: Precam Res 115:153-186.

Thorpe, R.I., 1999, The Pb isotope linear array for volcanogenic massive sulphide deposits of the Abitibi and Wawa subprovinces, Canadian Shield: Economic Geology Monograph 10, 1999, pp. 555-576.

Thurston, P.C., Ayer, J.A., Goutier, J., Hamilton, M.A., 2008, Depositional gaps in Abitibi Greenstone Belt Stratigraphy: a key to exploration for syngenetic mineralization; Economic Geology, v. 103, pp. 1097-1134.

Granitic magmatism in the Yilgarn Craton: implications for crustal growth and metallogeny

by

DC Champion[1] and KF Cassidy[2]

Introduction

The Archean Yilgarn Craton of Western Australia, is not only one of the largest extant fragments of Archean crust in the world, but is also one of the most richly-mineralised regions in the world. Understanding the evolution of the craton is important, therefore, for constraining Archean geodynamics, and the influence of such on Archean mineral systems. The Yilgarn Craton is dominated by felsic intrusive rocks - over 70% of the rock types. As such these rocks hold a significant part of the key to understanding the four-dimensional evolution of the craton, providing constraints on the nature and timing of crustal growth, the role of the mantle, and also the timing of important switches in crustal growth geodynamics. The granites also provide constraints on the nature and age of the crustal domains within the craton. Importantly, this crustal pre-history appears to have exerted a significant, but poorly understood, spatial control on the distribution of mineral systems, such as gold, komatiite-associated nickel sulphide and volcanic-hosted massive sulphide (VHMS) base metal systems.

Regional geology

The Archean Yilgarn Craton comprises a western cratoic nucleus, the Youanmi Terrane (YT; formerly the Southern Cross and Murchison Provinces of Gee et al., 1981), and a collage of terranes in the east — the Eastern Goldfields Superterrane (EGST; formerly Eastern Goldfields Province of Gee et al., 1981), as well as high-grade gneiss terranes along the western margin of the craton (see Cassidy et al., 2006). The craton is dominated by granite-greenstone terranes, largely formed between ca. 3.10 and 2.60 Ga, but also include older rocks (back to 3.8 Ga) within the gneiss terranes.

Volcanic and sedimentary rocks - in greenstone belts - range in age from >3.0 Ga to ca. 2.655 Ga, with three apparent age groups: ca. 3.0-2.9 Ga., ca. 2.8 Ga, ca. 2.75-2.65 Ga (e.g., Cassidy et al., 2006; Wyche, 2007 and references therein). Although age groups occur across the craton, the majority of the exposed older greenstone rocks (pre-2.7 Ga) are in Youanmi Terrane, and the majority of younger rocks (post ca. 2.72 Ga) are in the EGST. Like greenstone sequences elsewhere, those in the Yilgarn are dominated by high-Fe and high-Mg mafic and ultramafic volcanism but also include felsic volcanism, siliciclastic, volcaniclastic and chemical sediments, and, within the Kurnalpi Terrane, locally common intermediate volcanism.

Voluminous granites (up to 70% of all rocks) were emplaced into both the EGST and the YT, particularly within the period 2.73 to 2.63 Ga (Fig. 1, Table 1). Extant felsic plutonism older than this (to ~3.0 Ga) is poorly preserved, occurring largely as isolated, often gneissic, remnants and within the older greenstone belts.

Granitic magmatism

The bulk of granites of the Yilgarn Craton are mineralogically very similar, with >80% being biotite-bearing monzogranites or granodiorites (Table 1); accordingly geochemistry is required to help characterise and discriminate granite groups. Champion and Sheraton (1997), based on work in the eastern YT and northern EGST, recognised two major — High-Ca granites (TTGs) and younger (potassic) Low-Ca granites - and three minor (High-HFSE, Mafic and Syenitic) granite groups (Table 1; Fig. 1). Subsequent work has confirmed this subdivision across the whole craton (Cassidy et al., 2002), and shown that the craton is dominated by TTGs (~60%) and younger potassic granites (~20%), similar to many other Archean terranes. All groups, except the syenites, occur within both the YT and EGST; the syenites are localised within the latter (Table 1).

Geochemistry and petrogenesis

The High-Ca granites are felsic (68-77% SiO_2), dominantly sodic rocks (Table 1), that form a LILE-rich end-member

[1] Geoscience Australia, GPO Box 378, Canberra, ACT, 2601
[2] Alchemy Resources Ltd, GPO Box 2815, Perth, WA, 6001

Table 1. Characteristics of the five granite groups in the Youanmi Terrane and Eastern Goldfields Superterrane, Yilgarn Craton

Group Area %	Lithologies	Geochemistry	Isotopic signature	Youanmi Terrane	Kalgoorlie Superterrane	Comments
High-Ca >60%	sodic granodiorite, trondhjemite and granite Distributed both within and external to greenstone belts	high Na_2O, Na_2O/K_2O, low Th, LREE, Zr; mostly Y-depleted, Sr-undepleted. Range of LILE, LREE and Th contents; younger rocks extend to more LILE-enriched compositions	ε_{Nd} varies between +3.6 and -6.4, mostly between +2.5 and -2.0. Isotopic signature strongly terrane-specific (Fig. 2)	>3.0 Ga-2.9? Ga, ca. 2.81 Ga, ca. 2.76 to 2.66 Ga; mostly 2.73-2.68 Ga	ca. 2.8 Ga (minor remnants); 2.74-2.65 Ga; majority 2.685 to 2.655 Ga. Youngest members appear to occur within Kalgoorlie terrane	
Low-Ca >20%	potassic granodiorite, and granite Mostly external to greenstone belts	high K_2O, low Na_2O, high Rb, Th, LREE, Zr; moderately fractionated end-members	ε_{Nd} varies between +2.0 and -5.1. Like the High-Ca granites the isotopic signature is terrane specific	2.65-2.6? Ga; mostly 2.65 to 2.63 Ga. Possibly also 2.685 Ga	2.655 to 2.63 Ga	Occur broadly synchronously across the craton, including within the gneiss terranes
High-HFSE up to 5+%	granite, minor granodiorite Mostly internal or marginal to greenstone belts	distinctive combination of high FeO*, MgO, TiO_2, Y, Zr with low Rb, Pb, Sr, Al_2O_3	ε_{Nd} varies between +2.0 and -4.7. Strongly terrane specific, where measured	3.01 to 2.92 Ga?, ca. 2.81 Ga, 2.76 Ga to 2.74 Ga and younger?; also includes a post-greenstone 2655-2620 Ma subgroup	>2.72 Ga to 2.665 Ga; 2.7 to 2.68 Ga most common. Mostly geographically restricted to Kurnalpi Terrane and north-east Kalgoorlie Terrane	spatially associated with VHMS mineral systems
Mafic up to 5+%	diorite, granodiorite, granite, tonalite and trondhjemite	low SiO_2 (55-70+%), moderate to high Ni, Vr, MgO. Range of LILE, LREE and Th; subdivided into high- and low-LILE	Mostly ε_{Nd} of +2.8 to +1.0. Values of -1.7 and -2.8 for 2 samples in the western Youanmi Terrane. No correlation between geochemistry and isotopic signature	3.01 to 2.92 Ga?, ca. 2.81 Ga, 2.76 Ga to 2.71 Ga	>2.72 Ga to 2.65 Ga; possibly younger? LILE-enriched members tend to be ca. 2.665 and younger	common spatial association with gold mineralisation, especially the high-LILE members
Syenitic <5%	syenite, quartz syenite, monzonite, quartz monzonite	high total alkalis ($Na_2O + K_2O$) 10-12%; commonly low MgO, FeO*, TiO_2	all very similar, ε_{Nd} of +0.8 to +2.3, mostly all within error of each other: +1.5 to +2.0	none recorded	ca. 2.65 Ga, and 2.655-2.645 Ga	some spatial association with gold mineralisation

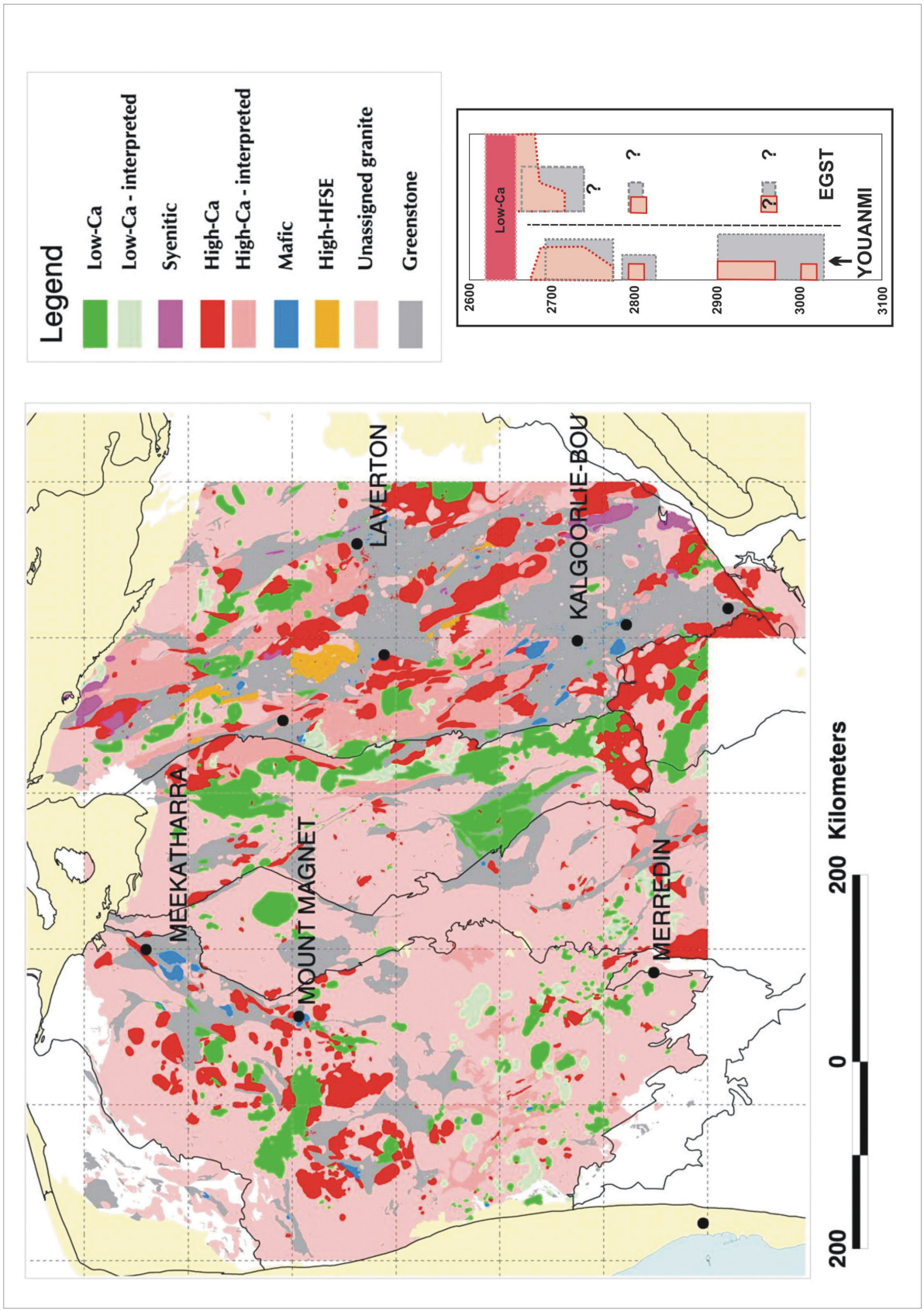

Figure 1. Distribution of granite groups within the Youanmi Terrane and Eastern Goldfields Superterrane of the Yilgarn Craton. Granite groups are as outlined in Table 1. Figure from Cassidy et al. (2002). Inset shows the relative age distributions of greenstone rocks and granites

to the ubiquitous tonalite-trondhjemite-granodiorite (TTG) group of granites found in all Archean cratons. They have chemical compositions consistent with derivation from a basaltic precursor but with an additional, crustal, component. Like TTGs elsewhere, the High-Ca granites are (mostly) characterised by Sr-undepleted, Y-depleted signatures, indicating they were produced at high pressures; either within thickened mafic crust or by melting of subducting oceanic crust.

The younger Low-Ca group are potassic, characterised by high-LILE, strong enrichments in LREE and some of the HFSE, and show evidence for crystal fractionation (Table 1). Their chemistry is consistent with derivation by partial melting of crust of broadly tonalitic composition; i.e., they represent reworking of older (High-Ca) felsic crust — an interpretation supported by field observations.

The volumetrically minor granite groups comprise: a) the high SiO_2 (>74%) High-HFSE group with distinctive A-type characteristics but low LILE contents, especially Rb and Pb, suggestive of low-pressure derivation from basaltic pre-cursors; b) a geochemically diverse but isotopically similar group of more mafic (<60 to >70% SiO_2) granites that exhibit large between-suite variations in LILE and LREE and include calc-alkaline andesites, sanukitoids and lamprophyres, strongly suggestive of subduction-related magmatism; and c) peralkaline syenitic rocks with calc-alkaline signatures suggestive of derivation from (arc-) metasomatised lithosphere (Table 1).

Geochronology

Available U-Pb zircon geochronology (e.g., Cassidy et al., 2002, 2006 and references therein; GSWA, 2006; Sircombe et al., 2007), indicates a range in the age of granite magmatism from ca. 3.0 to 2.63 Ga, with a peak between 2.73 and 2.63 Ga across the craton. It has also established there is a common sequence of felsic magmatism. The oldest granites are the High-Ca, High-HFSE and Mafic groups (3.0-2.65 Ga), which are syn- to post-greenstone in age. Syenitic magmatism is largely post-greenstone in age (2.65-2.64 Ga) but includes older units (ca. 2.665 Ga) within the Kurnalpi Terrane.

There are regional variations in the ages of these older granites. This is best illustrated by the timing of High-Ca peak magmatism: ca. 2.73-2.68 Ga in the YT; ca. 2.68-2.655 Ga in the EGST. Although it is evident that 2.82-2.74 Ga granites are largely absent from the eastern YT, suggesting High-Ca magmatism may have been diachronous (younging to the east), this is not supported by the widespread occurrence of 2.73-2.68 Ga granites across the whole YT.

High-Ca magmatism and the regional age variations effectively ended ca. 2.655 Ga with the initiation of Low-Ca magmatism (2.655 to 2.63 Ga), which occurred across the craton and records what must have been a voluminous craton-wide event. Although data is inconclusive, there is a suggestion that this event may have started earlier in the east (2.655 Ga) than the west (2.64 Ga). Magmatism contemporaneous with the Low-Ca granites includes Syenites and (poorly dated) lamprophyres in the EGST, and a minor group of late High-HFSE granites in the western YT.

Although the granites are dominantly ca. 2.73 Ga and younger, older granites are present. Granite age groups include ca. 2.63 to 2.76, 2.78-2.815 and 2.9 to >3.0 Ga in the YT, and 2.63-2.73, 2.75-2.77, 2.8-2.81, and possibly 2.94-2.96? Ga in the EGST. Inherited zircons are also relatively common in the granites, and include age populations of ca. 2.78-2.83 Ga and 2.9 to >3.0 Ga in the YT, and ca. 2.74-2.77, 2.8-2.81, 2.85 and 2.94-2.96 Ga in the EGST. The correlation between older granite and greenstone ages and the ages of inherited zircons in the granites strongly suggest that older felsic crust was originally much more extensive, in agreement with the evidence from the High-Ca granite geochemistry.

Sm–Nd isotopes and crustal development

Regional Sm-Nd isotopic confirm that there is a significant crustal component in both the High-Ca and Low-Ca granites and can be used to provide strong constraints on the crustal prehistory of the Yilgarn Craton. Champion and Cassidy (in prep.) used two-stage Nd depleted-mantle model ages (T_{2DM}), calculated from Sm-Nd isotopic data for the granites, to produce a contour map showing relative (not absolute) crustal ages for the Yilgarn Craton (Fig. 2). Data for these granites clearly identify a major isotopic break between the YT and the EGST (Fig. 2), subdividing the craton into a larger 'older' western crustal block (YT) and a significantly 'younger', economically-important, eastern block (EGST). The simplest interpretation for such a break is that it represents a major crustal boundary – an hypothesis supported by the close correspondence of its position with the large-scale Ida Fault. The isotopic data also delineate two isotopically 'younger' domains; one in the central part of the YT, co-incident with ca. 2.8 Ga layered mafic intrusives, and one within the EGST (Fig. 2).

Constraints from felsic magmatism on tectonic models for the Yilgarn

Although tectonic models based on granite data alone are equivocal, they can be used, in conjunction with the points raised above and the Sm-Nd isotopic data, to provide important constraints for tectonics of the Yilgarn Craton. Tectonic environments for the 2.8 Ga and older parts of the craton are the most equivocal. Apart from the High-Ca granites, which may either reflect slab-melting or melting of thickened mafic crust, there is little definitive evidence for arc-related tectonics. Most evidence would appear to better support vertical crustal growth in an episodic plume-environment. Regardless, the presence of ca. 2.8 Ga layered mafic rocks within the central part of the YT, the similar

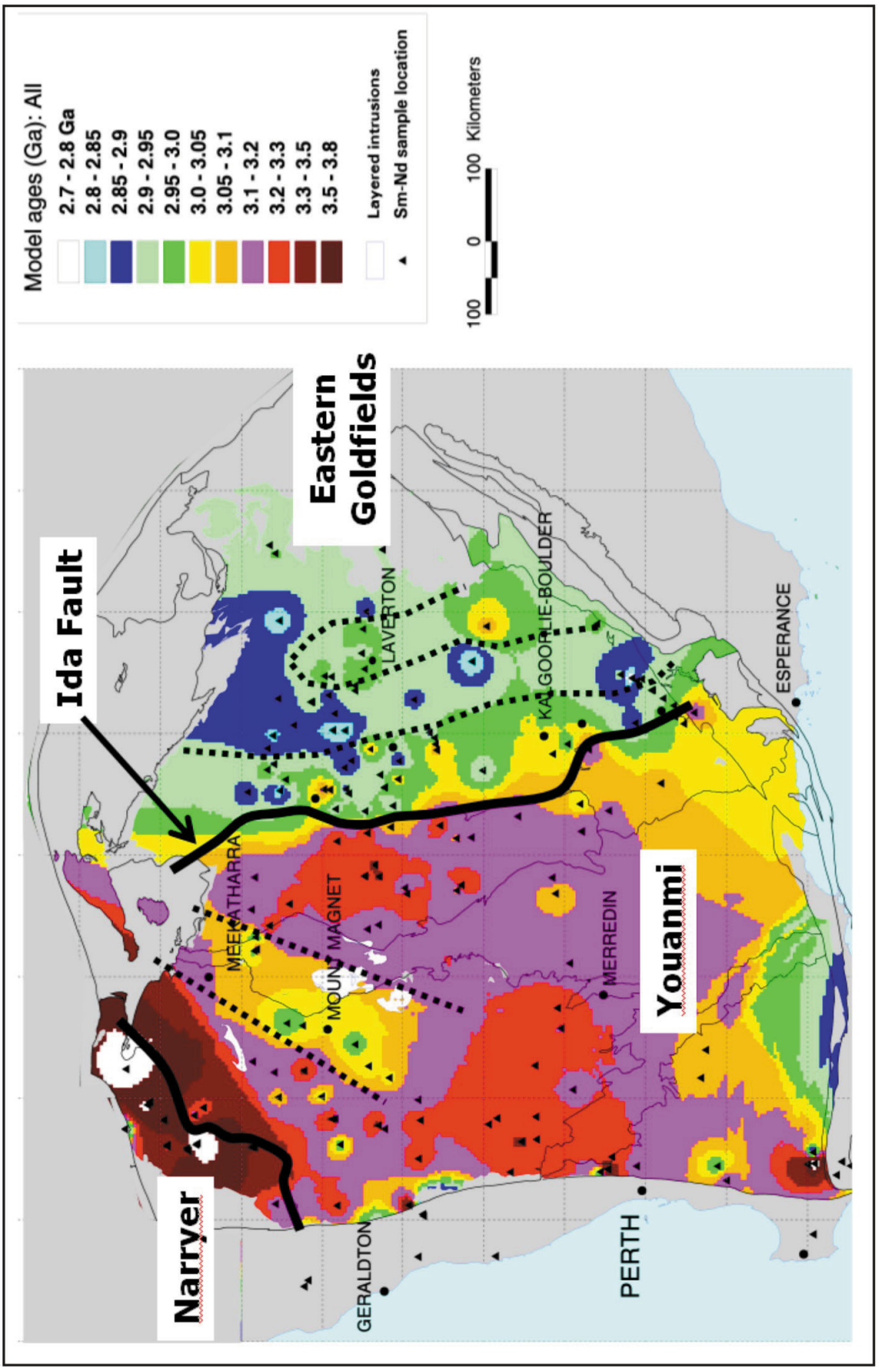

Figure 2. Nd depleted-mantle model age map of the Yilgarn Craton. Image produced by gridding Nd depleted-mantle model ages calculated from Sm-Nd point data (from Champion and Cassidy, in prep.)

greenstone ages and the T_{2DM} model ages, suggest the YT nucleus behaved as a coherent crustal block relatively early (possibly 2.9-3.0 Ga).

The best evidence for subduction-related magmatism in the YT is found within 2.78-2.71 Ga sanukitoid-like rocks of the Mafic Group. Much more evidence is present within the EGST including, ca. 2.72-2.7 Ga, calc-alkaline basalts and andesites in the Kurnalpi Terrane (e.g., Barley et al., 2003), minor but widespread, mostly ca. 2.665-2.55 Ga, sanukitoid-like mafic granites, as well as the presence of syenites and lamprophyres with strong calc-alkaline signatures. As such a variety of increasingly complex accretionary models have been suggested for the EGST, e.g., Cassidy et al. (2002), Barley et al. (2003). These are consistent with the Sm-Nd isotopic data which suggest lateral crustal growth and terrane accretion, not dissimilar to modern-style plate tectonics, though it is acknowledged that the isotopic zonation is also consistent with rifting, as has been suggested for parts of the EGST.

The 2.655 Ga change from High-Ca dominated to Low-Ca dominated magmatism reflects a significant change in magmatic style, and presumably represents some fundamental re-ordering of the tectonic environment at that time, interpreted by Champion and Cassidy (in Barley et al., 2003) to be the cessation of subduction. From this time on, but certainly post-2.648 Ga, there is no preserved (or recognised) record of any subduction-related Archean magmatism within the Yilgarn Craton. In this regard, the cessation of Low-Ca magmatism (ca. 2.63 Ga) marks the timing of effective cratonisation of the Yilgarn Craton as a whole.

Crustal isotopic domains and mineral systems

Consideration of the relationship between crustal age and the distribution of mineral deposits shows that there is a close spatial association between mineralisation and specific crustal domains, best expressed for the EGST. These associations are:

1) komatiite-associated nickel-sulphide deposits are concentrated in terranes with pre-existing crust; that is, Youanmi, Kalgoorlie, and the 'older' eastern part of the Kurnalpi Terrane.

2) VHMS base-metal systems appear spatially associated with terranes with juvenile crust, for example, the 'young' domains in the central Youanmi and Kurnalpi Terranes.

3) although occurring across the craton, the majority of the gold endowment is spatially restricted to areas underlain by crust of 'intermediate age' (Nd T_{2DM} ages of 2.95-3.1 Ga); specifically the Kalgoorlie Terrane and the 'older' eastern part of the Kurnalpi Terrane. In the EGST, at least, there is little significant gold mineralisation in domains with more juvenile signatures.

Huston et al. (2005) suggested that the high heat flow and extensional structures that are characteristics of juvenile crustal domains encourage formation of VHMS deposits. This relationship of metal endowment and specific crustal domains effectively explains why the Abitibi Subprovince in Canada is more endowed in VHMS mineralisation than the Yilgarn Craton; that is, the crust is not juvenile enough in the Yilgarn.

Why these apparent relationships hold for komatiite-associated nickel-sulphide and gold mineral systems is not entirely clear, and it is noted that the relationship for gold does not appear to hold for the extremely well (gold) endowed Abitibi Subprovince. Using empirical relationships it is possible that gold endowment in a specific terrane is related to the combined interaction of specific tectonic processes with pre-existing crustal and mantle reservoirs. For example, it is possible that the absence of a critical feature, such as plume-related komatiites in the 'young' crustal belt of the Kurnalpi Terrane, decreases the metal inventory and/or the ability to extract fertile material during orogeny, making these crustal domains less prospective (Cassidy et al., this volume).

Acknowledgements

The authors wish to acknowledge that many of the results presented here were made possible through a number of industry-funded AMIRA projects, especially P482 and P624. The authors would also like to acknowledge co-workers from UWA: Mark Barley, Stuart Brown, Ian Fletcher, Stephen Gardoll, David Groves, Bryan Krapez, Neal McNaughton, Jan Dunphy; Geoscience Australia: Richard Blewett, Paul Henson, Natalie Kositcin, Alan Whitaker; and the Geological Survey of Western Australia: Bruce Groenewald, Steve Wyche. Published with the permission of the Chief Executive Officer, Geoscience Australia.

References

Barley M.E., Brown S.J.A., Cas R.A.F., Cassidy K.F., Champion D.C., Gardoll S.J. and Krapež B. 2003, An integrated geological and metallogenic framework for the eastern Yilgarn Craton: developing geodynamic models of highly mineralised Archaean granite-greenstone terranes: Aust. Miner. Ind. Res. Assoc., Project P624, Final Report, 192 188p.

Cassidy K.F., Champion D.C., McNaughton N.J., Fletcher I.R., Whitaker A.J., Bastrakova I.V. & Budd A.R. 2002, Characterization and metallogenic significance of Archaean granitoids of the Yilgarn Craton, Western Australia: Aust. Miner. Ind. Res. Assoc. Project P482/MERIWA Project M281, Final Report, 514 p.

Cassidy K.F., Champion D.C., Krapež B., Barley M.E., Brown S.J.A., Blewett R.S., Groenewald P.B. and Tyler I.M. 2006, A revised geological framework for the Yilgarn Craton, Western Australia: Geological Survey of Western Australia, Record 2006/8, pp8.

Champion D.C. and Sheraton J.W. 1997, Geochemistry and Sm-Nd isotopic systematics of Archaean granitoids of the Eastern Goldfields Province, Yilgarn Craton, Australia: constraints on crustal growth: Precambrian Research, 83, 109-132.6.

Gee R.D., Baxter J.L., Wilde S.A. and Williams I.R. 1981, Crustal development in the Archaean Yilgarn Block, Western Australia. In: Glover J.E. & Groves D.I. (eds), Archaean Geology: Second International Symposium, Perth, 1980, Geol. Soc. Aust. Spec. Publ., 7, 43-56.

Geological Survey of Western Australia 2006, Compilation of geochronology data, June 2006 update: Geological Survey of Western Australia, Digital Data, ANZWA1220000726.

Huston D.L., Champion D.C. and Cassidy K.F. 2005, Tectonic controls on the endowment of Archean cratons in VHMS deposits: evidence from Pb and Nd isotopes. In: Mao J. & Bierlein, F.P. (eds), Mineral Deposit Research: Meeting the Global Challenge, Berlin/Heidelberg, Springer, 15-18.

Sircombe K.N., Cassidy K.F., Champion D.C. and Tripp G. 2007, Compilation of SHRIMP U-Pb geochronological data, Yilgarn Craton, Western Australia, 2004-2006: Geoscience Australia Record 2007/01, 182p.

Eastern Goldfields structural evolution

by

Richard Blewett[1], Karol Czarnota[1], Paul Henson[1] and Ben Goscombe[1]

Introduction

Most mineral deposits of the Eastern Goldfields Superterrane (EGST) are structurally controlled, so knowledge of their structure and tectonics is critical to understand the region's endowment and to predict new resources. A decade ago, at the 4th International Archaean Symposium (4IAS) meeting, the structural terminology for the Goldfields largely followed that of Swager (1997). This terminology consisted of a succession of contractional deformational events labelled 'D_1' to 'D_4'. Some authors proposed extension throughout parts of this compressive history although these were not enumerated (other than De or DE), or not particularly emphasised.

Building on the state of knowledge from a decade ago, we present a new structural framework for this meeting, the 5th International Archaean Symposium. Since the last meeting there has been a vast improvement in geochronology, geochemistry, isotopes, stratigraphy, deep seismic profiles, 3D models, together with new structural mapping from various GA, GSWA, AMIRA and pmd*CRC projects. This new framework integrates the greenstone stratigraphy, granite evolution, metamorphism, structure, tectonic mode, and mineralisation into a coherent structural evolution in time and 3D space.

A new integrated tectonic framework

D_1: long-lived extension and granite–greenstone formation

The D_1 event was extensional with a dominantly ENE-directed polarity and was likely the result of ENE directed roll-back of a subduction zone(s). Evidence of D_1 extension is preserved in: the broadly NNE trending distribution of the greenstone stratigraphy (Swager, 1997); the NNW trends in the granites εNd model age map (Cassidy and Champion, 2004); the subduction signature of the High-Ca granites (Champion and Sheraton, 1997); metamorphic patterns (Goscombe et al., 2009); the presence of unconformities and the excision of stratigraphy in the greenstone sequence (Swager, 1997; Krapěz et al., 2000); and, mesoscale structures in gneisses and older greenstone fragments (Blewett et al., 2004a; Blewett and Czarnota, 2007).

D_1 extension in the EGST was active from the earliest greenstone rock record (~2720 Ma) through to the onset of the first significant contraction at around 2665 Ma. Relicts of the older basement (maybe Youanmi Terrane) are preserved as the small slivers of >2750 Ma greenstones at Leonora, Duketon, Dingo Range, and Laverton. These may represent the rifted remnants of the older Youanmi Terrane. The voluminous High-Ca plutonism that occurred during this period likely initiated early elongate domes — 'sowing the seeds' of the domal architecture seen today.

D_2: termination of an arc and ENE–WSW contraction

The first significant contraction (D_2) occurred around 2670-2665 Ma, terminating volcanism in the greenstones. During this time interval disparate associations (in chemistry and age distribution) were juxtaposed at a time when the late arcs shut off in the Kalgoorlie Terrane.

In general D_2 developed without significant regional foliation development. Although in areas away from late basins and D_3 extension, structures here correlated with D_4 may well be associated with D_2 (as D_2 and D_4 are co-planar and may lack overprinting relationships). D_2 macroscopic structures indicate that shortening was oriented ENE-WSW, perpendicular to the grain of the D_1 extensional orogen. Accretion of an external body (an oceanic plateau) into the receding subduction zone is interpreted to have terminated volcanism and sent a wave of D_2 contraction across the orogen.

Blewett et al. (2004b) described two examples of regional macroscale F_2 folds. In the Kalgoorlie Terrane, a regional S-plunging anticline-syncline pair is overlain by the Kurrawang basin at Ora Banda. In the western Kurnalpi Terrane, the S-plunging upright Corkscrew Anticline is overlain by the Pig Well basin at Welcome Well. These

[1] Geoscience Australia, GPO Box 378, Canberra, ACT, 2601

* Deformation in quotes are from other workers. The structural nomenclature presented here is not placed in quotes.

examples show late basins unconformable on pre-folded greenstone sequences, providing an age constraint of >2660 Ma for the development of these folds (Blewett et al., 2004b).

To the east in the Kurnalpi Terrane, the map patterns of the Mt Margaret Anticline around Laverton also show that old greenstone sequences are folded more tightly than the upper surface of the domal batholith and the base of the folded Wallaby late basin (2665 ± 5 Ma). This relationship suggests that ENE-oriented shortening had at least commenced before the late basins were initiated. In the southern EGST, the ENE-directed Foster Thrust at Kambalda is interpreted as a D_2 structure.

D_3: extensional granite doming, mafic granites and late basin formation

The D_2 contraction was followed by a dramatic change in tectonic mode, as well as greenstone and granite type. The D_3 extensional event was associated with significant granite doming, a peak in High-Ca granite emplacement, late basin formation, and deformation. The event is characterised by extensional high-strain shear zones which wrap around major granite dome margins.

Late basins (Krapěz et al., 2000) display two geometrical forms, arcuate and elongate. The arcuate late basins are located in the hangingwall of extensional shear zones along the SSE margins of some major granite domes. The elongate late basins strike NNW, are rift-like, and are interpreted to have developed as a result of D_3 unidirectional ENE-down, asymmetric extension (inversion of D2 thrusts?).

The D_3 event was associated with the introduction of Mafic-type granite magmatism across the EGST. These magmas, with sanukitoid affinity, were derived from a metasomatised mantle source (a good source for gold and sulphur). Syenite magmatism (mantle sourced) commenced in the Kurnalpi and Burtville Terranes at this time. This dramatic change in felsic magmatism suggests that a fundamental geodynamic adjustment occurred, rather than the system returning to the previous D_1 extensional setting. Beakhouse (2007) attributed the change from slab melting (TTG) to metasomatised mantle melting in the Superior Province to be a function of slab detachment following collision.

Major granite domes controlled the locus of this D_3 extension, with a strong meso- and macro-scale record of extension at Lawlers, Leonora, and Mt Margaret. The accumulation/preservation boundaries of the main greenstone belts also record greenstone down extension along the Ida Fault to the west and the Pinjin shear zone to the east (Swager, 1997). At Leonora on the eastern margin of the large Raeside Batholith, extensional S-C-C' shear zone fabrics are well developed at the meso-scale, and at the macro-scale in seismic reflection images (Czarnota and Blewett, 2007). Furthermore large metamorphic grade jumps consistent with excision of stratigraphy have also been documented across extensional shear zones at Leonora (Williams and Currie, 1993). All scales infer granite-up and greenstone-down sense of movement (down to east), with elongate late basins (Pig Well: <2665 Ma) developed further east in the hangingwall to extensional shear zones.

Czarnota et al. (in press) proposed a model where the D_3 extension and its associated rock record in the EGST, were the result of detachment (or delamination) of the D_1 slab following D_2 collision. This detachment provided drivers, pathways and access to fertile sources for subsequent heat, gold-bearing fluids and magmas. The gross architecture of the EGST developed during the D_1 and D_3 phases of extension, not during contraction (Drummond et al., 2000).

D_4: Sinistral transpression

D_4 was a progressive sinistral transpressional event recorded across the terranes of the EGST, both within the granites and the greenstones. It has been subdivided into two distinct stages.

a) The first stage (D_{4a}) involved horizontal compression with σ_1 just north of E-W and a vertical σ_3 (co-planar to the D_2 stress field). D_{4a} is characterised by pure shear, basin inversion, NNW-striking upright folding and associated cleavage formation, reverse faulting, and tightening of earlier domes and D_2-D_3 folds. The geometrical result was the rotation and steepening of stratigraphy (including late basins) along the margins of E-facing granite domes.

b) The second stage (D_{4b}) involved the development of NNW-striking, steeply-dipping ductile sinistral shear zones, associated with a slight clockwise rotation of σ_1 to ESE-WNW and a horizontal σ_3. Sinistral strike-slip shear zones best developed in regions with steep-dipping stratigraphy (where thrusting and flattening ceased to be effective in dissipating the stress) and within the internal granites. This D_{4b} event equates to the 'D_3' deformation of Swager (1997).

Low strain structures associated with the D_{4b} event resolve a locally highly variable stress field with σ_1 ranging from ESE-WNW to N-S in orientation (e.g., main gold at Wallaby, Miller, 2006). This large variation in the local stress field is inferred to be a direct consequence of the development of sinistral strike-slip shear zones on a pre-existing highly anisotropic architecture, primarily composed of doubly plunging granite domes overlain by folded greenstones.

In a significant change from the Swager (1997) framework, the S-over-N thrusts from the Kambalda and Kanowna areas (*viz*, Foster, Tramways Republican, and Fitzroy), described as 'D_1' (Swager, 1997), are re-assigned to D_{4b}. This is based on regional map pattern superposition relationships where the 'D_1' thrusts overprint NNW-trending upright 'F_2' folds (see Henson et al., 2004). An analogy of how N-directed thrusts developed at a high angle to NNW-trending D_{4b} sinistral strike-slip faults exists in the eastern Gobi-Alty region of Mongolia (Bayasgalan et al., 1999). Thrusts in this example develop at the terminations of major strike-slip faults, acting as accommodation structures to rotational strain, and at restraining step-overs, accommodating displacement between

parallel strands of a strikes-slip fault system. Locally σ_1 was oriented NW- to N-striking across these transfer structures and restraining bends despite the regional stress field being oriented ESE-WSW.

D_5: dextral transtension and crustal melting

The D_5 event was developed in an overall dextral transtensional tectonic mode accompanying the emplacement of Low-Ca granites and characterised by brittle/ductile N- to NNE-striking dextral strike/oblique-slip faults. This D_5 event equates to the 'D_4' event of Swager (1997). Many past workers have suggested that it was a progressive event from earlier 'D_2' (e.g., Weinberg et al., 2003 and references therein). However, this study has shown that a significant rotation of the palaeostress field (~60°) occurred between the D_{4b} sinistral (σ_1 ESE-WNW) and the D_5 dextral (σ_1 NE-SW) events, so the transition was not progressive but probably marked a major plate reconfiguration.

This event is remarkably consistent across the EGST and thereby forms a good marker for structural correlation across the region. D_5 ductile high strain and locally transpressional shear zones occur along the most significant terrane boundaries such as Ida-Waroonga, Ockerburry and Hootanui Fault Systems. Distant from these terrane boundaries, the D_5 event is expressed as brittle faults with very well-developed quartz-carbonate slicken lines. The development of local transpressional/transtensional structures is controlled by pre-existing fault strike and the geometry of adjacent granite batholiths within a system where σ1 was inclined towards the SW.

D_6: low-strain systemic collapse

The last event inferred to be part of the EGST tectonic cycle (cratonisation of the Yilgarn) is systemic collapse. This event is characterised by mostly low strain crenulations, with sub-horizontal axial planes at a range of amplitudes from millimetres to metres. The fold hinges plunge variably. The structural style is brittle to locally brittle-ductile normal faulting. No specific vector of extension has been defined; and the driver for this extension may have been a readjustment of localised topographic highs from earlier events rather than a regional or far-field control. Structures ascribed to this event have been noted previously by Swager (1997), Davis and Maidens (2003) and Weinberg et al. (2003).

D_7: Proterozoic contractional events

The D_7 event occurred across the EGST and was associated with minor ENE-oriented contraction and the emplacement of dolerite dyke swarms and minor E-W sinistral strike-slip faults. Numerous small displacement faults occur in the granite pavements of the external granites (Blewett et al., 2004a). Swager (2007) also described similar structures. These are likely Proterozoic in age and may reflect events at the craton margin.

Implications for predictive gold discovery

Gold is associated with all of the events throughout the geodynamic history of the EGST, however significant gold mineralisation did not occur until the D_3 extension event. The genetic link between D_3 extension and late basin formation provides insight into the empirical observation that large gold deposits occur in proximity to late basins (Hall, 2007). This is because late basin distribution is associated with crustal penetrating shear zones developed during D_3 extension. These shear zones are necessary to tap deep fluids and metals (from the mantle). The emplacement of mantle-derived Mafic and Syenitic granites into the upper crust during D_3 extension reflects this deep connection. Furthermore extension is an efficient way to draw fluids down shear zones to facilitate fluid mixing (Sheldon et al., 2008). Significant gold mineralisation is hosted in high-strain extensional ductile shear zones at Gwalia, Lancefield, and the Lawlers camp. Extensional shear zones occur in other areas of the Yilgarn, so there is significant potential for finding Sons of Gwalia-like ore deposits. The D_3 extension is also responsible for setting up the domal architecture of the EGST which is critical for fluid focusing during subsequent events.

The D_4 sinistral transpression event was imposed on the highly anisotropic architecture developed largely during D_3. This resulted in the creation of numerous depositional sites with significant structural complexity and the development of locally variable and complex stress fields as the anisotropy in the orogen was being 'ironed out'. Gold is associated with brittle-ductile sinistral strike-slip shear zones at deposits such as Wallaby and Sunrise Dam, St Ives camp, Kalgoorlie, Kanowna Belle, Lawlers and Wiluna (Swager, 1997; Weinberg et al., 2003; Miller, 2006 and references therein).

The final gold event was associated with D_5 dextral shearing (brittle transtension), with deposits including Sunrise Dam and Wallaby, Transvaal, Wiluna camp, New Holland, Golden Mile, St Ives camp, and Kundana, being examples. In contrast to the earlier gold-dominated events (D_{3-4}), the mineralogy associated with D_5 included base metals and tellurides and may reflect the influence of basinal fluids (Goscombe et al., 2009).

Conclusions

This new tectonic framework will aid researchers to make informed regional correlations, to place local studies in a robust context, to provide input parameters to numerical modelling, and to make predictions for new and different mineral plays (e.g. D_3 extensional gold).

Acknowledgements

We thank the *pmd**CRC sponsors for their ongoing commitment to the Y4 project and the sponsors of the Y1-P763 project from which this work is based on. Thanks to GSWA for access to their vehicle for the fieldwork. Published with permission of the CEO of Geoscience Australia.

References

Bayasgalan, A., Jackson, J., Ritz, J.F., and Carretier, S., 1999, Field examples of strike-slip fault terminations in Mongolia and their tectonic significance: Tectonics, 18, 394-411.

Barley, M.E., Brown, S.J.A., Krapež, B., and Cas, R.A.F., 2002. Tectonostratigraphic Analysis of the Eastern Yilgarn Craton: an improved geological framework for exploration in Archaean Terranes: AMIRA Project P437A, Final Report.

Beakhouse, G.P., 2007, Structurally Controlled, Magmatic Hydrothermal Model for Archaean Lode Gold Deposits: A Working Hypothesis: Ontario Geological Survey Open File Report 6193, 133 p.

Blewett, R.S., Cassidy, K.F., Champion, D.C., and Whitaker, A.J., 2004a, The characterisation of deformation events in time across the Eastern Goldfields Province, Western Australia: Geoscience Australia Record, 2004/10. http://www.ga.gov.au/products/servlet/controller?event=GEOCAT_DETAILS&catno=47616.

Blewett, R.S., Cassidy, K.F., Champion, D.C., Henson, P.A., Goleby, B.R., Jones, L., and Groenewald, P.B., 2004b, The Wangkathaa Orogeny: an example of episodic regional 'D_2' in the late Archaean Eastern Goldfields Province, Western Australia: Precambrian Research, 130, 139-159.

Blewett, R.S., and Czarnota, K., 2007, The Y1-P763 project final report November 2005. Module 3 - Terrane Structure: Tectonostratigraphic architecture and uplift history of the Eastern Yilgarn Craton: Geoscience Australia Record 2007/15, 113p. http://www.ga.gov.au/image_cache/GA10678.pdf.

Blewett, R.S., Czarnota K., Henson, P.A., in press, Structural-event framework for the eastern Yilgarn Craton, Western Australia, and its implications for orogenic gold: Precambrian Research.

Cassidy K.F., and Champion D.C., 2004. Crustal evolution of the Yilgarn Craton from Nd isotopes and granite geochronology: implications for metallogeny. In Muhling, J., et al., (Eds), SEG 2004, Predictive Mineral Discovery Under Cover: The University of Western Australia, Publication 33, 317-320.

Champion, D.C., and Sheraton, J.W., 1997. Geochemistry and Nd isotope systematics of Archaean granites of the Eastern Goldfields, Yilgarn Craton, Australia; implications for crustal growth processes: Precambrian Research, 83, 109-132.

Czarnota, K., and Blewett, R.S., 2007, Don't hang it on a foliation to unravel a structural event sequence: an example from the Eastern Goldfields Superterrane, Specialist Group: Tectonics and Structural Geology: Geological Society of Australia Abstracts, Deformation in the Desert, Alice Springs, 9-13 July 2007, 75.

Czarnota, K., Champion, .D.C., Cassidy, K.F., Goscombe, B., Blewett, R.S., Henson, P.A., Groenewald, P.B., in press, The geodynamics of the Eastern Goldfields Superterrane: Precambrian Research.

Davis, B.K., and Maidens, E., 2003. Archaean orogen-parallel extension; evidence from the northern Eastern Goldfields Province, Yilgarn Craton: Precambrian Research, 127, 229-248.

Drummond, B.J., Goleby, B.R., and Swager, C.P., 2000, Crustal signature of Late Archaean tectonic episodes in the Yilgarn Craton, Western Australia: evidence from deep seismic sounding: Tectonophysics, 329, 193-221.

Goscombe, B., Blewett, R.S., Czarnota, K., Groenewald, B., Maas, R., 2009. Metamorphic evolution and integrated terrane analysis of the Eastern Yilgarn Craton: Rationale, methods, outcomes and interpretation: Geoscience Australia Record 2009/23, 270p. http://www.ga.gov.au/image_cache/GA15820.pdf.

Hall, G., 2007, Exploration success in the Yilgarn Craton: insights from the Placer Dome experience, the need for integrated research, *in* Proceedings of Geoconferences (WA) Inc. Kalgoorlie '07 Conference *edited by* FP Bierlein and CM Knox-Robinson: Geoscience Australia Record 2007/14, p. 199–202.

Henson, P.A., Blewett, R.S., Champion, D.C., Goleby, B.R. and Cassidy, K.F., 2004. Using 3D 'map patterns' to elucidate the tectonic history of the Eastern Yilgarn. In Barnicoat, A.C., and Korsch, R.J., (Eds), Predictive Mineral Discovery Cooperative Research Centre: Extended Abstracts from the June 2004 Conference. Geoscience Australia, Record 2004/9, 87-90.

Henson, P.A., Blewett, R.S., Champion, D.C., Goleby, B.R., and Czarnota, K., 2007, How does the 3D architecture of the Yilgarn control hydrothermal fluid focussing, *in* Proceedings of Geoconferences (WA) Inc. Kalgoorlie '07 Conference *edited by* FP Bierlein and CM Knox-Robinson: Geoscience Australia Record 2007/14, p. 57–61.

Krapež, B., Brown, S.J.A., Hand, J., Barley, M.E., and Cas, R.A.F., 2000, Age constraints on recycled crustal and supracrustal sources of Archaean metasedimentary sequences, Eastern Goldfields Province, Western Australia, Evidence from SHRIMP zircon dating: Tectonophysics, 322, 89-133.

Miller, J.M., 2006, Linking structure and mineralisation in Laverton, with specific reference to Sunrise Dam and Wallaby. In: A.C. Barnicoat, and R.J. Korsch (eds). Predictive Mineral Discovery CRC Extended Abstracts for the April 2006 Conference: Geoscience Australia Record 2006/7, 62-67.

Sheldon, H.A., Zhang, Y., Ord, A. 2008. Gold mineralisation in the Eastern Yilgarn Craton: Insights from computer simulations. In: Blewett R.S., (Ed.), Concepts to Targets: a scale-integrated mineral systems study of the Eastern Yilgarn Craton: pmd*CRC Y4 project Final Report, Part III, 177–190. http://www.pmdcrc.com.au/final_reports_projectY4.html.

Swager C.P., 1997, Tectono-stratigraphy of late Archaean greenstone terranes in the southern Eastern Goldfields, Western Australia: Precambrian Research, 83, 11-42.

Weinberg, R.F., Moresi, L., and van der Borgh, P., 2003, Timing of deformation in the Norseman-Wiluna Belt, Yilgarn Craton, Western Australia: Precambrian Research, 120, 219-239.

Williams, P.R. and Currie, K.L., 1993, Character and regional implications of the sheared Archaean granite–greenstone contact near Leonora, Western Australia: Precambrian Research, 62, 343-365.

Comparative lithogeochemistry of komatiites in the Eastern Goldfields Superterrane and the Abitibi Greenstone Belt, and implications for distribution of nickel sulphide deposits

by

Stephen J Barnes[1] and Marco L. Fiorentini[2]

Introduction

Very large volumes of research-quality lithogeochemical data on komatiites from the Eastern Goldfields Superterrane (EGST) and Abitibi Greenstone Belt (AGB) have been accumulated over the last three decades, and have been supplemented by an extensive database of platinum group element data (Barnes et al., 2004; Barnes et al., 2007; Fiorentini et al., in press; Sproule et al., 2002; Sproule et al., 2005). This data set enables statistical belt-scale comparisons to be made between two superficially similar greenstone terranes, both of which contain associations of komatiitic, tholeiitic, and felsic volcanic rocks. Both belts contain nickel sulphide mineralisation hosted by the komatiite component, but the relative endowments are greatly different. The EGST holds nine times more contained Ni metal content in komatiite-related sulphide ores than the AGB.

This contribution compares the major and trace element signatures of komatiites, komatiitic basalts and associated cumulate bodies in the EGST and AGB sequences, taking a broad-brush approach based on a combined database of more than 4500 analyses. All analyses have been incorporated into a single relational GIS database, and have been processed through a consistent recalculation procedure to standardise the treatment of ferrous and ferric iron ratio and to correct for volatile enrichment during alteration and for minor sulphide components (Barnes et al., 2004, 2007). The results are plotted on data density contour diagrams. Attempts have been made in both belts to sample the different lithologies in rough proportion to their abundance, although it is likely that spinifex-textured rocks are slightly over-represented in the data set relative to olivine cumulates. Randomised under-sampling is used to eliminate bias due to over-represented localities.

[1] CSIRO Earth Science and Resource Engineering, Perth, Western Australia. steve.barnes@csiro.au

[2] Centre for Exploration Targeting, The Universsity of Western Australia, Nedlands 6009

Results

MgO–FeO Trends

Komatiitic suites have major and trace element compositional arrays which to a first approximation are controlled by mass sorting of olivine, by processes including variable degrees of partial melting, fractional crystallisation and accumulation of liquidus phases to form cumulates. Plots of MgO vs FeO are useful in this context in that they represent the range and proportion of lithologies present, and also give an indication of magma composition in relation to the average bulk composition of accumulated (or fractionated) olivine (Figure 1). Projections of linear trends among rocks representing liquids and cumulates indicate the average composition of liquidus olivine.

Figure 1 compares subsets from both belts: the Kalgoorlie Terrane of the EGST, which contains the heavily endowed Agnew-Wiluna and Kambalda domains; and the Tisdale and Kidd-Munro assemblages of the Abitibi belt, which contain all the known Ni mineralisation within the AGB. Clear contrast between the different terranes is immediately apparent. The EGST-Kalgoorlie group (Figure 1A) contains a high proportion of samples falling on or very close to the pure olivine line, representing mesocumulates and nearly pure adcumulates with olivine forsterite contents ranging from 90 to 94 mol percent, with a high proportion of samples (mostly from the dunite complexes of the Agnew-Wiluna Belt) between Fo_{93} and Fo_{94}. These are exceptionally primitive olivine compositions, almost unique to komatiites, aside from same rare examples in kimberlites and boninites, and are closely (although not invariably) associated with ore deposits. This data grouping is substantially less well represented in all other greenstone terranes for which comparable data are available. Extreme olivine rich cumulates are completely missing from most of the Abitibi Belt. However, it is noteworthy that highly magnesian olivine cumulates are found within one specific region of the Abitibi Belt, the Shaw Dome area, which is the part of the belt most richly endowed with nickel sulphide deposits

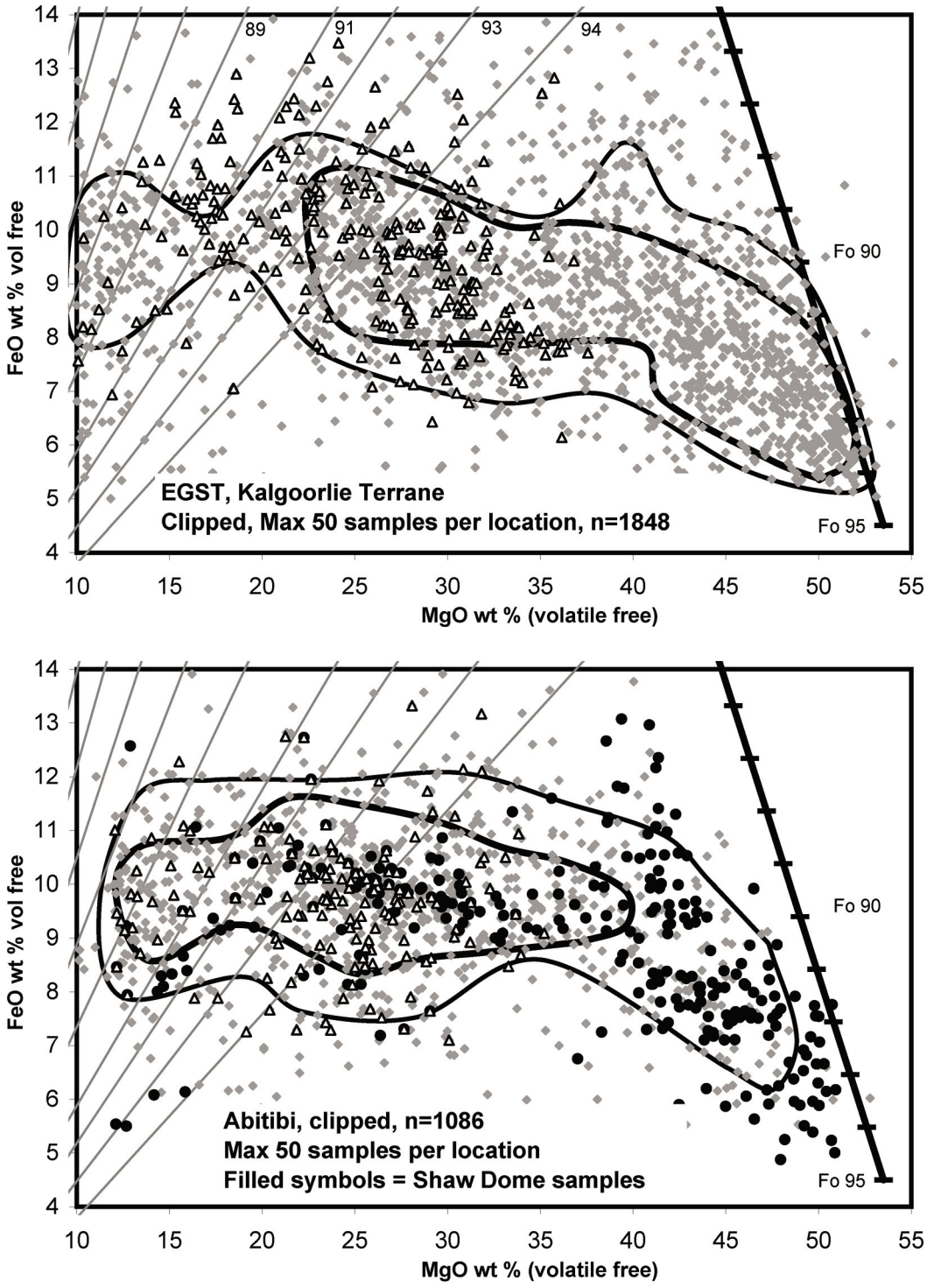

Figure 1. Plot of MgO-FeO for Eastern Goldfields Superterrane and Abitibi Greenstone Belt. Data clipped to reduce sample numbers from over-represented localities. Top (A): Eastern Goldfields Superterrane (EGS), Kalgoorlie Terrane incorporating Agnew-Wiluna belt. Bottom (B): Abitibi Greenstone Belt, Kidd-Munro and Tisdale Assemblages only; filled symbols indicate samples from the Shaw and Bartlett Dome areas. Contours on the densest 50%, and 80% of the data in each plot. Samples identifiable as spinifex textured as open triangles. Heavy sloping line on right indicates pure olivine compositions (allowing for 0.5% NiO plus CaO), ticks indicate mol % forsterite. Light grey sloping straight lines indicate olivines in equilibrium with olivine of forsterite content ranging from 86 mol % (left) to 94 mol% (right) – see labels on top left plot

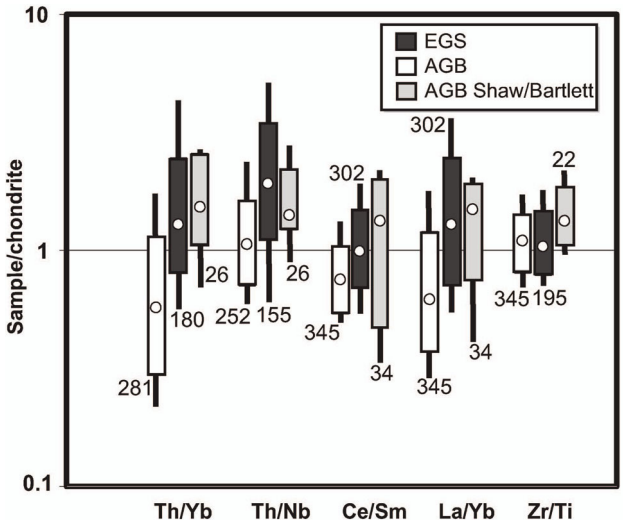

Figure 2. Box-whisker plots showing the ranges (median, 80th and 90th percentiles) on various ratios of incompatible trace elements within the EGST and AGB, plus data for the subset of samples from the Shaw and Bartlett Domes

(Barnes et al., 2007). Liquid compositions, as approximated by spinifex textured rocks in the range of MgO from 10-30%, are similar between the two belts, and the ranges of implied olivine compositions (mainly Fo_{90} to Fo_{94}) are indistinguishable. In summary, the critical difference is the much higher abundance within the EGST of very olivine-rich, very high-MgO cumulates, including large bodies of nearly pure olivine adcumulate. A large proportion of the total endowment of nickel sulphide in the EGST is directly associated with these dunite bodies.

Incompatible lithophile element ratios

Ratios of strongly to moderately incompatible lithophile elements such as La/Sm and Th/Nb have been used widely as indicators of crustal contamination in komatiite suites, and crustal contamination has been implicated directly in the origin of most known nickel sulphide deposits. Statistics on various of these ratios are summarised in Figure 2.

On all the indices except one, the EGST sample array shows significantly higher degrees of enrichment of the more lithophile element, and hence higher degrees of implied contamination. It is very difficult to eliminate the superimposed effects of alteration (Barnes et al., 2004), and there is some evidence that the elements La, Th and Zr may be susceptible to mild mobility during intense carbonate alteration. However, there is no clear relationship between trace element ratios and extent or style of alteration in the EGST, leading Barnes et al. (2004) to conclude on a number of lines of evidence that contamination was the predominant source of the variance. Thus, it seems likely that the EGST komatiites have been as a whole more strongly contaminated that their AGB equivalents. The greater variation in Th/Nb reflects the fact that Th is much more strongly enriched and Nb is much less enriched during contamination by upper continental crust (Lesher et al., 2001), and the lesser variation in Zr/Ti reflects the fact that these elements are less incompatible and are therefore less enriched in upper continental crust.

Figure 2 also shows a subset of the AGB data for localities from the Shaw Dome and Bartlett Dome, the portions of the Ontario Abitibi which host the great majority of known Ni sulphide deposits. This data subset is much more similar to the EGST dataset than to the remainder of the Abitibi data, a feature which is also evident in the MgO-FeO plots in Figure 1. This confirms both the association between contamination and assimilation of felsic crustal rocks, and the utility of contamination indices as exploration indicators.

Considering the least contaminated component of the data sets for the two belts, there is no detectable difference between the REE and incompatible lithophile element patterns (Barnes and Fiorentini, Econ Geol, in review). Primitive uncontaminated magmas in both belts have the characteristic signal of source depletion and high degree partial melting characteristic of komatiites worldwide (Arndt et al., 2008).

Platinum group elements

Platinum group element data are available on a spectrum of komatiite compositions, both distal from and closely associated with mineralisation. The EGST komatiite array as a whole contains a higher proportion of samples showing anomalous PGE enrichments and depletions, directly associated with sulphide liquid accumulation and segregation, but outside the immediate ore environments there is no evidence that the EGST komatiites were any more or less enriched or depleted in PGEs than typical komatiites of this type and age from the AGB, or any other belt (Fiorentini et al., in press). Komatiites of the same petrogenetic type and age are evidently remarkable consistent in the PGE contents worldwide, and komatiites from both EGST and AGB fall within that narrow range except in the immediate vicinity of ore deposits. There is clear evidence, from the general lack of systematic PGE depletion anywhere outside ore-bearing flows, that the EGST and AGB komatiites were erupted sulphide-undersaturated in almost all cases, and the pattern of PGE and incompatible trace element chemistry is entirely consistent with, and strongly supportive of, a substrate erosion model for local derivation of sulphur by supracrustal or near-surface assimilation of sulphidic sedimentary or clastic volcanic rocks (Bekker et al., 2009).

Age and extent of komatiites

The persistence of komatiitic volcanism over a period from 2750 Ma to 2706 Ma within the Western AGB (Ayer, 2002) contrasts with the burst of essentially coeval komatiite volcanism within the Kalgoorlie Terrane of the EGST over a strike length of more than 500 km (Nelson, 1997). The

komatiite history of the AGB records multiple plume events, while the EGST stratigraphy in the Kalgoorlie Terrane records a single major plume head arrival at around 2705 Ma. Alternatively, the AGB may be recording the prolonged history of a single plume tail; the Abitibi sequence may be akin to modern oceanic hot spot trails, interacting with a series of convergent margins, while the EGST represents a plume-head related LIP analogous to modern continental flood basalt provinces or oceanic plateaus.

Conclusions

On a variety of criteria – major element chemistry, PGEs and incompatible lithophile trace elements — the populations of primitive, uncontaminated komatiites erupted in the two belts appear to have been remarkably similar. However, the EGST komatiite suite has a much higher proportion of highly olivine-enriched cumulates, and is generally more contaminated, than the AGB suite, both factors which are likely contributors to its much higher Ni sulphide resource endowment. The more highly endowed regions of the AGB, such as the Shaw and Bartlett Dome area, also have higher proportions of low-porosity cumulates, and are very similar to the Kambalda area of the EGST in lithogeochemical terms. The combination of high degrees of contamination and presence of olivine adcumulates in the EGST attests to the presence of exceptionally high-intensity, prolonged eruptions, capable of forming long-lived entrenched magma pathways, represented by highly olivine-enriched cumulates, and capable of melting substrates to form orebodies. This is in contrast with more episodic, lower volume eruptions in the AGB. The contrast is unlikely to be due to the size and temperature of the underlying mantle plume (or plumes), which produced very high-Mg melts over a comparable area in both belts. The cause may have more to do with differences in tectonic evolution of the two belts, the AGB being generally more juvenile and less influenced by pre-existing continental crust and lithosphere structure. The high Ni endowment of the western part of the EGST may be associated with channelling of magmas by a deep seated trans-lithospheric structure associated with the eastern margin of the older Youanmi terrane cratonic block (Begg et al., 2009). Alternatively, or additionally, the contrast may be one between prolonged plume-tail hot-spot track activity (AGB) compared with a major plume head LIP event (EGST).

Acknowledgements

The EGST PGE data reported in this contribution were collected as part of AMIRA project P710a, funded by BHP Billiton Ltd., Norilsk Nickel Australia Ltd., Lion Ore Australia NL, Independence Group NL and MERIWA.

References

Arndt, N. T., Lesher, C. M., and Barnes, S. J., 2008, Komatiite: Cambridge, Cambridge University Press, 467p.

Ayer, J., Amelin, Y., Corfu, F., Kamo, S., Ketchum, J., Kwok, K., and Trowell, N., 2002, Evolution of the southern Abitibi greenstone belt based on U-Pb geochronology: autochthonous volcanic construction followed by plutonism, regional deformation and sedimentation: Precambrian Research, v. 115, p. 63- 95.

Barnes, S. J., Hill, R. E. T., Perring, C. S., and Dowling, S. E., 2004, Lithogeochemical exploration for komatiite-associated Ni-sulphide deposits: strategies and limitations: Mineralogy and Petrology, v. 82, p. 259-293.

Barnes, S. J., Lesher, C. M., and Sproule, R. A., 2007, Geochemistry of komatiites in the Eastern Goldfields Superterrane, Western Australia and the Abitibi Greenstone Belt, Canada, and implications for the distribution of associated Ni-Cu-PGE deposits: Applied Earth Science (Transactions of the Institute of Mining and Metallurgy Series B), v. 116, p. 167-187.

Begg, G. C., Hronsky, J. M. A., O'Reilly, S., Griffin, W. L., and Hayward, N., 2009, Plumes, Cratons and Nickel Sulphide Deposits: SGA Biennial meeting, Townsville, Qld., 2009, p. 147-148.

Bekker, A., Barley, M. E., Fiorentini, M. L., Rouxel, O. J., Rumble, D., and Beresford, S. W., 2009, Atmospheric sulphur in Archean komatiite-hosted nickel deposits: Science, v. 326, p. 1086-1089.

Fiorentini, M. L., Barnes, S. J., Lesher, C. M., Heggie, G., Keays, R. R., and Burnham, O. M., in press, Platinum-group element geochemistry of mineralized and non-mineralized komatiites and basalts: Economic Geology.

Lesher, C. M., Burnham, O. M., Keays, R. R., Barnes, S. J., and Hulbert, L., 2001, Trace-element geochemistry and petrogenesis of barren and ore-associated komatiites: Canadian Mineralogist, v. 39, p. 673-696.

Nelson, D. R., 1997, Evolution of the Archaean granite-greenstone terranes of the Eastern Goldfields, Western Australia: SHRIMP U-Pb zircon constraints: Precambrian Research, v. 83, p. 57-81.

Sproule, R. A., Lesher, C. M., Ayer, J. A., Thurston, P. C., and Herzberg, C. T., 2002, Spatial and temporal variations in the geochemistry of komatiites and komatiitic basalts in the Abitibi greenstone belt: Precambrian Research, v. 115, p. 153- 186.

Sproule, R. A., Lesher, C. M., Houle, M., Keays, R. R., Thurston, P. C., and Ayer, J. A., 2005, Chalcophile element geochemistry and metallogenesis of komatiitic rocks in the Abitibi Greenstone Belt, Canada: Economic Geology and the Bulletin of the Society of Economic Geologists, v. 100, p. 1169-1190.

Localization of komatiite-associated Ni–Cu–(PGE) mineralization in the Abitibi greenstone belt, Superior Province, Canada

by

MG Houlé[1] and CM Lesher[2]

Introduction

Most of the komatiite-associated Ni-Cu-(PGE) deposits in the ~2.7 Ga Abitibi greenstone belt (AGB) are similar to those in other areas in many respects (presence of both Type I basal stratiform and Type II internal disseminated mineralization, thick olivine mesocumulate-adcumulate host units, localization in footwall embayments, association with S-rich footwall rocks, evidence for local thermomechanical erosion), but they differ in several important aspects (common presence of mineralization at multiple stratigraphic levels) and there are several small but important exceptions (local presence of heterolithic breccia host rocks). Because they are superbly exposed in glacially-polished outcrops, they provide a variety of information critical in developing exploration models for deposits of this type.

Spatial and temporal distribution of komatiites in the AGB

Komatiitic rocks are widely distributed within the ~2.7 Ga Abitibi greenstone belt (AGB), but represent only a small proportion of volcanic rocks in the belt. Based on very large high-precision U-Pb single zircon geochronological database, komatiites occur mainly within four main time intervals (Ayer et al., 2005, Thurston et al., 2008): the 2750-2735 Ma Pacaud volcanic episode (~4% komatiitic rocks), the 2723-2720 Ma Stoughton-Roquemaure volcanic episode (~3% komatiitic rocks), the 2720-2710 Ma Kidd-Munro volcanic episode (~11% komatiitic rocks), and 2710-2704 Ma Tisdale volcanic episode (~7% komatiitic rocks), and rarely within the 2730-2720 Ma Deloro volcanic episode (<1% komatiitic rocks). Unlike the occurrences in many other Archean greenstone belts, the distribution of komatiites within each volcanic episode of the AGB is often variable and relatively discontinuous, typically occurring at multiple stratigraphic levels (Berger et al., 2010, Houlé et al., 2008).

[1] Geological Survey of Canada, Québec City, Québec, Canada G1K 9A9
michel.houle@nrcan.gc.ca

[2] Mineral Exploration Research Centre, Department of Earth Sciences, Laurentian University, Sudbury, Ontario, Canada P3E 2C6
mlesher@laurentian.ca

Petrogenesis and sulfide saturation history of komatiites in the AGB

Komatiitic rocks throughout the AGB, regardless of age or petrogenetic affinity (Al-undepleted, Al-depleted, Ti-enriched, Fe-rich) are only very rarely and very locally depleted in highly chalcophile elements (PGE-Cu–Ni-Co), indicating that most if not all of the parental magmas were undersaturated in sulfide prior to emplacement and therefore represent favourable magma sources for Ni-Cu-(PGE) mineralization (Sproule et al., 2005). They also only locally exhibit geochemical evidence (HILE enrichment, negative Nb-Ta-(Ti) anomalies) for crustal contamination, suggesting that such contamination occurred only locally and that it does not reflect contamination in the source and/or during ascent (Sproule et al., 2002).

Komatiite-associated Ni–Cu–(PGE) deposits in the AGB

The 2720-2710 Ma Kidd-Munro and the 2710-2704 Ma Tisdale volcanic episodes host almost the entire Ni-Cu-(PGE) endowment of the AGB. Of the 29 most significant mines, deposits, and occurrences associated with komatiites in the AGB, 12 occur within the 2720-2710 Ma volcanic episode and 16 occur within the 2710-2704 Ma volcanic episode, but only one occurrence (Bruce Lake) has been found thus far within the 2730-2720 Ma volcanic episode (see Table 1, Figure 1).

Mineralization appears to be clustered on the regional scale, occurring wherever favourable host rocks are exposed: 1 mine (Alexo-Kelex), 2 deposits (Dundeal, Dundonald South), and several occurrences (e.g., Sox, Small Pit) in the Dundonald area; 4 mines (Langmuir #1 and #2, Redstone, McWatters), 2 deposit (Hart, Langmuir W4), and several occurrences (e.g., Langmuir W2, Galata, MA05-01) around the Shaw Dome; 1 mine (Texmont) and several occurrences (e.g., Texmont DDH A-8, Bruce Lake/Deloro-aged rocks) around the Bartlett Dome; 1 deposit (Sothman) around the Halliday Dome; 1 deposit (C Zone) and several occurrences

Table 1. Nickel–copper–(PGE) mines, deposits and occurrences in the Abitibi greenstone belt

Volcanic Episode	Mines	Deposits	Occurrences
Kidd–Munro volcanic episode			
La Motte Dome Area, Qc	Marbridge 1-3-4	Bilson	Cubric
	Marbridge 2		Ataman
Amos Area, Qc		Dumont	
Dundonald Area, On	Alexo–Kelex	Dundeal	Sox
		Dundonald South	Small Pit
Munro Area, On			Mickel
Tisdale volcanic episode			
Shaw Dome, On	Langmuir #1	Hart	Galata
	Langmuir #2	Langmuir W4	Langmuir W2
	McWatters		Langmuir W3
	Redstone		MA05-01
Bartlett Dome, On	Texmont		Texmont DDH A-8
			Bruce Lake (Deloro-age rocks)
Halliday Dome, On		Sothman	
Bannockburn Area, On		C Zone	B Zone
			Thalweg

NOTES: Mines: mineralization that has been exploited totally or partially; Deposits: mineralization that has been defined, but not yet exploited; Occurrences: mineralization with small and undefined resource; On: Ontario; Qc: Québec

(e.g., Thalweg, B Zone) in the Bannockburn area; 2 mines (Marbridge #1-3-4, Marbridge #2), 1 deposit (Bilson), and several occurrences (e.g., Cubric, Ataman) in the La Motte Dome area; and 1 deposit (Dumont) in the Amos area (see Table 1).

The restriction of komatiite-associated Ni-Cu-(PGE) deposits to the Kidd-Munro and Tisdale volcanic episodes can be attributed to the much greater abundance of thick Mg-rich cumulate units and the much greater abundance of S-rich country rocks (metasediments and metavolcanic rocks) than in the Pacaud, Stoughton-Roquemaure, or Deloro volcanic episodes. Contrary to previous interpretations, Ni-Cu-(PGE) mineralization is not restricted to specific stratigraphic contacts, but may occur in any environment (intrusive, subvolcanic, or volcanic) throughout the stratigraphy where lava channels/magma conduits have had access to external S. Three main types of volcanic successions host Ni-Cu-(PGE) mineralization: 1) quasi-uninterrupted thick packages of komatiites and komatiitic basalts (e.g., Bartlett Dome), 2) interlayered komatiites and intermediate to felsic calc-alkaline/transitional volcanic rocks (e.g., lower part of Shaw Dome), and 3) interlayered komatiites and mafic to intermediate tholeiitic volcanic rocks (e.g., upper part of Shaw Dome).

Although most of the komatiites in the AGB have been previously considered to be extrusive, an increasing number of units have been shown to be intrusive (e.g., Houlé et al. 2008) and it now appears that komatiite-associated Ni-Cu-(PGE) mineralization in the AGB occurs within a spectrum of environments ranging from intrusive (Dumont, Sothman) through subvolcanic (Kelex, Dundeal, Dundonald South, McWatters) to extrusive (Alexo, Marbridge, Hart, Langmuir #1 and #2, Redstone, Langmuir W4, Texmont, C Zone). Mineralization in the Kidd-Munro volcanic episode is interpreted to occur near the base of the sequence at several stratigraphic levels in Dundonald Township (Alexo, Kelex, Dundeal, Dundonald South) and likely at higher levels in Munro Township (Mickel) and LaMotte Township (Marbridge). Mineralization in the Tisdale volcanic episode is interpreted to occur at several levels near the base of the sequence in the Shaw Dome (Galata, Langmuir #1 and #2, Redstone, McWatters), in Bannockburn Township (C Zone, Thalweg), and the Halliday Dome (Sothman), and stratigraphically higher in the Bartlett Dome (Texmont).

Regardless of volcanic setting, however, all deposits are hosted by relatively undifferentiated olivine mesocumulate cumulate units that have been interpreted as lava channels (Figure 2), subvolcanic sills, or feeder dikes (which normally have very distinctive geophysical/geochemical signatures) and most are associated with S-rich country rocks, but one is hosted by olivine adcumulate rocks (Dumont) and one is partly hosted by autoclastic komatiitic breccias (Bannockburn C Zone). Almost all deposits are localized within transgressive footwall embayments produced or enhanced via thermomechanical erosion (e.g., Alexo, Dundeal, Dundonald South/Beach, Hart, Langmuir #1 and #2, Redstone, Thalweg, Galata, and Mickel) and most exhibit evidence of magma-wallrock interaction (e.g., xenoliths, geochemical contamination), consistent with them having formed in dynamic systems.

The evidence for thermomechanical erosion at Alexo is particularly compelling (Houlé et al. *accepted*): 1) the contact between komatiite and andesite is very sharp but delicately scalloped, marked by a thin selvedge of black devitrified glass, and clearly transgresses pillow structures and interpillow breccias in the andesite without any evidence of a regolith, shearing, or folding, producing multiple nested embayments on scales from 100s of metres to a few centimetres; 2) the andesites have been contact metamorphosed and altered along the entire length of the outcrop and the degree of metamorphism/alteration is thicker and more intense around embayments; 3) xenoliths of andesite in komatiite are more common within embayments; 4) komatiitic dikes

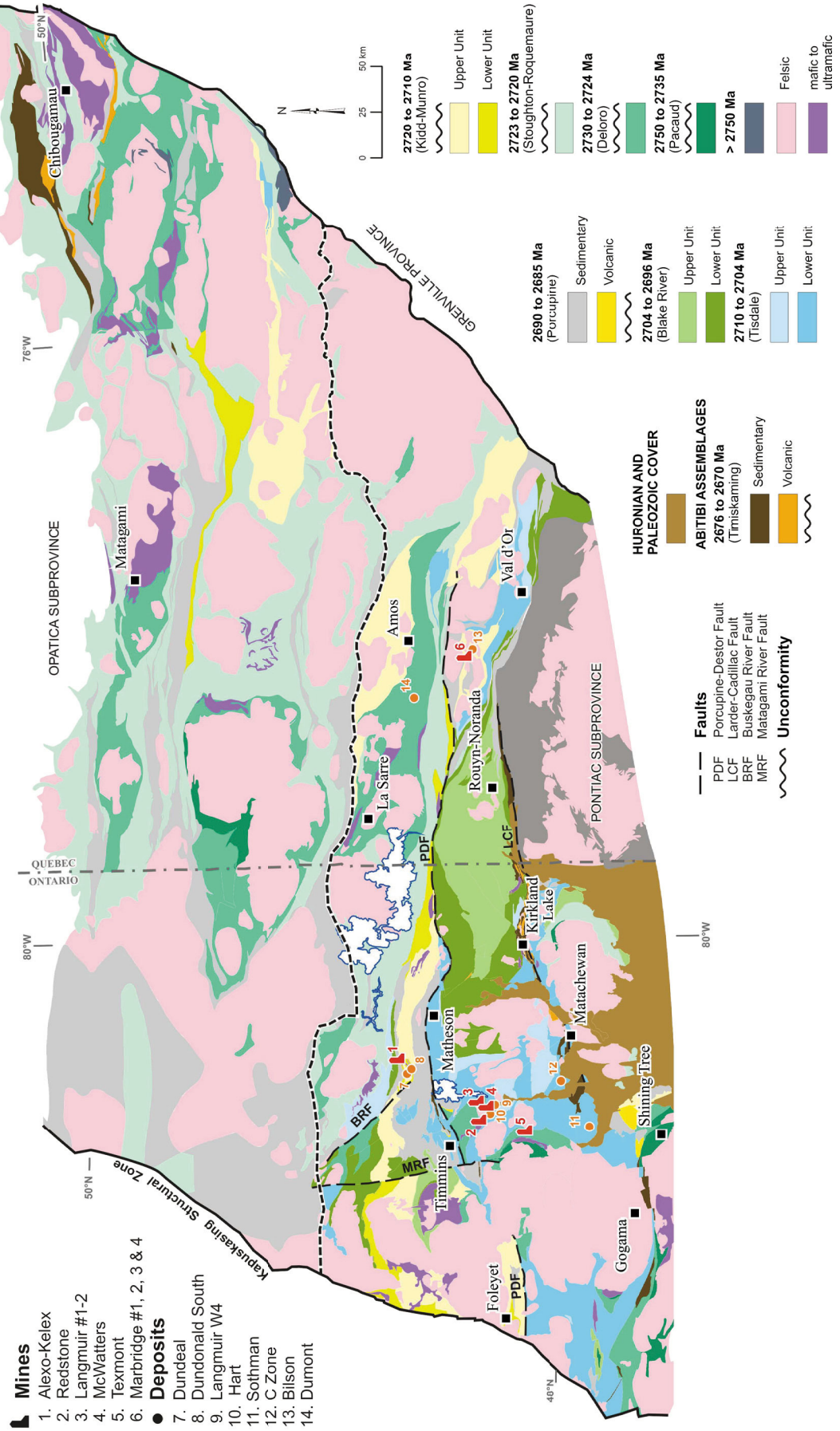

Figure 1. Simplified lithotectonic assemblages map showing the different komatiite-associated Ni–Cu–(PGE) deposits and/or occurrences in the Abitibi greenstone belt (adapted from Thurston et al., 2008)

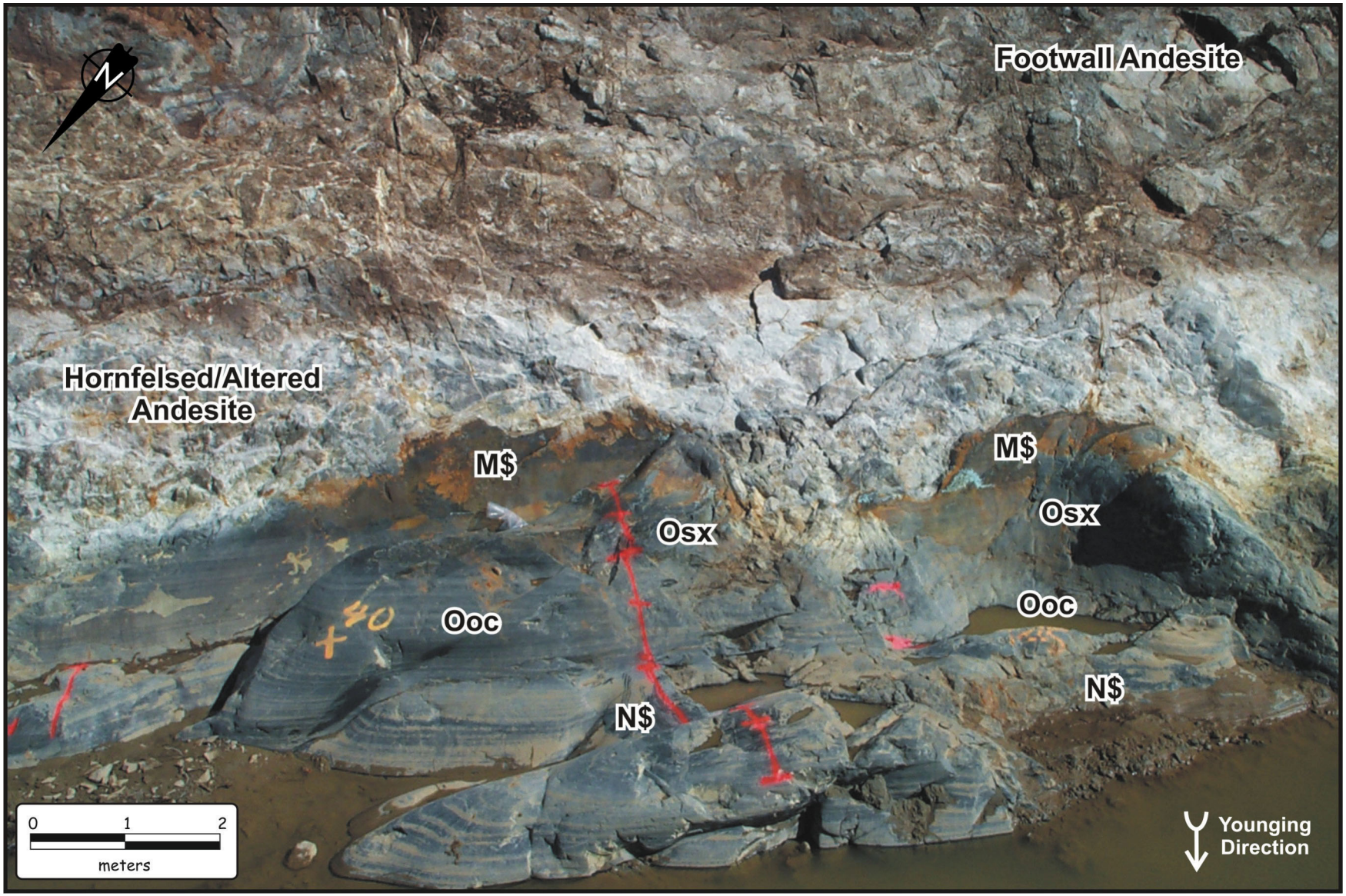

Figure 2. Typical example of komatiite-associated Ni–Cu–(PGE) sulfide mineralization located at the base of komatiitic lava channel at the Alexo mine, Dundonald Township. M$: massive sulfides, N$: net-textured sulfides, Ooc: olivine orthocumulate, Osx: olivine spinifex textures

penetrate downward into underlying andesites, primarily along the lateral margins of embayments, and 5) many of the dikes and marginal rocks exhibit geochemical evidence of contamination. This evidence for thermomechanical erosion, combined with S isotopic evidence for a major component of non-magmatic country-rock S in the ores, provides additional support for the roles of thermomechanical erosion and incorporation of country-rock S in the genesis of komatiite-associated Ni-Cu-(PGE) deposits. The detailed mapping also reveals that the stratigraphy of the ore zone is considerably more complex than previously reported, indicating that the sulfides were emplaced in several stages, confirming the dynamic nature of the ore emplacement process in komatiite-associated Ni-Cu-(PGE) deposits.

Discussion

Although komatiitic systems in the AGB exhibit all of the critical factors required to generate Ni-Cu-(PGE) mineralization, no komatiite-associated Ni-Cu-(PGE) ore systems of the sizes of those in the Thompson Nickel Belt (Manitoba), Cape Smith Belt (New Québec), Pechenga Belt (Russia), or Norseman–Wiluna Belt (Australia) have been discovered. The main reason for this is believed to be that the mineralized intrusive and extrusive units discovered thus far in the AGB appear to be smaller, less dynamic, and/or less extensive, probably reflecting less favourable deep crustal structure in the AGB compared to that in the other areas (see discussion by Lesher and Keays, 2002; Barnes et al., 2008). As a consequence, the volcanic stratigraphy in AGB is more complex and more variable, and the mineralization occurs in a wider range of volcanic-subvolcanic settings and stratigraphic locations (Houlé et al., 2008). Houlé et al. (2008) have also suggested there is a spectrum of komatiite volcano types between those characterized by flow-dominated successions (e.g., Munro Township, Bartlett Dome), which are more likely to be extrusive, and those characterized by volcaniclastic and/or sediment-dominated successions (e.g. Dundonald Township, Shaw Dome), which are more likely to be both intrusive and extrusive. Within this spectrum it is the nature of the near-surface rocks that plays a critical role in developing the architecture of submarine komatiitic volcanoes, their subvolcanic plumbing systems, and where Ni-Cu-(PGE) sulfides will segregate and accumulate. Although it appears that the deposits in the AGB may be smaller, they are also more likely to occur in a wider range of stratigraphic settings and at a wider range of stratigraphic levels.

Concluding remarks

Our recently increased understanding of the volcanology and stratigraphy of komatiites in the AGB indicates that with increased exploration there is potential for the discovery of new Ni-Cu-(PGE) deposits associated with komatiites in both less explored (e.g., Bartlett Dome) and also more explored camps (e.g., Langmuir W4 deposit in the Shaw Dome). However, the smaller, less dynamic and less extensive systems in the AGB make it more difficult to predict the location of mineralized lava channels or channelized sheet flows/sills within different komatiitic successions. Thus far, almost all komatiitic successions in the AGB are prospective for komatiite-associated Ni-Cu-(PGE) deposits, but the Kidd-Munro- and the Tisdale-aged komatiitic rocks remain most prospective, which are also the only volcanic episode that contain both abundant magma/lava pathways (magma conduits, feeder sills, lava channels, and channelized sheet flows) and external sources of S. A multidisciplinary approach including geological mapping, volcanic facies mapping, geophysical surveys, and geochemical studies is required to aid in the exploration for these new deposits and to facilitate the recognition of favourable volcanic sequences that may host nickel sulfide mineralization.

References

Ayer, J.A., Thurston, P.C., Bateman, R., Dubé, B., Gibson, H.L., Hamilton, M.A., Hathway, B., Hocker, S.M., Houlé, M.G., Hudak, G., Ispolatov, V.O., Lafrance, B., Lesher, C.M., MacDonald, P.J., Péloquin, A.S., Piercey, S.J., Reed, L.E. and Thompson, P.H. 2005. Overview of results from the Greenstone Architecture Project: Discover Abitibi Initiative; Geological Survey, Open File Report 6154, 146pp.

Barnes, S.J., Lesher, C.M., and Sproule, R.A., 2008, Geochemistry and petrogenesis of komatiites and komatiitic basalts in the Eastern Goldfields Superterrane, Western Australia and the Abitibi Greenstone Belt, Canada, and implications for the distribution of associated Ni-Cu-PGE deposits: Insitution of Mining and Metallurgy, v. 116, no. 4, p. 167-187.

Berger, B.R., Pilote, P., Houlé, M.G., Ayer, J.A., Dinel, E., and Bleeker, W., 2010, Stratigraphy of the 2720-2710 Ma Kidd-Munro volcanic episode in the Abitibi Greenstone Belt: Implications for base metal mineralization: Fifth International Archean Symposium, Perth, Yilgarn–Superior workshop: Geological Survey of Western Australia Record 2010/20, p. 42–46.

Houlé, M.G., Gibson, H.L., Lesher, C.M., Davis, P.C., Cas, R.A.F., Beresford, S.W., and Arndt, N.T., 2008, Komatiitic Sills and Multigenerational Peperite at Dundonald Beach, Abitibi Greenstone Belt, Ontario: Volcanic Architecture and Nickel Sulfide Distribution: Economic Geology, v. 103, p. 1269-1284.

Houlé, M.G., Lesher, C.M., and Davis, P.C. *accepted*, Thermomechanical erosion at the Alexo Mine, Abitibi Greenstone Belt, Ontario: Implications for the genesis of komatiite-associated Ni-Cu-(PGE) mineralization: Mineralium Deposita.

Lesher, C.M. and Keays, R.R. 2002, Komatiite-associated Ni-Cu-PGE deposits: geology, mineralogy, geochemistry and genesis; in The geology, geochemistry, mineralogy and mineral beneficiation of platinum-group elements: Canadian Institute of Mining, Metallurgy and Petroleum, Special Volume 54, p. 579-618.

Naldrett, A.J. 2004. Magmatic sulfide deposits: geology, geochemistry and exploration: Springer-Verglag, Berlin, 727pp.

Sproule, R.A., Lesher, C.M., Ayer, J.A., Thurston, P.C., and Herzberg, C.T. 2002, Spatial and temporal variations in the geochemistry of komatiitic rocks in the Abitibi greenstone belt: Precambrian Research, v. 115, p. 153-186.

Sproule, R.A., Lesher, C.M., Houlé, M.G., Keays, R.R., Ayer, J.A., and Thurston, P.C. 2005, Chalcophile element geochemistry and metallogenesis of komatiitic rocks in the Abitibi greenstone belt, Canada: Economic Geology, v. 100, p. 1169-1190.

Thurston, P.C., Ayer, J.A., Goutier, J., Hamilton, M.A., 2008, Depositional gaps in Abitibi greenstone belt stratigraphy: a key to exploration for syngenetic mineralization: Economic Geololgy, v. 103, p. 1097-1134.

What happens when there is no volcanism: BIFs and how greenstones have developed in the Superior and elsewhere

by

PC Thurston[1], BS Kamber[1], JA Ayer[2], and GJ Baldwin[1]

Introduction

Archean greenstone belts are dominated by volcanic rocks with sparse sedimentary rocks. To understand the processes of belt development, we must constrain the depositional setting and the rates of volcanism and sedimentation. Most belts, regardless of craton, consist of a komatiite/tholeiite basal unit overlain by varying proportions of intermediate to felsic volcanics capped by a sedimentary interface zone (SIZ) consisting of mixtures of clastic and chemical sedimentary rocks followed by another cycle of volcanism etc. commonly followed by a successor basin. This style of volcanism represents variable proportions of possibly plume-derived komatiites and tholeiites and mafic to felsic rocks with arc trace element signatures. In multi-cycle belts, we observe total durations of ~50 to ~300 My or more. "Arc" systems represent an influx of mantle-derived mafic material interacting with a mantle wedge or obtaining the distinctive trace element signature through the presence of residual rutile in the source. Volume estimates of mantle-derived mafic magma in modern arcs range from 0.01-1 km^3 yr per volcanic system (Shaw, 1985) to 5 km^3/year/km of arc length (Scholl and von Hueme, 2004) whereas plumes represent 0.15-8.2 km^3/yr (Condie, 2001). Using the volume for the 2734-2724 Ma mafic-felsic episode in the Abitibi greenstone belt as an example, (vol.=750,000 km^3) we estimate accumulation times for the volcanic cycles at: 1) 7,500-75,000 yr (Shaw method), 2) 4.1 x 10^3/ yr, or <2000 yr for a 600 km long arc (the Scholl and Von Hueme method), and 3) 100,000 yr-5 × 10^6 yr for the plume-based estimate (Condie, 2001) (Thurston et al., 2008). As this volcanic unit represents deposition over a 10 My interval, these estimates of accumulation time especially on a possibly hotter Archean mantle suggest that active volcanic deposition lasted a much shorter (100-1000×) duration than the entire time represented by a geologically preserved cycle such as the Deloro assemblage (Figure 1). What occurs during these apparently lengthy volcanic hiatuses?

[1] Laurentian University, Sudbury, Ontario, Canada
[2] Ontario Geological Survey, Sudbury, Ontario, Canada

Sediment geochemistry

In modern systems, submarine unconformities are loci of extensive rock-water interaction, which produces extensive development of mass flow units by down-slope movement from more proximal locales, accumulations of Mn nodules, chert nodules, or glauconitic sands in distal settings. In Archean greenstones, SIZ units capping volcanics consist of complex mixtures of clastic and chemical sediments. We can divide hydrogenous sediments (autochthonous sediments derived from basin waters) into those influenced dominantly by 1) open marine seawater, 2) terrigenous sources, and 3) hydrothermal fluids (e.g., (Allwood et al., 2010; Bolhar et al., 2004). In shale-normalized diagrams, modern seawater is characterized by: 1) depletion of the LREE, 2) Y/Ho above chondritic values (i.e. >26), positive anomalies for La, Gd, and perhaps Lu, and 4) a variably negative Ce anomaly. The first three features are caused by stability of REE complexes during estuarine removal of a part of the dissolved river load (e.g. Kamber, 2010). Many microbial carbonates, cherts and phosphates have been shown to exhibit seawater patterns (Shields and Webb, 2004) will commonly exhibit seawater patterns. High T hydrothermal fluids, though poorly characterized, are enriched in LREE and Eu and chondritic Y/Ho. Terrigenous sediments are made up of colloidal and particulate components. The latter strongly affects geochemistry with incompatible elements enriched in continental crust (e.g. Th, Zr, Ga and Sc). This usually will flatten the REE pattern when normalized to shales which in turn represent average continental compositions.

Origin of sedimentary interface zones (SIZ)

SIZ units at the top of volcanic cycles represent major hiatuses in volcanism with the duration of non-volcanic intervals ranging from fractions of a million years to several tens of millions of years. What occurs during these lengthy hiatuses? There are three alternatives: 1) Very slow rates of sedimentation produce "condensed sections" or zones with very low rates of sedimentation down-dip from thicker near shore sections in a shelf environment. For example in the

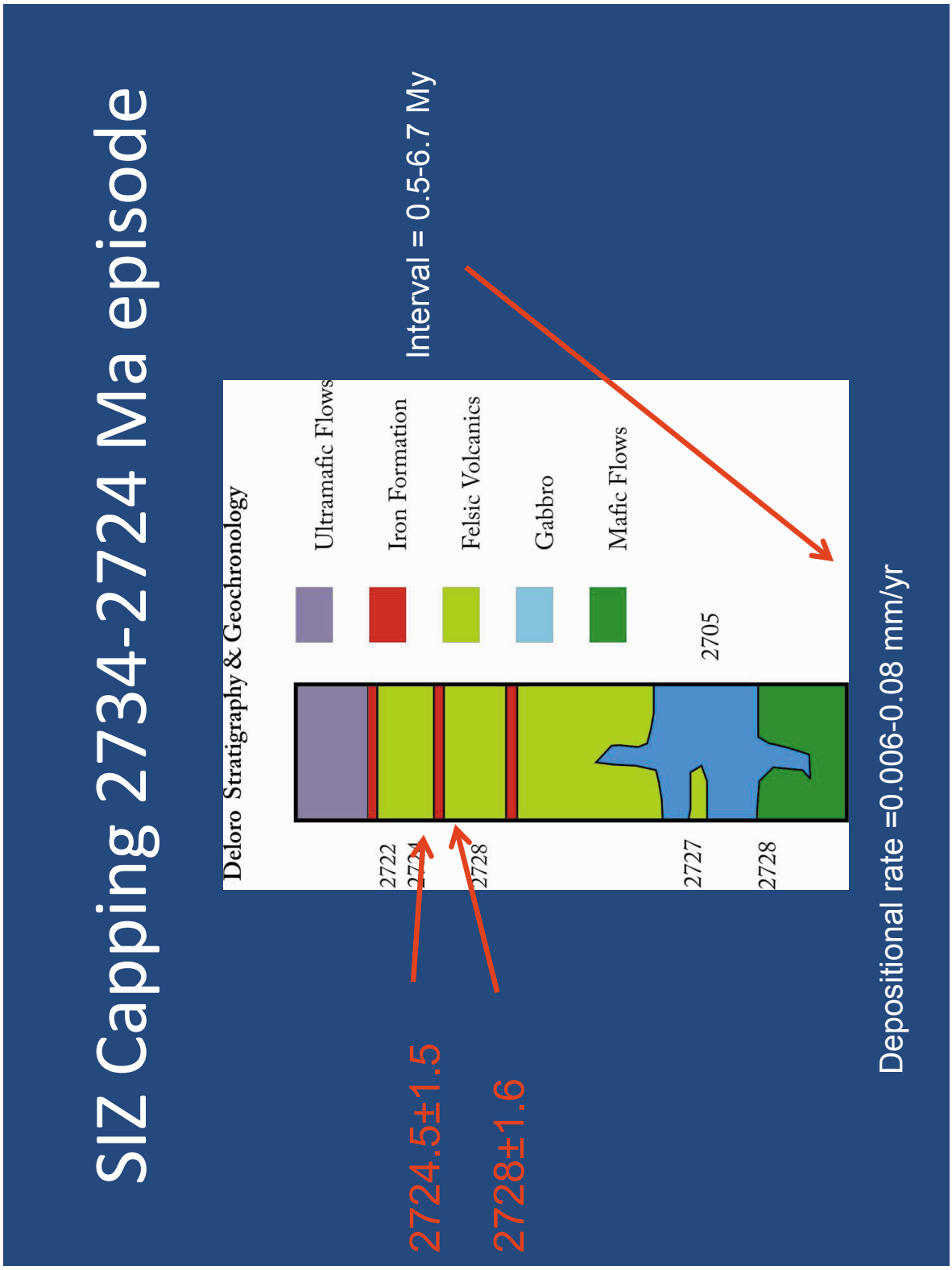
SIZ Capping 2734-2724 Ma episode
Deloro Stratigraphy & Geochronology
Ultramafic Flows
Iron Formation
Felsic Volcanics
Gabbro
Mafic Flows
2722
2724
2728
2727
2705
2728
Interval = 0.5-6.7 My
2724.5±1.5
2728±1.6
Depositional rate =0.006-0.08 mm/yr

Figure 1.

Deloro assemblage of the Abitibi belt, an iron formation is bounded above and below by rhyolite. The lower rhyolite has an age of 2728.1±1.6 Ma and the upper rhyolite 2724.5±1.5 Ma, indicating the duration of iron formation deposition was 0.5-6.7 My. These units normally show a complex mixture of seawater, hydrothermal, and terrigenous geochemical signatures (Figure 2). 2) Hydrothermal circulation can produce chert breccias forming cross-cutting veins and stratiform chert breccia units both having hydrothermal geochemical signatures. 3) Rock-water exchange processes in shelves or abyssal environments will produce silicification of pre-existing units, "hard ground", Mn nodules glauconite, sulfide zones, etc. (Krapez et al., 2003). In summary the SIZs produced during volcanic hiatuses represent very slow sedimentation and/or rock-water interaction. Thus the SIZ units represent alternatively submarine unconformities, condensed sections, or correlative conformities.

Role of SIZ in syngenetic mineralization

There may be an association of lengthy hiatuses in volcanism with production of thick SIZs with economic thicknesses and grades of iron formation. The examples of Table 1 are listed on the basis of their lengthy depositional gaps. Those in bold type have economic iron deposits whereas the other occurrences are examples of SIZ units serving as regional scale marker units.

The regional scale marker units vary from SIZ units capping basalt/komatiite to rhyolite sequences to iron formations within basalt sequences. In either stratigraphic situation, SIZs represent appreciable hiatuses in volcanism (Table 2). Volcanic hiatuses are also commonly marked by chert/argillite marker units in VMS districts ranging from cm to metre-scale units in districts ranging in age from Phanerozoic (Peter et al., 2003) to Archean (Gibson and Galley, 2007) in age. The hiatuses in volcanism occur at the group, formation and member level. The hydrothermal systems giving rise to the VMS deposits are a product of hydrothermal systems leaching metals from the volcanic pile on or beneath the seafloor during gaps in volcanism. The hiatus also represent intervals of regional hydrothermal activity as indicated by the metal contents and alteration associated with the SIZ units. For example, the 110 Mt of VMS ore produced from the Deloro assemblage to date are all from deposits with ages of 2728 to 2724 Ma, the same timeframe for deposition of the SIZ unit discussed above.

The big picture and shield to shield comparisons

Iron formations can display features indicative of shallow water deposition both within the BIF and along strike e.g. stromatolites and flaser bedding (Thurston et al., 2008, and references therein). This textural evidence, coupled with the arguments advanced by Kamber (2010) lead us to suggest that much of Archean greenstone stratigraphy was quite possibly deposited in an oceanic plateau environment. Archean greenstone belts worldwide display similar dome and keel architecture with autochthonous juvenile komatiite/tholeiite to rhyolite stratigraphy capped by SIZ units and commonly with various types of successor basins arrayed along major strike-slip shear zones. There are confusing factors such as the presence of calc-alkaline sequences lacking a komatiite/tholeiite base and alkaline (e.g., shoshonitic) volcanic units. The simplest Australian example with features similar to Abitibi stratigraphy is the eastern Pilbara (Van Kranendonk et al., 2007). However, the Yilgarn appears to be similar to the Abitibi stratigraphically (Kositcin et al., 2008) and to the Superior Province in a tectonic sense (Wilde et al., 1996) albeit complicated by strike-slip structures. Differences appear to lie in large-scale structural interpretation e.g. (Middleton et al., 1995) vs. (White et al., 2003).

Table 1. Selected depositional gaps in Archean greenstones and associated iron formations

Area/craton	Ages below to above iron formations	Possible depositional gap	Reference
Bartlett dome/Superior	2728.1±1.6/2724.5±1.5	0.5-6.7 My	(Baldwin, 2009)
Steeprock/Superior	**2780/2735 Ma**	**45 My**	**(Stone, 2010)**
Confederation/Superior	2880/2771 Ma	~109 My	(Rogers, 2000)
Temagami/Superior	**2766-2722 Ma**	**~44 My**	**(Ayer et al., 2006)**
Michipicoten/Superior	**2750-2700 Ma**	**~ 50 My**	**(Sage and Heather, 1991)**
Kostomuksha/Baltic	**2843/2757 Ma**	**~114 My**	**(Puchtel et al., 1998)**
Manjeri Fm /Zimbabwe	2.80-2.74 Ga	~60-120 My	(Prendergast, 2004)

Hydrogenous sediments

Hydrothermal

Argillite

Seawater

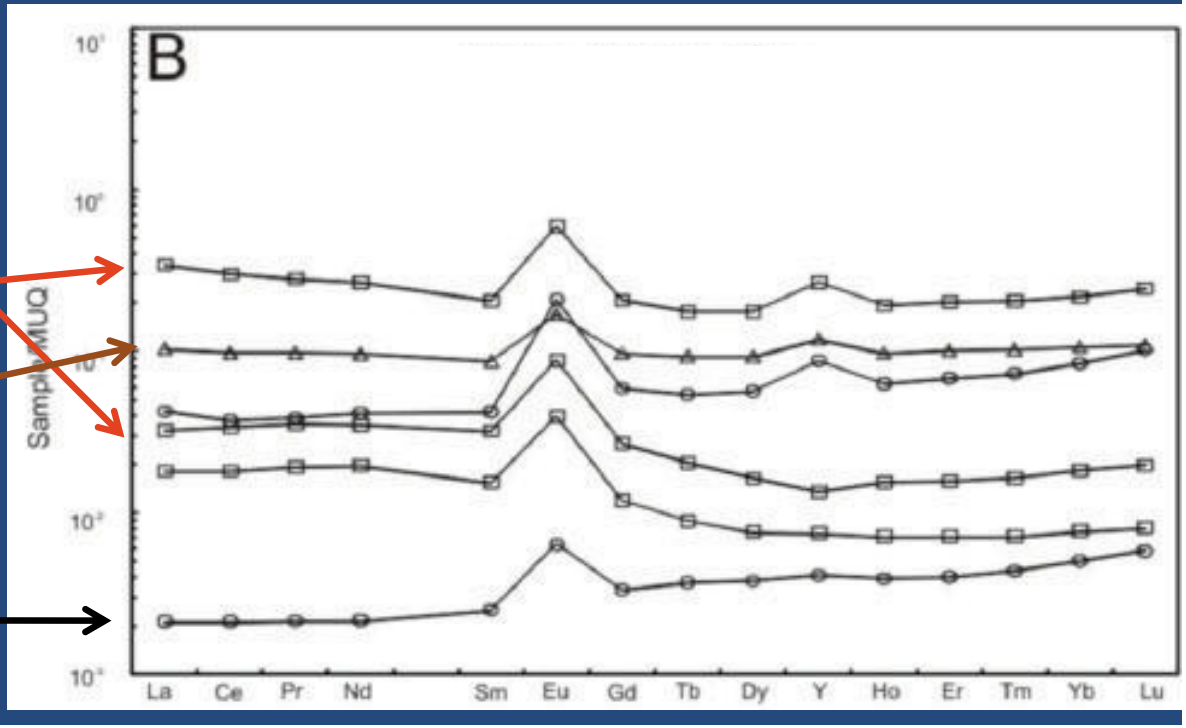

Fiogure 2.

Table 2. Syngenetic deposits in the Abitibi greenstone belt (after Thurston et al., 2008)

Time interval	VMS mineralization	Komatiite-associated Cu-Ni-PGE mineralization
2704-2695 Ma	Jameland, Kam-kotia, Can. Jamieson, Rouyn-Noranda Camp	
2710-2704 Ma	Val-d'Or Camp	Langmuir, Redstone,Texmont
2719-2711 Ma	Kidd Creek, Potter, Potterdoal, Langlois	Alexo, Dundonald, Dumont, Marbridge
2723-2720 Ma	Estrades	
2734-2724 Ma	Shunsby, Hunter Mine, Normétal, Selbaie, Matagami Camp, Joutel Camp	
2750-2735 Ma	Tretheway-Ossian, Amity, Gemini-Turgeon	

References

Allwood, A. C., Kamber, B. S., Walter, M. R., Burch, I. W., and Kanik, I., 2010, Trace elements record depositional history of an Early Archean stromatolitic carbonate platform: Chemical Geology, v. 270, p. 148-163.

Ayer, J., Chartrand, J. E., Grabowski, G. P. D., Josey, S., Rainsford, D., and Trowell, N. F., 2006, Geological compilation of the Cobalt-Temagami area, Abitibi greenstone belt: Ontario Geological Survey, Preliminary Map P. 3581.

Bolhar, R., Kamber, B. S., Moorbath, S., Fedo, C. M., and Whitehouse, M. J., 2004, Characterization of early Archaean chemical sediments by trace element signatures: Earth and Planetary Science Letters, v. 222, p. 43-60.

Condie, K. C., 2001, Mantle Plumes and Their Record in Earth History: Cambridge, Cambridge University Press, 306p.

Gibson, H. L., and Galley, A. G., 2007, Volcanogenic Massive sulphide Deposits of the Archean, Noranda District, Québec, *in* Goodfellow, W., ed., Mineral Deposits of Canada: A Synthesis of Major Deposit-types, District Metallogeny, The Evolution of Geological Province, and Exploration Methods, 5, Mineral Deposits Division Geological Association of Canada, p. 533-552.

Kamber, B. S., 2010, Archean mafic-ultramafic volcanic landmasses and their effect on ocean-atmosphere chemistry: Chemical Geology, v. 274, p. 19-28.

Kositcin, N., Brown, S. J. A., Barley, M. E., Krapez, B., Cassidy, K. F., and Champion, D. C., 2008, SHRIMP U/Pb zircon age constraints on the late Archaean tectonostratigraphic architecture of the Eastern Goldfields Superterrane, Yilgarn Craton, Western Australia: Precambrian Research, v. 161, p. 5-33.

Krapez, B., Barley, M. E., and Pickard, A. L., 2003, Hydrothermal and resedimented origins of the precursor sediments to banded iron formation: sedimentological evidence from the Early Palaeoproterozoic Brockman supersequence of Western Australia: Sedimentology, v. 50, p. 979-1011.

Middleton, M. F., Wilde, S. A., Evans, B. J., Long, A., Dentith, M. C., and Morawa, M., 1995, Implications of a geoscientific traverse over the Darling fault zone, Western Australia: Australian Journal of Earth Sciences, v. 42, p. 83-93.

Peter, J. M., Goodfellow, W., and Doherty, W., 2003, Hydrothermal Sedimentary Rocks of the Heath Steele Belt, Bathurst Mining Camp, New Brunswick: Part 2. Bulk and Rare Earth Element Geochemistry and Implications for Origin, *in* Goodfellow, W., McCutcheon, S. R., and Peter, J. M., eds., Massive Sulfide Deposits of the Bathurst Mining Camp, New Brunswick and northern Maine: Economic Geology Monograph 11: Boulder CO, Economic Geology.

Prendergast, M. D., 2004, The Bulawayan Supergroup; a late Archaean passive margin-related large igneous province in the Zimbabwe Craton: Journal of the Geological Society of London, v. 161, p. 431-445.

Sage, R. P., and Heather, K. B., 1991, The Structure, Stratigraphy and Mineral Deposits of the Wawa area, Geological Association of Canada: Mineralogical Association of Canada, Society of Economic Geologists Field Trip A6 Guidebook, p. 118.

Scholl, D. W., and von Hueme, R., 2004, Recycling of continental crust at modern subduction zones, implicatioins for Precambrian crustal growth, supercontinent constructions, and littering the mantle with continental debris: Geological Society of America Abstracts with Programs, v. 36, p. 205-206.

Shaw, H. R., 1985, Links between magma-tectonic rate balances, plutonism and volcanism: Journal of Geophysical Research, v. 90, p. 11275-11288.

Shields, G. A., and Webb, G. E., 2004, Has the REE composition of seawater changed over geological time?: Chemical Geology, v. 204, p. 103-107.

Thurston, P., Ayer, J., Goutier, J., and Hamilton, M. A., 2008, Depositional Gaps in Abitibi Greenstone Belt Stratigraphy: a key to exploration for syngenetic mineralization: Economic Geology, v. 103, p. 1097-1134.

Van Kranendonk, M. J., Smithies, R. H., Hickman, A. H., and Champion, D. C., 2007, Secular tectonic evolution of Archaean continental crust: interplay between horizontal and vertical processes in the formation of the Pilbara Craton, Australia: Terra Nova, v. 19, p. 1-38.

White, D., Musacchio, G., Helmstaedt, H., R.M., H., Thurston , P. C., van der Velden, A., and Hall, K., 2003, Images of a lower-crustal oceanic slab: Direct evidence for tectonic accretion in the Archean Western Superior Province: Geology, v. 31, p. 997-1000.

Wilde, S. A., Middleton, M. F., and Evans, B. J., 1996, Terrane accretion in the southwestern Yilgarn Craton; evidence from a deep seismic crustal profile: Precambrian Research, v. 78, p. 179-196.

The Abitibi Subprovince: its evolution and its VMS deposits — an overview

by

Jean Goutier[1], Patrick Mercier-Langevin[2], Vicki McNicoll[3], and John Ayer[4]

Introduction

The Abitibi Subprovince (ASP) is the largest greenstone belt in the World (lozenge shape 310 km × 720 km) and the richest part of the Archean Superior Province. The ASP is known for its unique endowment in volcanogenic massive sulfide deposits (VMS), Ni-Cu-PGE magmatic deposits, and orogenic gold deposits among others. It contains the second largest concentration of VMS deposits of the World. Although generally well preserved (metamorphic grade varies from lower greenschist to amphibolite facies), the ASP is cut by numerous high-strain zones and crustal-scale faults limiting part of the reconstruction and stratigraphic correlation.

The ASP was formed over a period that spans approximately 150 m.y. (2790-2640 Ma). More than a hundred VMS deposits were formed in the ASP over a period of about 42 m.y., with a cumulative tonnage of approximately 760 Mt of base and precious metal-rich ore. Two VMS deposits of the ASP can be considered super-giant (>150 Mt: ~198 Mt, Horne H&G+Zone 5; ~183 Mt, Kidd Creek), one can be considered super large (50-100 Mt: ~67 Mt, LaRonde Penna;), whereas two can be considered large (25-50 Mt: ~47 Mt, Selbaie; ~26 Mt, Mattagami Lake). Also, twelve of the VMS are rich in gold. Of these twelve deposits, eight are located in the 2704-2695 Ma Blake River Group (BRG), with seven of these Au-rich VMS deposits being world-class gold deposits (>1 million ounces; Mercier-Langevin et al., in press). Two of these Au-rich VMS are located in the Noranda mining camp (Horne and Quemont) whereas the other five are located in the Doyon-Bousquet-LaRonde mining camp, 50 km east of Rouyn-Noranda (DBL: LaRonde Penna, Bousquet 2, Dumagami, Bousquet 1 and Westwood). Horne (~330 t Au) and LaRonde Penna (~268 t Au) are the two largest Au-rich VMS deposits ever discovered.

The ASP, and more specifically the BRG, represents one of the best places in the world to explore for Au-rich VMS deposits. The work undertaken by the Ministère des Ressources Naturelles et de la Faune du Québec (MRNF), the Geological Survey of Canada (GSC), the Ontario Geological Survey (OGS), universities and industry under the Targeted Geoscience Initiative 3 (TGI-3) and the Plan Cuivre aimed at better define the geological setting of the base and precious metal-rich deposits of the ASP. This presentation will present an overview of the geological setting in which the main VMS deposits of the ASP are found.

[1] Géologie Québec, Rouyn-Noranda, Québec, Canada
[2] Geological Survey of Canada, Québec, Québec, Canada
[3] Geological Survey of Canada, Ottawa, Ontario, Canada
[4] Ontario Geological Survey, Sudbury, Ontario, Canada

The Abitibi Subprovince subdivisions

The Abitibi Subprovince has been subdivided into eight episodes of major submarine volcanic activity based on recent regional and detail mapping and compilation. Although numerous major faults and high-strain corridors cut across the ASP, stratigraphic sections are commonly well preserved. These volcanic episodes are therefore well constrained (figure 1): 1) ~2790 Ma; 2) ~2758 Ma; 3) 2750-2735 Ma; 4) 2734-2724 Ma; 5) 2723-2720 Ma; 6) 2719-2711 Ma; 7) 2710-2704 Ma; 8) 2704-2695 Ma and many now of episodes are favorable periods for VMS formation. This new framework also enables us to better understand the evolution of the ASP which was previously thought to systematically young to the south.

Geologic setting and distribution of the VMS deposits of the Abitibi

The oldest volcanic rocks in the ASP, dated from 2790 to 2758 Ma, are located in the NE part of the Abitibi. These rocks represent the probable extension of the Frotet-Evans belt, located further north of the ASP. The 2750-2735 Ma volcanic episode is the oldest VMS-bearing episode of the ASP. Base and precious metal-rich VMS occurrences (Gemini-Turgeon) are found in the Théo Formation, in the northern Abitibi. The occurrences are associated with a significant Fe-carbonate alteration that is overprinted by

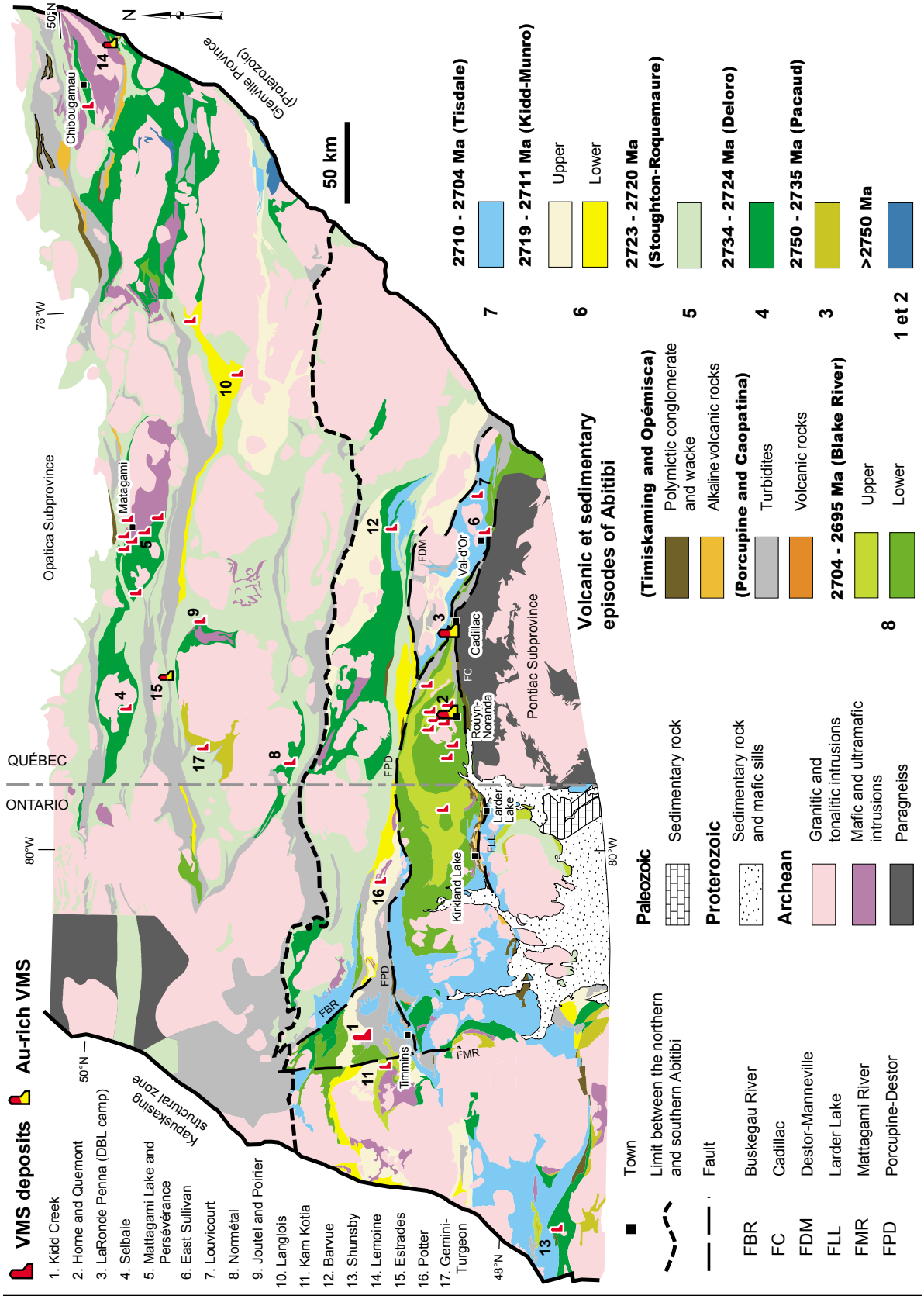

Figure 1. Map of volcanic and sedimentary episodes of the Abitibi Subprovince, with location of VMS and Au-rich VMS deposits. Modified from Thurston et al. (2008)

discordant chlorite and sericite alteration zones close to the ore. The sulfides are dominantly hosted in calc-alkaline felsic volcaniclastic rocks.

The 2734-2724 Ma volcanic episode was very fertile with 40 VMS deposits, totaling ~134 Mt. The major mining camps of the northern Abitibi are within the volcanic rocks of this episode and are characterized by a variety of mineralization types: Zn ±Cu (Matagami), Cu-Zn (Joutel, Chibougamau, Normétal), Au-Zn-Cu (Chibougamau) and possibly a "hybrid type" polymetallic VMS (Selbaie). Major synvolcanic plutons of gabbro-anorthosite of the ASP (Rivière Bell and Lac Doré) are associated with this episode and are adjacent to a number of VMS deposits. There is a link between the variation of geochemical affinity (calc-alkaline and tholeiitic), and the number of VMS more abundant in the Matagami sector that are the youngest of this episode.

The VMS deposits of the Matagami camp are exceptionally rich in Zn. The Matagami VMS lenses were mainly formed along a marker horizon called the "Key Tuffite". This sedimentary/exhalative horizon marks the contact between tholeiitic rhyolites in the footwall and a basalt-basaltic andesite sequence in the hanging wall. The Selbaie polymetallic deposit is characterized by veins of sphalerite-galena-chalcopyrite associated with lenses of massive pyrite. The ore at Selbaie is mainly developed in transitional to calc-alkaline felsic volcaniclastic units.

The 2723-2720 Ma volcanic episode is one of the largest in terms of volume of volcanic rocks generated (tholeiitic basalt, magnesian basalt and less komatiite) and geographic extent. This episode reflects the fragmentation of the large volcanic arc (2734-2724 Ma) during a short period of rapid expansion. Despite its extent, this episode contains only a single Au-Zn-Cu-Ag-rich VMS deposit (Estrades) in a bimodal volcanic package of tholeiitic affinity.

The 2719-2711 Ma volcanic episode hosts the super giant Kidd Creek deposit. This deposit is hosted in a sequence of ultramafic volcanic rocks (base), overlain by coherent to brecciated tholeiitic rhyolites (mineralized horizon) that are covered by massive porphyritic rhyolites and basalts (see Berger et al., this volume). This volcanic episode is also associated with the formation of the Zn-Cu Langlois (formerly Grevet) and Zn-Cu-Co Potter VMS deposits.

The fifth VMS-bearing volcanic episode (2710-2704 Ma), in the southern Abitibi, has a distinct lateral variation of lithological and geochemical affinity. To the west, this episode is basalt and komatiite, with deposits associated Ni-Cu (Timmins), while in the east, tholeiitic to transitional polymictic tuff and transitional to calc-alkaline, intermediate to felsic volcaniclastics strata are found associated with VMS deposits districts Barraute (Barvue) and Val-d'Or (Louvicourt). During this same episode the northern Abitibi underwent intusion of large syntectonic TTG plutons and sedimentation with turbidites (Caopatina Fm) with detritus derived from erosion of metamorphic and plutonic sources in the Opatica Subprovince north of the ASP. This indicates that during this period the northern part of the Abitibi was in contraction, while the south was undergoing extension.

VMS and Au-rich VMS deposits of the 2704–2695 Ma volcanic episode

The 2704-2695 Ma volcanic episode of is the richest in terms of total accumulation of metals with 365 Mt of ore and 34 ore deposits, which comprises the Blake River Group (BRG) that contains the most important concentration of VMS deposits of the Superior Province. Approximately half of the total VMS tonnage of the ASP is located in the BRG, and about 90% of the total VMS gold of the ASP is found in the BRG. Horne (54 Mt plus 144 Mt of sub-economic sulfides) and LaRonde Penna (~67 Mt) together contain more than 40% of the total VMS gold of the entire ASP (Mercier-Langevin et al., 2010). Extensive and very precise U-Pb geochronology in the BRG enables us to differentiate four VMS-bearing secondary volcanic episodes or time-stratigraphic intervals in the BRG (Goutier et al., 2009).

The VMS deposits of the Rouyn-Noranda district, especially those located in the central camp, define the archetypal "Noranda model". These deposits are characterized by lenses or masses of sulfides sitting on top of discordant sulphide stringers (feeders) that are formed near tholeiitic to transitional effusive centers. The VMS deposits that are located outside the main camp (Horne and Bouchard-Hébert) are generally larger, tabular in shape and were formed, at least in part, by sub-seafloor replacement of felsic volcaniclastics rocks. They are associated with extensive, concordant to locally discordant sericite and quartz alteration envelopes and proximal zones of chlorite ± carbonate alteration of varying intensity.

The Doyon-Bousquet-LaRonde mining camp is characterized by an exceptional concentration of Au-rich volcanogenic mineralization forming disseminated, semi-massive and massive sulphide lenses that are locally rich in base metals. These Au-rich lenses are associated with widespread sericitization and with significant concordant to discordant proximal garnet-biotite-sericite±quartz-chloritoid-rutile alteration zones or with proximal aluminous alteration zones (staurolite, kyanite, andalousite, quartz, sericite, sulfides). The mineralization and its associated alterations are preferentially developed in a sequence dominated by transitional to calc-alkaline felsic volcaniclastic units.

The first time-stratigraphic interval of the BRG (2704 to 2701.7 Ma) is associated with the formation of a tholeiitic lava plain and isolated felsic centres. The Horne and Quemont Au-rich VMS deposits are associated with this early volcanic event. The second time-stratigraphic interval (2701.7 to 2699.3 Ma) is characterized by bimodal volcanism in the central part of the BRG and by the emplacement of large synvolcanic plutons. The Aldermac, Ansil and Corbet VMS deposits were formed during this bimodal volcanic event. The third time-stratigraphic interval (2699.3 to 2696.7 Ma) is the most prolific of in terms of VMS deposits generation. It includes the Mine Sequence VMS deposits (Amulet, Millenbach, Waite, Norbec), which are hosted in a bimodal volcanic package. The Au-rich VMS deposits of the Doyon-Bousquet-LaRonde mining camp were formed at about the same time, although in a different environment

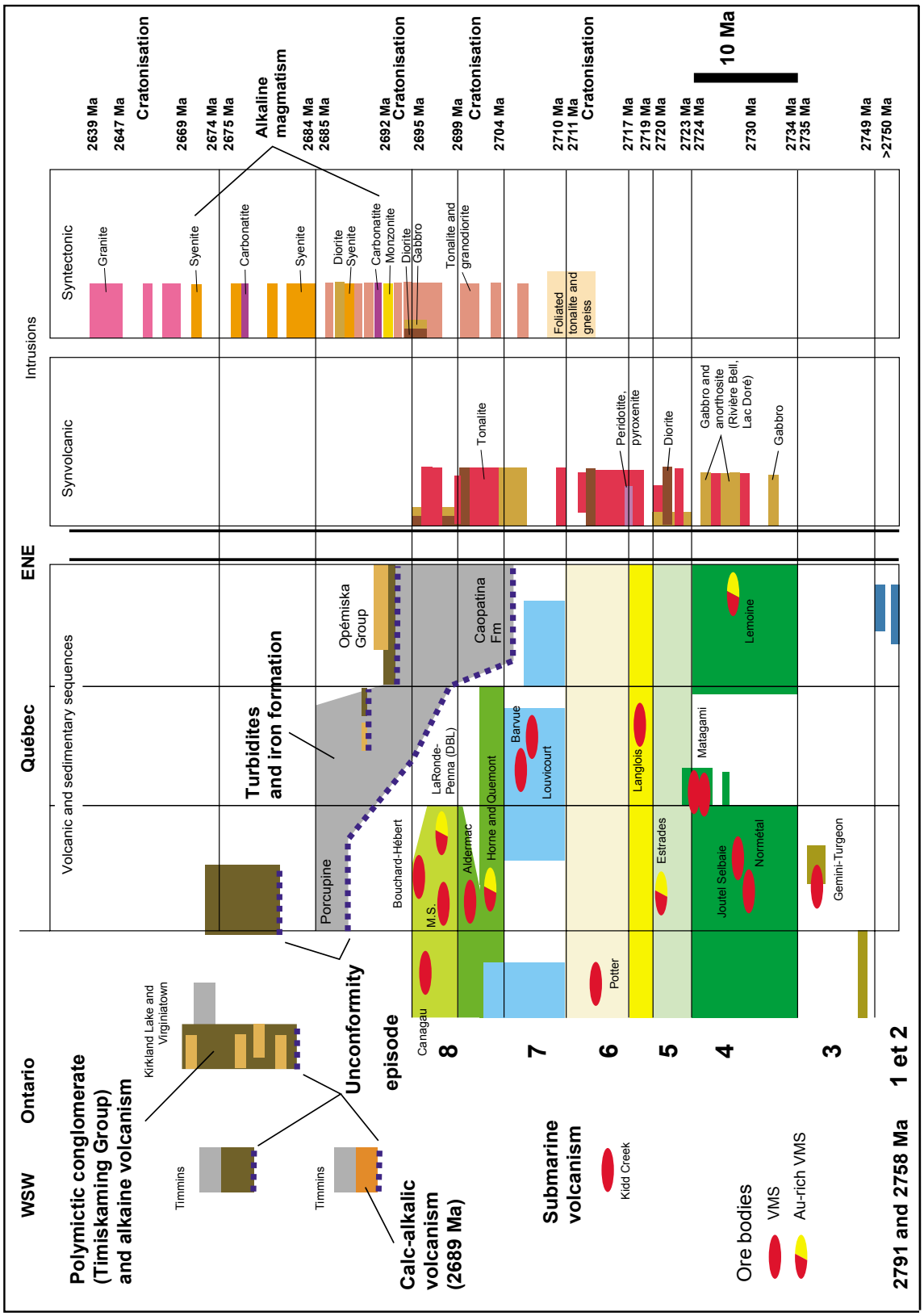

Figure 2. Chronostratigraphic relationship between volcanic, sedimentary, plutonic rocks and VMS deposits of the Abitibi Subprovince. M.S. = Mine sequence (Amulet, Millenbach, Waite, Norbec); DBL = Doyon-Bousquet-LaRonde mining camp

characterized by transitional to calc-alkaline, intermediate to felsic flow-domes and associated volcaniclastic rocks. The fourth time-stratigraphic interval of the BRG (2696.7 to 2695 Ma) consists of felsic volcanic rocks and mafic-intermediate pyroclastic rocks. They include several tholeiitic rhyolites and synvolcanic plutons. The VMS deposits of the Bouchard-Hébert mine and that of Canagau in Ontario were formed during this last BRG-related volcanic event.

Discussion

The ASP is characterized by one of the most significant concentration of VMS deposits of the World, with deposits of varying composition, size, and alteration and mineralization styles. VMS deposits have been found in six of the eight volcanic episodes of the ASP so far, indicating a favorable period for this type of mineralization that spans about 42 m.y. (figure 2).

In general, the oldest deposits are slightly richer in Zn and Ag, whereas those found in younger rocks are clearly richer in gold. Although Au-rich examples are found in most volcanic episodes, the two largest deposits in this type (Horne and LaRonde Penna) in the Abitibi region (and worldwide) are located in the BRG (episode 2704-2695 Ma).

The association between VMS deposits and tholeiitic felsic centers long established, recent research in the Abitibi and elsewhere demonstrated the several, and some of the most significant VMS deposits of the ASP are directly associated with or hosted in transitional to calc-alkaline felsic to intermediate volcanic units (Mercier-Langevin et al., 2007; Mercier-Langevin et al., in press).

In the Blake River Group, each time-stratigraphic interval, which corresponds to magmatic episodes, contains at least one significant VMS deposit. The VMS forming events in the BRG occurred approximately every 2 m.y. The BRG is distinct from the other volcanic sequences of the ASP formed in the older volcanic episodes: it has a great variety of volcanic rocks, it is exceptionally rich in metals, and it is characterized by at least four episodes of mineralization formed in a relatively short period of time. Improved understanding and geological modelling of entities such as the BRG and its ore-bearing volcanic units will allow for more effective exploration and target identification on surface and at depth, in the BRG as well as in the ASP, and perhaps elsewhere in Archean greenstone belts.

References

Goutier, J., McNicoll, V., Dion, C., Lafrance, B., Legault, M., Ross, P.-S., Mercier-Langevin, P., Cheng, L-Z., de Kemp, E., and Ayer, J., 2009, L'impact du Plan cuivre et de l'IGC-III sur la géologie de l'Abitibi et du Groupe de Blake River: Extended abstract, Abitibi 2009, MRNF-OGS-GSC, report GM 64195, p. 9-14.

Mercier-Langevin, P., Dubé, B., Hannington, M.D., Richer-Laflèche, M, and Gosselin, G., 2007, The LaRonde Penna Au-rich volcanogenic massive sulfide deposit, Abitibi greenstone belt, Québec: Part II. Lithogeochemistry and paleotectonic setting: Economic Geology, v. 102, p. 611-631.

Mercier-Langevin, P., Dubé, B., Hanninton, M., Monecke, T., McNicoll, V., Gibson, H., Galley, A., Goutier, J., Davis, D., and Bécu, V., 2010, Gold-rich deposits of the Abitibi Greenstone Belt: Distribution, main geological attributes and implications for exploration: Prospectors and Developers Association of Canada Convention, Toronto, March 2010.

Mercier-Langevin, P., Hannington, M., Dubé, B., and Bécu, V., in press, The gold content of volcanogenic massive sulfide deposits: Mineralium Deposita.

Thurston, P. C., Ayer, J.A., Goutier, J., Hamilton, M.A., 2008, Depositional Gaps in Abitibi Greenstone Belt Stratigraphy: A Key to Exploration for Syngenetic Mineralization: Economic Geology, v. 103, p. 1097–1134.

Stratigraphy of the 2720–2710 Ma Kidd–Munro volcanic episode in the Abitibi greenstone belt: implications for base metal mineralization

by

BR Berger[1], P Pilote[2], MG Houlé[3], JA Ayer[1], E Dinel[4] and W Bleeker[3]

Introduction

The Abitibi greenstone belt (AGB) represents a collection of coherent, autochthonous lithostratigraphic packages that are divisible into seven predominantly volcanic and four predominantly sedimentary episodes based mainly on time (Ayer et al., 2005, Thurston et al., 2008). The Kidd-Munro volcanic episode is a predominantly metavolcanic assemblage that was formed between 2720 and 2710 Ma and contains several Cu-Zn VMS and komatiite-associated Ni-Cu-(PGE) deposits including the giant world-class Kidd Creek Volcanogenic Massive Sulfide (VMS) deposit (>150 Mt Cu-Zn ore). Rocks of the Kidd-Munro episode occur scattered throughout the AGB, but the most extensive unit consist of a relatively narrow belt (<25 km wide) over long distance extending >450 km truncated by the Kapuskapsing Structural Zone in the west and by the Grenville Front in the east. The area of focus of this presentation is the prolific base-metal bearing portions extending ~300 km from north of Timmins, Ontario to north of Val D'Or Québec (Figure 1).

Results from recent collaborative mapping and research demonstrate that the Kidd-Munro episode in the study area can be subdivided into 4 ages based on mapping and an intensive campaign of high precision ID-TIMS U-Pb zircon geochronology. These stratigraphic subdivisions are: 2720-2717 Ma, 2717-2715 Ma, 2715-2712 Ma and 2712-2710 Ma (Figure 2). Each age is spatially restricted within the Kidd-Munro episode, has dominant rock types, volcanic morphologies, geochemical affinities and distinctive base metal prospectivity.

[1] Ontario Geological Survey, Ministry Northern Development, Mines and Forestry, Ontario, Canada
[2] Ressources naturelles et Faune, Québec, Canada
[3] Geological Survey of Canada, Canada
[4] University of Toronto, Ontario, Canada

Kidd–Munro volcanic episode

The 2720-2717 Ma age is composed of tholeiitic and transitional mafic, intermediate and rare felsic subaqueous metavolcanic flows and fragmental deposits that are intermixed with each other. Very little komatiite is reported within this cycle and most rocks of this age occur in Québec (Figure 1). Volcanic facies indicate deposition in a subaqueous environment medial to distal from volcanic vents; possibly as an oceanic plateau or back arc basin. Minor base metal mineralization is associated with rocks of this age.

The 2717-2715 Ma age is characterized by a bimodal suite of tholeiitic mafic and high silica felsic metavolcanic flows with lesser pyroclastic deposits; a komatiite suite composed of subvolcanic dikes, sills and thick cumulate textured flows and a transitional suite of mafic, intermediate and felsic metavolcanic rocks (Figure 1). These rocks occur as intercalated units throughout the Kidd-Munro volcanic episode with the greatest concentration in the area of the Kidd Creek base metal deposit. Rare calc–alkalic rocks occur as spatially restricted mafic flows that are intercalated with mafic and intermediate tholeiitic flows.

Tholeiitic felsic metavolcanic rocks of this age are widespread and are host to VMS mineralization such as the giant Kidd-Creek deposit and several smaller occurrences. Mafic magma that was erupted synchronous with the komatiite locally hosts potentially economic copper-zinc VMS mineralization (such as the Potter deposit) and account for over 5 million tons of ore (Préfontaine et al., 2008). This style of mineralization is poorly understood and under explored given that over 80% of the Kidd-Munro episode is composed of mafic metavolcanic rocks. Kambalda style Ni-Cu-(PGE) mineralization (over 500 Kt) occurs in thick komatiite flows/sills within footwall embayments produced by thermo-mechanical erosion and are spatially associated with peperitic komatiitic dikes and sills within this cycle (Houlé et al., 2008). These prospective units appear to be under explored given the extent of komatiite magmatism

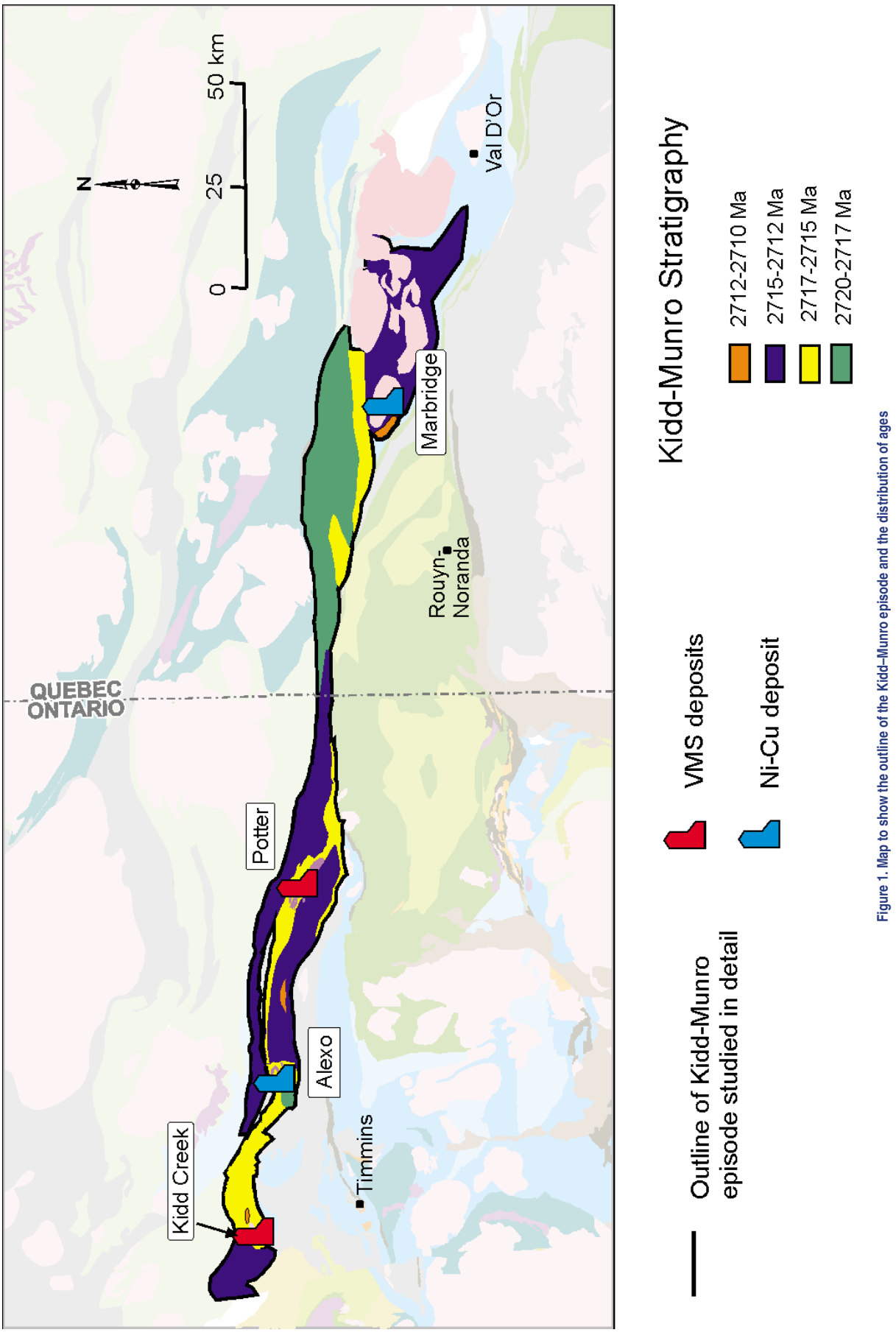

Figure 1. Map to show the outline of the Kidd–Munro episode and the distribution of ages

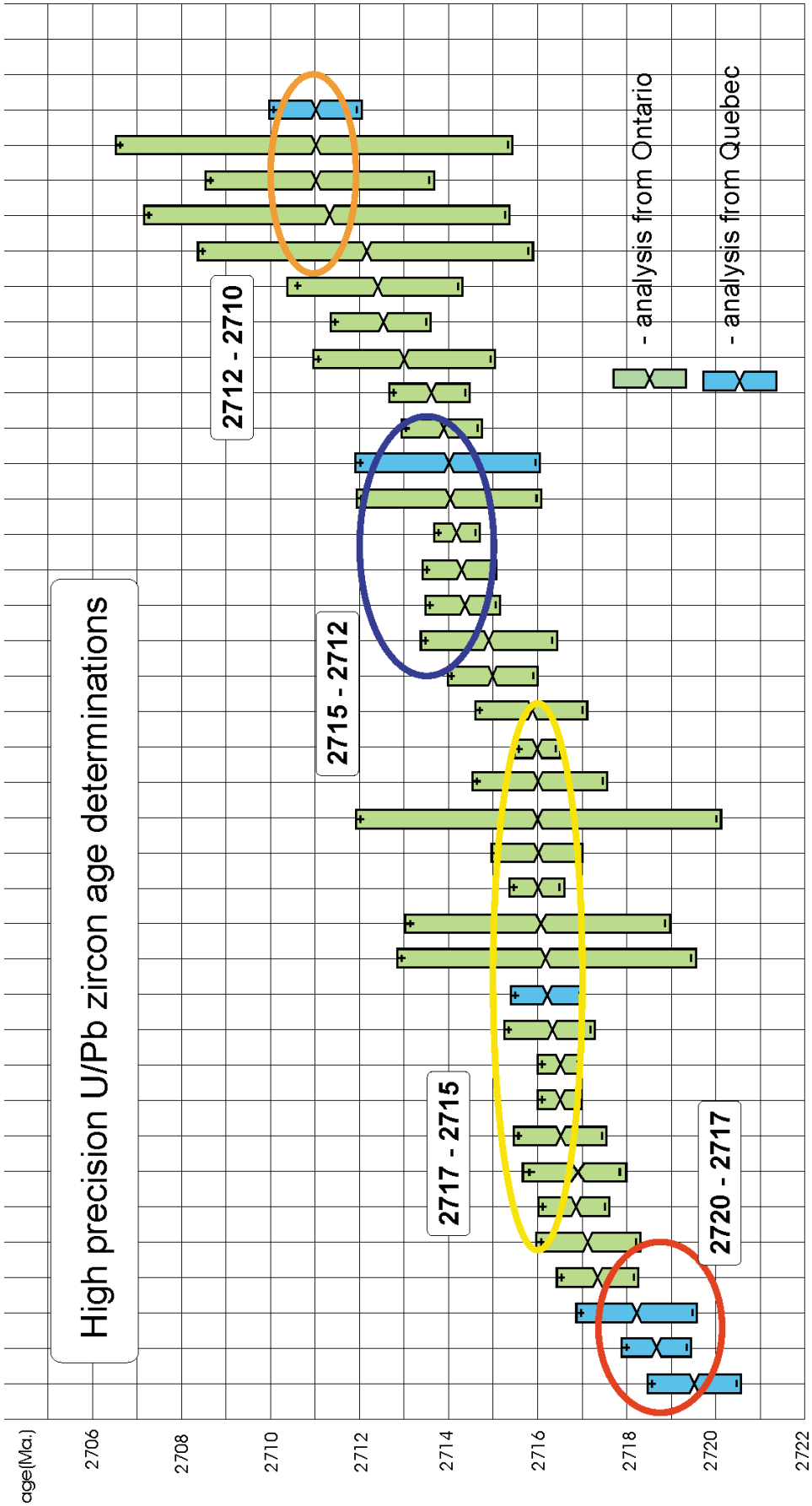

Figure 2. High precision U/Pb zircon age dating techniques were used to define four distinct ages within the Kidd–Munro episode

of this age. The 2717-2715 age is most prospective for base metal mineralization in the Kidd-Munro episode.

The 2715-2712 Ma age is composed mostly of mafic tholeiitic lava flows with subordinate high silica rhyolite sub-volcanic sills, lava flows, autoclastic breccia and tuff (Figure 1). Calc-alkalic andesite and dacite pyroclastic and epiclastic deposits are restricted to a separate sub-unit at this interval but still interpreted to form a single event of volcanism. A second generation of komatiite formed thin organized lava flows typically with cumulate textured bases and spinifex-textured tops. Kambalda-style Ni-Cu-(PGE) deposits (such as the Marbridge deposit in Québec with >700K tons Ni-Cu ore) indicate that the komatiite lava flows at this age are also fertile to hosts nickel sulphide mineralization. Zinc-rich VMS mineralization is hosted in some high silica rhyolite units and calc-alkalic pyroclastic rocks and indicates a second generation of base metal mineralization, albeit minor, occurred within the Kidd-Munro episode.

Rocks of the 2712-2710 Ma age are restricted is a few small areas and are composed mostly of tholeiitic and transitional felsic tuff, flows, epiclastic deposits and reworked metasedimentary rocks (Figure 2). Thin discontinuous, spinifex and cumulate textured basaltic and peridotitic komatiite flows are intercalated with the felsic rocks providing confirmation of a third komatiite generation in the Kidd-Munro volcanic episode. Minor base metal mineralization appeared to be associated with this age.

Geodynamic interpretation

The geologic setting is inferred to be very dynamic between 2717-2715 Ma with invasion of the crust by a mantle plume. The plume initiated rifting at multiple centers that permitted outpouring of extensive thick cumulate textured komatiite lava flows and intrusion of subvolcanic komatiite dikes and sills. The high heat flow that accompanied the mantle plume resulted in subsequent partial melting of older mafic strata thus generating significant amounts of high silica rhyolite (F-III) magmas, and a hydrothermal system resulting in genesis of the giant Kidd Creek VMS deposit, associated with the same rifts that the komatiites exploited. Calc-alkalic volcanism was also initiated at this time either by arc-related subduction or melting of mafic residues at the base of the crust by underplating processes.

The geologic setting, between 2715-2712 Ma, is inferred to involve the interaction of mantle plume and arc — like processes (cf. Wyman et al., 1999). Subduction — like processes were most active with rapid build up of a volcanic pile represented by the calc-alkalic subunit. The mantle plume is inferred to have spread under a thickened crust resulting in a lower volume of high silica rhyolite generated by more widespread and lower heat flow. Rifting of the substrate was restricted to fissures that resulted in venting of less komatiite with more diverse flow morphologies. Retreat of the mantle plume, between 2712-2710 Ma, resulted in cessation of the calc-alkalic volcanism and signalled a more quiescent geologic setting. Residual heat from the retreating plume generated point source felsic volcanic centers and conduits for minor komatiite eruptions. The limited extent of these rocks limits the potential for base metal mineralization at this age.

Implication for base metal deposits

Base metal mineralization includes a variety of felsic metavolcanic hosted copper-zinc VMS deposits formed at or near the ancient sea floor and is directly analogous to "black smoker" base metal mineralization forming in the modern seafloor environment (cf. Franklin et al., 2005). This style of mineralization is characterized by a regional, semi-conformable alteration zone containing greenschist grade minerals such as quartz, epidote, chlorite and sericite and a more proximal alteration zone containing talc, cordierite, garnet, aluminosilicates, carbonate and iron-rich chlorite. Chemical vectors include zones of sodium and calcium depletion and zones of potassium, magnesium and iron enrichment (Hannington, 2007). The Kidd Creek deposit is exceptionally large and displays many of the typical features of VMS mineralization and was formed in a graben environment dominated by komatiite flows in the footwall (Bleeker, 1999). The high heat associated with generation of komatiite magmas may play a crucial role in the genesis of Archean VMS deposits. Other high silica rhyolite units of the 2717-2715 age are prime targets for additional discoveries of VMS mineralization.

Although the presence of felsic metavolcanic rocks is important, they are not essential for VMS mineralization in the Kidd-Munro episode. Mafic and ultramafic metavolcanic hosted copper-zinc mineralization such as the Potter Mine is a subordinate, but economically important, type of VMS deposit within the Kidd-Munro volcanic episode. This style of mineralization also formed at or near the seafloor; however, alteration patterns and mineralization are less well understood but are distinctive from the felsic metavolcanic hosted VMS deposits (Préfontaine et al., 2008). The potential for new VMS discoveries of this type is largely untested in the Kidd-Munro episode.

Kambalda-style nickel-copper mineralization is associated with komatiites at 2717-2715 Ma and 2715-2712 Ma in the Kidd-Munro volcanic episode (Houlé et al 2008; Pilote et al., 2009). This type of mineralization is typically composed of massive and net textured sulfides with high nickel grades but low tonnage. However, stacked ore lenses, multiple vent areas and mineralization associated with synvolcanic sills increase the overall potential for economic nickel deposits in the Kidd-Munro volcanic episode.

Conclusion

High precision ID-TIMS U-Pb zircon geochronology combined with detailed and regional geologic mapping has resulted in a better understanding of the internal stratigraphy of the Kidd-Munro volcanic episode in the AGB. Four ages are recognized and each is spatially restricted, has dominant

volcanic morphologies, geochemical affinities and different base metal potential. VMS mineralization at the 2717-2715 Ma age is hosted in felsic and mafic metavolcanic rocks associated with mantle plume derived komatiites that were deposited in graben or rift environments. Kambalda-style nickel mineralization is most prospective in two of the ages of komatiitic magmatism. New opportunities for base metal exploration are identified by the study.

References

Ayer, J.A., Thurston, P.C., Bateman, R., Dubé, B., Gibson, H.L., Hamilton, M.A., Hathway, B., Hocker, S.M., Houlé, M.G., Hudac, G., Ispolatov, V.O., Lafrance, B., Lesher, C.M., MacDonald, P.J., Péloquin, A.S., Piercey, S.J., Reed, L.E. and Thompson, P.H. 2005. Overview of results of the Greenstone Architecture Project: Discover Abitibi Initiative: Ontario Geological Survey, Open File Report 6154, 146p.

Bleeker W., 1999. Structure, Stratigraphy, and Primary setting of the Kidd Creek volcanogenic massive sulphide deposit: a semiquantitative reconstruction: Economic Geology Monograph 10, The Giant Kidd Creek Volcanogenic Massive sulphide Deposit, Western Abitibi Subprovince, Canada, pp. 71-122

Franklin, J.M., Gibson, H.L., Galley, A.G. and Jonasson, I.R, 2005. Volcanogenic massive sulfide deposits; Economic Geology, 100th Anniversary Volume.

Hannington, M., 2007. Hydrothermal Ore Deposits: University of Ottawa/ Laurentian University, modular course on Submarine Hydrothermal systems and VMS deposits, February 17-24, 2007.

Houlé, M.G., Gibson, H.L., Lesher, C.M., Davis, P.C., Cas, R.A.F., Beresford, S. W. and Arndt, N. T., 2008. Komatiitic sills and multigenerational peperite at the Dundonald Beach, Abitibi Greenstone Belt, Ontario: Volcanic architecture and nickel sulphide distribution: Economic Geology, v. 103, pp. 1269-1284.

Pilote, P., McNicoll, V., Daigneault, R. and Moorhead, J. 2009. Géologie et nouvelles corrélations dans la partie ouest du Groupe de Malartic et dans le Groupe de Kinojévis, Québec: Congrès Abitibi 2009 du 28 Septembre au 2 Octobre 2009, Abitibi Cuivre — programme de conférences, p. 55-59.

Préfontaine, S, Gibson, H. L., Houlé, M. G., Mercier-Langevin, P. and Gamble, A.D.P., 2008. Project Unit 08-022. Preliminary Results of the Alteration and Mineralization Study of the Potter Mine, Munro Township, Abitibi Greenstone Belt; Summary of Field Work and other Activities 2008: Ontario Geological Survey, Open File Report 6226, p. 9-1 to 9-5.

Thurston, P.C., Ayer, J.A., Goutier, J., and Hamilton, M.A. 2008. Depositional gaps in Abitibi greenstone belt stratigraphy: A key to exploration for syngenetic mineralization: Economic Geology, v. 103, p. 1097 – 1134.

Wyman, D.A., Bleeker, W. and Kerrich, R., 1999. A 2.7 Ga komatiite, low Ti tholeiite, arc tholeiite transition, and inferred Proto-arc geodynamic setting of the Kidd Creek deposit: evidence from trace element data: Economic Geology Monograph 10, The Giant Kidd Creek Volcanogenic Massive sulphide Deposit, Western Abitibi Subprovince, Canada, pp. 511-528.

Yilgarn volcanogenic massive sulphides

by

Susan Vearncombe[1]

The Yilgarn is 750,000 km^2 of meta-volcanic and meta-sedimentary rocks, gabbros, and granites formed between 3.05 and 2.6 Ga. The Yilgarn is a major producer of gold and nickel ores, to a lesser extent but with increasing emphasis, iron ore, vanadium, uranium and volcanogenic massive sulphides; the latter rarely rates a mention.

Canada is well endowed with VMS deposits that vary in style, age and size. This includes Archaean-age VMS camps whereas in contrast, the Yilgarn is struggling to make its mark. We can count on one hand the VMS 'camps' discovered, namely the Youanmi Terrane (4) and the Gindalbie Terrane (3). Why? Is the Yilgarn prospective for VMS? If yes, are we approaching our search the right way? Is the paucity of VMS deposits a function of knowledge and commitment?

Canadian Archaean VMS environments are commonly used as reference regions for VMS deposits elsewhere. After all, this is where much of the literature describing such systems is derived. Comparisons are great, so long as we appreciate that perhaps the Yilgarn and the Canadian counterparts are not directly comparable/transposable. The Yilgarn Craton has its own unique set of conditions and issues when it comes to exploring for VMS deposits. Some of the research has tended to make direct comparisons and emphasize reasons for the lack of endowment here. There are plenty of reasons to believe that we should be more positive regarding VMS potential in the Yilgarn. Perhaps there is a more positive way in which we can drive our science.

***Corporate mindsets that have hindered the Yilgarn VMS search*:**

- deposits viewed as too small, take too long to get into production
- too small for large companies
- too slow and expensive for small companies
- difficult to 'get off the bench' as there is little support for greenfields exploration
- gold in particular, and nickel are viewed as a faster avenue to production
- terrane-scale research sends negative or inconclusive conclusions
- lack of understanding of VMS, unwillingness to step off the treadmill and out of the comfort zone.

In consequence, very few companies have VMS as part of their dedicated metal search.

***Yilgarn geological VMS issues*:**

- deep weathering profiles commonly to +100 m depth
- deformation state, structural overprinting and disruption
- lack of outcrop
- problems extrapolating stratigraphy which herald difficulties in the current understanding of litho-stratigraphy in these terranes
- age dating of rocks is improving all the time, but there is not enough. Stratigraphic correlation is unreliable over relatively short distances
- electromagnetics is an excellent aid but not a panacea. Major hindrances to EM surveys include large tracts of saline ground/groundwaters, deep weathering profiles up to 200 m depth, conductive cover sequences including transported cover, conductivity dependent upon Cu–FeS (copper–pyrrhotite) bodies, graphitic sequences, and it is expensive
- transposing directly Canadian parameters to the Yilgarn isn't working.

***VMS prospectivity in the Yilgarn*:**

Volcanogenic massive sulphide deposits in the Yilgarn are located in the Murchison Province of the Youanmi Terrane (Golden Grove, ?Mt Gibson, Austin, Just Desserts) and the Gindalbie Terrane (Jaguar / Teutonic Bore / Bentley).

These deposits share many similar characteristics — Cu–Zn type, bimodal mafic; Pb does not feature significantly and, excepting at Golden Grove, Pb tends to remain unreported. There is no Pb associated with the Austin and Just Desserts deposits. Just Desserts does not report Zn and is a Cu–Au deposit (D. Sargeant, pers comm).

Chemically from rare earth and extended trace element analyses, Golden Grove and Austin, including the greater Quinns region that hosts Austin can be interpreted to fall within an intra-oceanic rifted arc setting, transitional to a continental margin arc (Kerrich, 2009a, b). There is no

[1] Silver Swan Group Limited, email: susan@silverswangroup.com.au

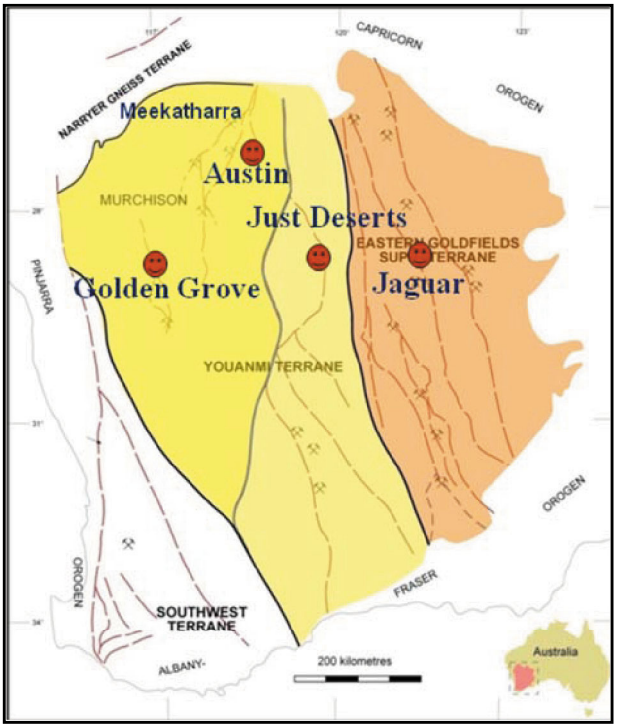

Figure 1.

chemical information on the volcanic sequence hosting the Just Desserts deposit. However, it is likely to sit within the same setting based on the age and relationship to the Youanmi intrusion (Ivanic et al., 2010). On Tb/Yb vs Nb/Yb and Ce/Nb vs Th/Nb diagrams, Golden Grove and Austin plot nicely along the same trend from a back-arc to a continental margin arc setting. Jaguar/Teutonic Bore is also indicative of a rifted system, albeit crossing an interpreted terrane boundary. The Melita volcanic complex hosting Jaguar has been interpreted variously as a back-arc, proto-arc to evolved arc, intra-arc and rifted marginal arc. Nd-isotopes values from Golden Grove and Teutonic Bore also support zones of rifting, e.g. Pb from sulphide ores at Teutonic Bore are isotopically primitive (Huston et al., 2005), and both are associated with juvenile crust (Cassidy et al., 2005; Huston et al., 2005). Similarly, the Yandal Belt, which hosts the northern felsic extensions to the stratigraphy at Teutonic Bore, has been interpreted to represent the northern part of a relict N–S oriented arc – back-arc system (Messenger, 2000). This further extends the existence of rifted sequences in the Eastern Goldfields.

Were they all related once? There is a circa 250 Ma period from Golden Grove (2.95 Ga; Wang et al., 1998) eastward to Austin and Just Desserts (2.82 Ga; GSWA unpubl.) and eastward to Jaguar (2.69 Ga) — see Figure 1. But all could sit nicely within a modern day Sea of Japan oceanic arc to continental margin arc setting (Fig. 2).

The VMS deposits of the Murchison, and the Gindalbie Terrane potentially highlight a once substantial extensional system(s) several hundred kilometres in width capable of hosting numerous VMS camps. These areas remain largely unexplored for VMS deposits: but they will be buried deposits?

The Lady Alma igneous 'intrusion' is a layered ultramafic-mafic complex several hundred metres thick and lies about 20 km NE of Quinns. Quinns volcanic stratigraphy, hosting the Austin VMS deposit, can be traced to the hangingwall position of complex. However, intrusive relationships to the volcanic sequence are not apparent and trace element geochemistry from the intrusion records evidence for intense hydrothermal alteration by reduced, evolved-seawater, and hydrothermal fluids, indicative of a subvolcanic intrusive setting at <4 km crustal depth (Kerrich, 2009c). A similar relationship can be seen at Barrambie and Youanmi in which the 'intrusion' is contemporaneous with the overlying volcanic sequence.

Are the hangingwall volcanic sequences to these complexes prime targets for VMS mineralisation? Do they represent Neoarchean analogues such as the ultramafic-mafic Kidd volcanic complex, hosting the Kidd Creek VMS deposit, or the Bell Allard gabbro–anorthosite complex, subjacent to the Matagami VMS camp? We believe there is such a connection

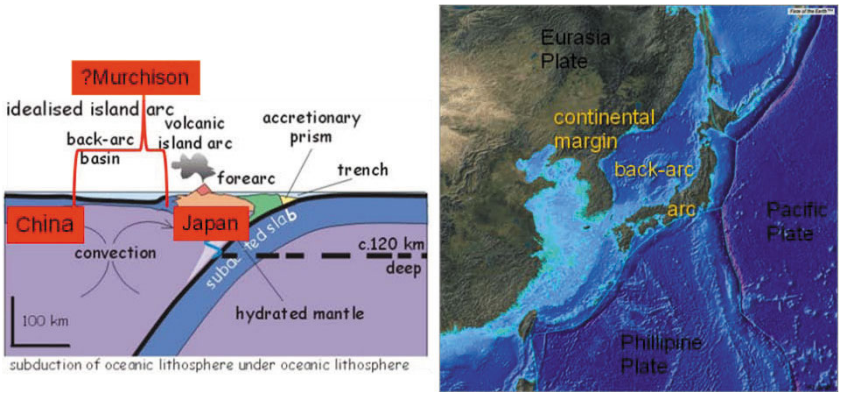

Figure 2. Murchison geodynamic setting: Sea of Japan equivalent?

Yilgarn Craton examples	*Classification*	*Style*	*Combined total resource*	*Age*
Teutonic Bore	Bimodal-mafic	Cu-Zn	1,554,000 t @ 1.6% Cu,` 3.1% Zn, 49 g/t Ag	2.69-2.68 Ga
Jaguar	Bimodal mafic	Cu-Zn	2,551,000 t @ 2.4% Cu, 5.6% Zn, 78 g/t Ag	2.69-2.68 Ga
Bentley	Bimodal-mafic	Cu-Zn-Pb	2,303,000 t @ 1.8% Cu, 9.8% Zn, 0.6% Pb, 121 g/t Ag	2.69-2.68 Ga
Golden Grove (Gossan Hill and Scuddles)	Bimodal-mafic	Cu-Zn	Remaining combined resource ?19 Mt @ 2.8% Cu, 0.2% Zn, 10.9 g/t Ag	2953±7 Ma -2945±4 Ma
Austin	Bimodal mafic Basalt-rhyolite	Cu-Zn	1,484,241 t @ 1.02% Cu, 1.41% Zn, 3.51 g/t Ag	2817±3 Ma (Lady Alma igneous complex 2821±5 Ma)
Just Desserts	Tuffs, ? rhyolite	Cu-Au	1,070,000 t @ 1.82% Cu, 0.78 g/t Au	(Youanmi igneous complex 2814±14 Ma)

between the Austin VMS deposit, the Quinns stratigraphy and the Lady Alma 'intrusion'. Such areas elsewhere have not been considered for VMS potential.

Useful exploration methodologies:

- *Rare earth (REE) and extended trace element geochemistry* — it works and is not expensive, although dependent upon outcropping rock and drillhole material.
- *Geophysics* — an essential part in the search for VMS discovery, particularly VTEM, MLEM and DHEM. MLTEM and FLTEM appear to have depth limitations particularly where mineralization is likely to be steeply dipping. It is dependent upon good conducting material — pyrrhotite-chalcopyrite.
- *Groundwater* — there are changes in groundwater signatures regionally, but this science currently is too broad to be useful in locating VMS deposits. Not aware of any literature that looks at groundwater at the camp-scale of VMS.
- *Bioleaching* of surface material tracking metals transported via fluctuations in the water table — Austin — see through 60 m of transported cover.
- More geochronology and stratigraphic correlations required.
- Large regional VTEM surveys required.

Conclusion

There is potential for more VMS camps in the Yilgarn. Deposits will be buried, hence harder to find. They require commitment, good quality geology and understanding of the larger geological picture. The volcanic sequences across the Murchison and across many areas of the Eastern Goldfields are poorly constrained. Research covering the various facets required to evaluate prospectivity for VMS camps in the Yilgarn is patchy. There are some really good research papers related to geodynamics and VMS mineralization but they exist in isolation. Continuity of this research is desperately required. We simply do not have the data to "write the Yilgarn off" in terms of potential size of VMS endowment. VMS present an excellent challenge across many facets of geology — this is what makes them so interesting. At the moment there are too few willing to take that challenge.

References

Cassidy, K.F, Champion, D.C and Huston, D.L. 2005, Crustal evolution constraints on the metallogeny of the Yilgarn Craton. *in* Mineral deposits research: Meeting the global challenge *edited by* J. Mao and F.P. Bierlein: Berlin, Springer-Verlag, p. 901–904.

Huston, D.L., Champion, D.C and Cassidy, K.F. 2005, Tectonic controls on the endowment of Archean cratons in VHMS deposits: Evidence from Pb and Nd isotopes. , *in* Mineral Deposit Research: Meeting the Global Challenge *edited by* J. Mao and F. P. Bierlein: Proceedings of the Eighth Biennial SGA Meeting, Beijing, China, 2005, Berlin/Heidelberg, Springer, p. 15–18.

Ivanic T.J., Wingate, M.T.D., Kirkland, C.L., Van Kranendonk, M.J and Wyche, S. 2010, Age and significance of voluminous mafic-ultramafic magmatic events in the Murchison Domain, Yilgarn Craton: Austr. Jn Earth Sciences v. 57, 5, 597–614.

Kerrich. R., 2009a, Austin Cu–Zn VMS Deposit Murchison Province, Australia: Report to Silver Swan Group by OreGeodynamics Inc., January 2009 (unpublished).

Kerrich. R., 2009b, Geochemistry of the Andalusite-Schists and Felsic Volcanic Sequence, Quinns, Meekatharra, Western Australia: Implications for VMS Mineralization and Intercomparisons with Austin and Yagahong: Report to Silver Swan Group by OreGeodynamics Inc., April 2009 (unpublished).

Kerrich. R. 2009c, Geochemistry of the Copper Hills-Yagahong Intrusive Complex, Murchison Province, Australia. Implications for Ni-Cu±PGE and VMS Mineralization: Report to Silver Swan Group by OreGeodynamics Inc., February 2009 (unpublished).

Messenger, P.R. 2000, Geochemistry of the Yandal belt metavolcanic rocks, Eastern Goldfields Province, Western Australia: Austr. Jn Earth Sciences v. 47, 6, 1015–1028.

Wang. Q. Schiotte, L. and Campbell, I.H. 1998, Geochronology of supracrustal rocks from the Golden Grove area, Murchison Province, Yilgarn Craton, Western Australia: Austr. Jn Earth Sciences v. 45, 4, 571–577.

Gold systems in the eastern Yilgarn Craton: scale-integrated signatures and targeting criteria

by

KF Cassidy[1]

Introduction

Poorly exposed Neoarchean granite-greenstone terranes of the eastern Yilgarn Craton include some of the world's most highly-mineralized belts hosting world-class gold deposits (Robert et al., 2005). In general, models for such deposits have emphasised a number of empirical relationships, including proximity to major fault systems, flexures along and intersections of subsidiary faults with the fault systems, modelled areas of dilatancy and importance of specific host lithologies, with models showing increasing sophistication over the past twenty five years (Groves et al., 2003). Empirical observations, such as 'every 30 km along major fault zones' or 'within 1 km of unconformity with late basins', many of which have been estabished for over twenty years (e.g., Hall, 2007), reflect physical attributes of complex systems and continue to provide practical exploration criteria to mineral explorers. Such empirical relationships formed input parameters to GIS-based prospectivity studies without providing either an increased understanding of the complex systems responsible for gold deposition or any substantive predictive capability in areas with limited information (Bierlein et al., 2007).

Over the past ten years there has been increasing realization that gold deposits are end products of much larger-scale systems of energy and mass flux (Hronsky and Groves, 2008). Gold systems are scale-dependent with some factors apparent at lithospheric-scale whereas other factors are important at terrane-, camp- and (intra-) deposit-scale. The acquisition and interpretation of new and enhanced geological, geochemical and geophysical datasets is permitting delineation of critical processes at the lithospheric-, terrane- and camp-scale as well as processes active at the site of deposition (Blewett et al., 2008). This realisation is leading to improved predictive capability at the terrane to camp-scale, although has not led to significant improvement in the detection of mineralised systems at the intra-camp scale. In particular, enhanced acquisition and interpretation of regional geophysical datasets (seismic reflection, receiver function, magneto-telluric, inversion of potential fields) have provided whole of crust imaging providing constraints on influence and impact of continental lithospheric mantle and lower crustal features (Blewett et al., 2010). In addition, improvements to existing and emerging technologies, including geochronology, lithogeochemistry, hyperspectral datasets (HyLogger, HyMap), and numerical modelling, have allowed better spatial and temporal constraints on the 'footprint' of hydrothermal fluid flux responsible for ore deposition (Halley, 2007; Potma et al., 2007; Vielreicher et al., 2010).

Detailed regional studies, including geochronological and geochemical studies of felsic and mafic lithologies, tectonostratigraphic analysis of volcano-sedimentary sequences, complex metamorphic histories, have provided base-line craton-scale representations of the complex punctuated evolution of the granite-greenstone terranes that make up the craton (Cassidy et al., 2002; Barley et al., 2003; Czarnota et al., 2008; Goscombe et al., 2009). Advancements in the application of geochronological techniques have led to recognition of multiple gold events (e.g., Kalgoorlie gold camp: Vielreicher et al., 2010) over a short time period that overlapped with and continued after intrusion of mantle-derived 'Mafic' granites and a period of (trans-)extension responsible for deposition of fault-bound siliciclastic sequences (Czarnota et al., 2008).

Notably, the critical lithospheric- and terrane-scale factors now clearly established for gold systems in the eastern Yilgarn are consistent with features that control gold systems in other Archean terranes (e.g., Superior and Slave provinces of Canada: Robert et al., 2005; Bleeker and Hall, 2007). In addition, although similarities between the 'giant' Kalgoorlie and Timmins gold camps have been recognised for decades, contextual placement of such gold camps within their host terranes, and the highly-endowed host terranes within cratons, has led to a greater understanding of the development of gold systems and their relationships to lithospheric- to terrane-scale processes.

Emphasis in this contribution is placed on the lithospheric-, terrane- and camp-scale features of gold systems in the eastern Yilgarn Craton that provide criteria to develop predictive targeting models. Use of these scale-dependent

[1] Bare Rock Geological Services, Fremantle, WA, 6160, and School of Earth and Environment, The University of Western Australia, Nedlands, WA, 6009

features has the potential to result in more effective targeting through iterative area reduction and consequently to mineral exploration success. Additional challenges exist at the intra-camp-scale, where direct detection of mineralisation competes with prediction (Hronsky and Groves, 2008). Advances in the understanding of gold systems at the intra-camp-scale have not resulted in greatly improved predictive capability, with use of traditional and evolving detection technologies more appropriate at this scale.

Gold systems — scale-dependent features

Lithospheric-scale

At the lithospheric-scale, there is increasing recognition of the role of subcontinental lithospheric mantle (SCLM) in the formation of gold systems in Archean provinces. Ground-breaking research on the architecture and history of SCLM across the globe suggests that lithospheric mantle domains strongly influence the generation of major mineral systems (Begg et al., 2009), with the edges of lithospheric domains providing zones of focussed strain and passage of mantle-derived magmas and fluids. In a review of lithospheric controls on gold-rich provinces, Bierlein et al. (2006) suggest that gold endowment is likely related to the conjunction of periods of rapid growth of continential crust and associated mantle instability, intrinsically thin or thinned lithosphere prior to episodes of gold mineralisation and location of major (terrane-scale) fault zones. The Yilgarn Craton contain elongate terranes that show evidence for unique conjunction of these primary factors. The architecture of the lithospheric mantle to the Yilgarn Craton, primarily interpreted from mantle tomography, magneto-telluric profiles and geochemistry of mantle xenoliths, has resulted in a delineation of domains with lithospheric-scale anomalies spatially coincident with the highly-endowed terranes in the eastern Yilgarn (Blewett et al., 2010).

In the eastern Yilgarn Craton, there is abundant evidence for a thin or thinned crustal lithosphere just prior to the major gold mineralisation event(s). Geochemistry, geochronology and Sm-Nd and Lu-Hf isotopic data from Yilgarn felsic magmatic rocks (Cassidy et al., 2002; Champion and Cassidy, 2008), in conjunction with detailed greenstone studies (Barley et al., 2003), indicate that the bulk of the craton can be subdivided into two major provinces — an older (>2.8 Ga) craton nucleus, the Youanmi Terrane, and a collage of broadly younger terranes in the east — the Eastern Goldfields Superterrane (EGST). Gold mineralisation occurs in all terranes across the Yilgarn Craton, however, the majority of the gold endowment is spatially restricted to the Kalgoorlie and the eastern Kurnalpi Terrane in the EGST and an elongate domain of the central Youanmi Terrane (i.e. areas underlain by crust with Nd depleted-mantle model ages of 2.95-3.1 Ga: Cassidy et al., 2005; Champion and Cassidy, 2008). In the EGST, at least, there is little significant gold mineralization in domains (western Kurnalpi Terrane) with the most juvenile signatures. The highly-endowed EGST, in particular the Kalgoorie Terrane, possibly represents a pericontinental rift margin with thinned lithosphere that was the site of subsequent 2.75 to 2.67 Ga plume- and arc-related magmatism (Czarnota et al., 2008).

Komatiites have long been recognized as noble metal rich and are a possible source for gold (Hodgson, 1993). A by-product of such magmatism may have been primary gold enrichment of the lithosphere. Re-melting of metasomatized mantle, developed by either hot upwelling of asthenospheric mantle or related to slab dehydration in a back-arc environment produces fertile material that may retain high metal contents particularly where there has been interaction with concurrent or previous plume-magmatism (McInnes et al., 1994). The Kalgoorlie and eastern Kurnalpi terranes contain abundant mafic-ultramafic volcanic rocks, and in particular komatiites. In contrast, the more juvenile belt in the western Kurnalpi Terrane contains abundant high-Mg basaltic rocks and limited komatiites and has the smallest gold endowment (Cassidy et al., 2005). Differences in the source composition and temperature and depth of mantle melting controls the type of ultramafic magma generated and may be important for gold endowment. A corollary to models in which the presence of komatiitic volcanism is intrinsically important to gold endowment is that the while the well-endowed Abitibi subprovince, Superior Province, contains significant thicknesses of komatiites, the MgO content of the parent ultramafic magmas is lower in komatiites in the Abitibi subprovince than that for komatiites in the Kalgoorlie Terrane (Barnes et al., 2007).

The Kalgoorlie and Kurnalpi Terranes contain abundant 2.66-2.64 Ga sanukitoid-like 'Mafic' and syenitic granites derived from metasomatized or subduction-modified mantle (Cassidy et al., 2002; Champion and Cassidy, 2008). In contrast, there is limited evidence for this type of magmatism in less mineralized parts of the Yilgarn Craton. Importantly, generation and emplacement of sanukitoid-like magmatism in the Yilgarn Craton, in association with discrete episodes of crustal extension is important in understanding the fertility of the major gold belts in Archean cratons. The generation of the sanukitoid-like felsic-intermediate magma component likely involved the melting of a small amount of Archean SCLM that had been previously metasomatized and enriched in large ion lithophile elements, metals and sulfur (Stern et al., 1989). Lithospheric structures are likely to have served as conduits for felsic to lamprophyric, calc-alkaline magmas during a short-lived event associated with extension and deposition of the late basins. Gold potential was likely enhanced where late to post accretionary fluid events exploiting lithospheric-scale plumbing systems were able to interact with the gold-rich lithospheric ource rocks.

Terrane-scale

At terrane-scale, highly-mineralized gold belts are confined to fault-bounded crustal domains containing thin (<7 km) greenstone sequences with abundant komatiites. Geophysical techniques, in particular seismic reflection and magneto-telluric studies, outline the location and architecture of

major fault systems and delineate the structural connectivity between mantle and crustal features (Blewett et al., 2010). Such fault systems are likely pathways for mantle-derived and deep-crustal fluids and magmas. Interpretation of seismic reflection data is consistent with chemical alteration associated with enhanced fluid flow along the interpreted major fault systems as well as the presence of large zones of possibly pervasively altered rock in the lower/mid-crust below some of the major fault systems (Chopping, 2008).

In general, terrane-bounding fault systems (e.g., Ida, Ockerburry, Hootanui: Blewett and Czarnota, 2007), unless reactivated during gold-related deformation events, are poorly mineralized. Controlling structures are domainal (e.g., Boulder-Lefroy, Zuleika, Waroonga in Kalgoorlie Terrane) with location of gold camps generally predictable along the fault systems (Weinberg et al., 2004). For instance, Weinberg et al. (2004) demonstrate the gold camps within terranes are localised along segments of the domain-bounding fault systems with the greatest deviation from the regional trend. Gold camps are regularly spaced at approximately 30-35 km along the domain-bounding fault systems (Hall, 2007), which is interpreted to reflect the efficiency of gold systems (Weinberg et al., 2004). On a practical level, the domain-bounding fault zones are defined by areally-significant, pervasively altered rocks, which are geochemically recognised by higher concentrations of H_2O and CO_2 relative to less altered regions (Goscombe et al., 2009).

The recognition of specific granite types and their evolution through the 2680 Ma to 2620 Ma interval in the eastern Yilgarn Craton has helped to better appreciate the role of granites and associated fluids in the location and evolution of gold systems (Champion and Cassidy, 2008). Fault systems active immediately prior to and during gold mineralising events generally contain mantle-derived felsic/intermediate intrusions (sanukitoid-like 'Mafic' granites, syenitic intrusions, lamprophyres). Such intrusions have geochemical characteristics that are spatially-restricted to specific fault systems (Smithies and Champion, 1999; Cassidy et al., 2002). For instance, sanukitoid-like 'Mafic' granites and syenitic intrusions associated with fault systems in the southern Kalgoorlie terrane are generally Ba- and Sr-enriched with respect to similar suites associated with fault systems in the Kurnalpi and northern Kalgoorlie Terranes (Cassidy et al., 2002). This LILE-enriched chemistry likely reflects enriched mantle source features, and may be significant in that the southern Kalgoorlie terrane has the highest gold endowment. Connectivity of the domain-bounding faults systems and camp-scale subsidiary fault zones are critical in transferring magmas and fluids to higher structural levels.

Key studies within the seven-year research program of the pmd*CRC have led to new geodynamic, structural and metamorphic histories for the eastern Yilgarn (Blewett and Czarnota, 2007; Czarnota et al., 2008; Goscombe et al., 2009). A number of results are directly relevant to gold systems. Firstly, is the recognition of discrete episodes of extension during a sixfold (D_1–D_6) deformation framework (Blewett and Czarnota, 2007). In particular, an episode of ENE-WSW-directed extension (D_3 of Blewett and Czarnota, 2007) resulted in lithospheric extension and core complexes. A series of extensional shear zones and development of domal features established the gross architecture (granite cored domes and synclinal greenstones) of the region. It was this architecture that was inverted during two subsequent contractional deformation events (D_4 and D_5: Blewett and Czarnota, 2007). Although gold mineralisation was associated with each of these deformation events, the major gold events post-date the D_3 orogenic extension (Czarnota et al., 2008). The first of these deformation events involved regional E-W directed transpression that folded the 'late basins' and developed NNW-striking, sinistral strike-slip faults that are related to gold mineralisation in the Golden Mile and St Ives gold camps.

Secondly, syntectonic siliciclastic basins, referred to as 'late basins', are associated with the D_3 extension event. The development of the 'late basins' is contentious, with both strike-slip (Krapez et al., 2008) and extensional graben (Blewett and Czarnota, 2007) models proposed. Irrespective of geodynamic model for their development, the 'late basins' represent an episode of deposition that is unconformable and/or in fault contact with pre-folded older volcanic-dominated sequences, and provide a terrane-scale rock package that may have acted as a regional 'seal'. The spatial and temporal conjunction of major structures, 'late basins', and mantle-derived 'Mafic' granites and syenites, with linear, (now 'uplifted') basal parts of the greenstone belts (e.g. St Ives and Kalgoorlie gold camps), is a natural consequence of the juxtaposition of these basal and upper parts through extension and rapid inversion/transpression.

Thirdly, are the findings of detailed studies of the metamorphic history of the eastern Yilgarn Craton (Goscombe et al., 2009). The critical elements of this ground-breaking study highlight discrete metamorphic events (M1, M2, M3) characterised by differences in thermal gradient, peak temperatures and pressures and linked to regional compressional (M2) and extensional (M1 and M3) events. The M2 metamorphism overlaps with emplacement of the volumetrically abundant 'High-Ca' granites and D_2 regional folding, with devolatilisation of the greenstone belts likely peaking during this metamorphic event. Metamorphic fluid produced during the M2 event would have been expelled from the crust quickly (about 2 m.y.), which is certainly outside the mineralization window in the eastern Yilgarn Craton which is 10 to 20 m.y. later than this principal metamorphic event (Goscombe et al. 2009), suggesting that unless the M2 fluids were "trapped and stored" and later released they were not involved in the gold mineralization process. The D_3-related 'late basins' and extensional shear zones record metamorphic PTt paths, that define a M3a metamorphic event, that are characteristic of lithospheric extension (Goscombe et al., 2009). High heat flow likely peaked during the M3b event associated with the switch from D_3 extension to transpressional deformation (D_4 and D_5), and is thought to have been driven by the dehydration of hydrous minerals in 'late basins' (Goscombe et al., 2009). The major episodes of gold mineralisation are also associated with the high geothermal gradient M3 event, which likely contributed fluids to the mineralisation events.

Camp-scale

At camp-scale, larger gold camps (Kalgoorlie, Kanowna Belle, St Ives, Wallaby) are spatially associated with domal or anticlinorial structures (Blewett et al., 2008; Davis et al., 2010), with deposits hosted in structures subsidiary to domain-scale faults and displaying evidence of multiple ore-related fluids (St Ives: Neumayr et al., 2008). Late-stage breaches of the domes during basin inversion and subsequent contractional deformation may have allowed gold-bearing fluids either generated during high geothermal gradient metamorphism associated with extension or stored within the domical structures to migrate higher along formed or reactivated structures in the crust.

Gold camps have a complex and long-lasting structural history with domes, domain-bounding fault zones and their subsidiary structures being the key structural elements. The early rift architecture associated with initial greenstone development was likely controlled by pre-existing basement boundaries, and may have had a major influence on the geometry of fault zones and associated folds generated during subsequent deformation events, e.g., early extension, regional folding, late extension and strike-slip deformation (e.g. St Ives: Miller et al., in press). Strike-changes on major faults in many cases correlate with early basin structures, which through reactivation can control gold mineralization (Weinberg et al., 2004; Miller et al., in press). The changes in strike can correlate with dilational and contractional jogs, overstepping faults, and/or intersecting faults all of which represent significant fault perturbation in segments of these faults and locally host gold mineralisation. These areas are also the focus for ascending magmas as evidenced by the widespread location of 'Mafic' granite, syenites and lamprophyre intrusions in these segments of the fault zones. In essence, the application of structural analysis (Miller et al., 2007) to predict possible target zones remains the primary technique used to delineate drill targets.

In the Laverton gold belt in the eastern Kurnalpi Terrane, gold deposits are associated with domain-scale fault systems form linear trends and cluster-like distribution. It is interpreted that strike-slip ruptures can repeatedly trigger restricted clusters of aftershocks that delineate pipe-like domains, whereas thrust or reverse ruptures trigger continuous, diffuse domains of aftershocks along the entire strike-length of the rupture (Micklethwaite, 2007). Furthermore, ruptures along regional strike-slip faults are able to trigger ruptures on pre-existing thrust faults at the deposit-scale which, in turn, generate an increase in permeability with fluid flow paths to be highly complex thereby increasing fluid-rock interaction or potential fluid mixing.

The definition of camp-scale hydrothermal 'footprints' of gold systems using multispectral analyses including Aster, HyMap and PIMA/ASD spectra from diamond core or bottom-of-hole samples, has allowed a better understanding of the location and role of discrete flow episodes of hydrothermal fluids. Reduced and oxidized sulfide-oxide mineral assemblages are used to delineate distinct hydrothermal alteration systems, which are interpreted to map camp-scale fluid pathways, with high redox gradients marking the location of high-grade gold mineralization (e.g., Kanowna Belle, St Ives: Neumayr et al., 2008). It is important to note, in this context, that the recognition of different redox minerals or hydrothermal fluids does not necessarily imply that these fluids or precipitation of redox minerals were necessarily 'active' at the same time.

Recent development of three-dimensional (3D) camp-scale maps have been useful to delineate targets at depth. This will be even more significant in the future as the majority of drilling is to less than 200 m depth, making it obvious that robust models are necessary to gain confidence in delineating deep targets. The use of 3D modelling programs, such as GeoModeller and GOCAD, has been useful, in addition to the inversion of potential field data such as magnetic and gravity. Further refinements include the usage of potential field data to map in three dimensions the hydrothermal alteration signature of gold systems. This work involves the inversion of rock mass and integration with known mineral susceptabilities and specific gravity characteristics of hydrothermal alteration minerals. The increasing integrated application of the spectrum of techniques available in the explorers' tool-kit, when combined with improved conceptual models for gold systems at the lithospheric- to camp-scale, provides an avenue to delineate significant new targets and resources.

Acknowledgements

This paper reflects the personal views of the author and is based on a decade of research supported by the pmd*CRC, AMIRA, MERIWA, ARC and many mining companies. KFC acknowledges the extraordinary contribution of former colleagues at Geoscience Australia, including Richard Blewett, David Champion, Karol Czarnota and Paul Henson, the strong support from industry leaders, including Greg Hall and Jon Hronsky, and discussions with Steffen Hagemann, Gary Beakhouse, David Rhys, Gerard Tripp, Rob Kerrich, Howard Poulsen and Francois Robert, in helping shape this position on gold systems.

References

Barley, M.E., Brown, S.J.A., Cas, R.A.F., Cassidy, K.F., Champion, D.C., Gardoll, S.J., and Krapež, B., 2003, An integrated geological and metallogenic framework for the eastern Yilgarn Craton: Developing geodynamic models of highly mineralized Archaean granite-greenstone terranes: AMIRA International, Project P624, Final Report.

Barnes, S.J., Lesher, C.M., and Sproule, R.A., 2007, Geochemistry of komatiites in the Eastern Goldfields Superterrane, Western Australia and the Abitibi Greenstone Belt, Canada, and implications for the distribution of associated Ni-Cu-PGE deposits: Transactions of the Institute of Mining and Metallurgy, B – Applied Earth Science, v. 116, p. 167-187.

Begg, G.C., Griffin, W.L., Natapov, L.M., O'Reilly, S.Y., Grand, S.P., O'Neill, C.J., Hronsky, J.M.A., Poudjom Djomani, Y., Swain, C.J., Deen, T., and Bowden, P., 2009, The lithospheric architecture of Africa: Seismic tomography, mantle petrology, and tectonic evolution: Geosphere, v. 5, p. 23-50.

Bierlein, F.P., Groves, D.I., Goldfarb, R.J. and Dube, B., 2006, Lithospheric controls on the formation of provinces hosting giant orogenic gold deposits: Mineralium Deposita, v. 40, p. 874- 887.

Bierlein, F.P., Groves, D.I., Brown, W.M., Murphy, F.C., Fraser, S.J., and Lees, T., 2007, Scale-integrated prospectivity analysis: a pragmatic approach to exploration targeting in the Archaean Yilgarn Craton, Western Australia: *in* Proceedings of Geoconferences (WA) Inc. Kalgoorlie '07 Conference, 25-27 September 2007, Kalgoorlie, Western Australia *edited by* F.P. Bierlein and C.M. Knox-Robinson: Geoscience Australia Record 2007/14, p. 221-225.

Bleeker, W., and Hall, B., 2007, The Slave Craton: Geology and metallogenic evolution, *in* Mineral Deposits of Canada: A Synthesis of Major Deposit-Types, District Metallogeny, the Evolution of Geological Provinces, and Exploration Methods *edited by* W.D. Goodfellow: Geological Association of Canada, Mineral Deposits Division, Special Publication No. 5, p. 849-879.

Blewett, R.S., and Czarnota, K., 2007, The Y1-P763 Project Final Report, Module 3 — Terrane Structure: Tectonostratigraphic architecture and uplift history of the Eastern Yilgarn Craton, Geoscience Australia Record 2007/15.

Blewett, R.S., and the Y4 Team, 2008, Part II: Practical Targets for the Explorer, *in* pmd*CRC Project Y4 Final Report – Parts I and II, January 2005–July 2008, Concepts to targets: a scale-integrated mineral systems study of the Eastern Yilgarn Craton, Volume 1, p. 33-162.

Blewett, R.S., Henson, P.A., Roy, I.G., Champion, D.C., and Cassidy, K.F., 2010, Scale-integrated architecture of a world-class gold mineral system: the Archean eastern Yilgarn Craton, Western Australia: Precambrian Research, doi: 10.1016/j.precamres.2010.06.004.

Cassidy K.F., Champion, D.C., McNaughton, N.J., Fletcher, I.R. Whitaker, A.J., Bastrakova, I.V., and Budd, A.R., 2002, Characterisation and metallogenic significance of Archaean granitoids of the Yilgarn Craton, Western Australia, Project M281: Minerals and Energy Research Institute of Western Australia, Report No. 222, 514p.

Cassidy, K.F., Champion, D.C., and Huston, D.L., 2005, Crustal evolution constraints on the metalloneny of the Archean Yilgarn craton, *in* Mineral deposits research: Meeting the global challenge *edited by* J. Moa, and F.P. Bierlein: Berlin, Springer-Verlag, p. 901–904.

Champion, D.C., and Cassidy, K.F., 2008, Geodynamics: Sm-Nd isotopes and the evolution of the Yilgarn and similar terrains, *in* New perspectives: The foundations and future of Australian exploration. Abstracts for the June 2008 pmd*CRC Conference *edited by* R.J. Korsch, and A.C. Barnicoat: Geoscience Australia, Record 2008/09, p. 7–16.

Chopping, R., 2008, Architecture: Mapping the distribution of alteration: what different techniques can reveal, *in* New perspectives: The foundations and future of Australian exploration, Abstracts for the June 2008 pmd*CRC Conference *edited by* R.J. Korsch and A.C. Barnicoat: Geoscience Australia, Record 2008/09, p. 17–22.

Czarnota, K., Champion, D.C., Goscombe, B., Blewett, R.S., Henson, P.A., Cassidy, K.F., and Groenewald, P.B., 2008, Question 1: Geodynamics of the Eastern Goldfields Superterrane: in pmd*CRC Project Y4 Final Report — Parts III and IV, January 2005–July 2008: Concepts to targets: a scale-integrated mineral systems study of the Eastern Yilgarn Craton, Volume 2, p. 10-52.

Davis, B.K., Blewett, R.S., Squire, R., Champion, D.C., and Henson, P.A., 2010, Granite-cored domes and gold mineralisation: Architectural and geodynamic controls around the Archaean Scotia-Kanowna Dome, Kalgoorlie Terrane, Western Australia: Precambrian Research, doi: 10.1016/j.precamres.2010.01.011.

Goscombe, B.D., Blewett, R.S., Czarnota, K., Groenewald, B.A. and Maas, R., 2009, Metamorphic evolution and integrated terrane analysis of the Eastern Yilgarn Craton: rationale, methods, outcomes and interpretation: Geoscience Australia, Record 2009/23.

Groves, D.I., Goldfarb, R.J., Robert, F., and Hart, C.J.R., 2003, Gold Deposits in Metamorphic Belts: Overview of Current Understanding, Outstanding Problems, Future Research, and Exploration Significance: Economic Geology, v. 98, p. 1-29.

Hall, G., 2007, Exploration success in the Yilgarn Craton: Insights from the Placer Dome experience – the need for integrated research, *in* Proceedings of Geoconferences (WA) Inc. Kalgoorlie '07 Conference, 25-27 September 2007, Kalgoorlie, Western Australia *edited by* F.P. Bierlein and C.M. Knox-Robinson: Geoscience Australia, Record 2007/14, p. 199-202.

Halley, S.W., 2007, Mineral mapping — how can it help us explore in the Yilgarn Craton, *in* Proceedings of Geoconferences (WA) Inc. Kalgoorlie '07 Conference, 25-27 September 2007, Kalgoorlie, Western Australia *edited by* F.P. Bierlein and C.M. Knox-Robinson: Geoscience Australia, Record 2007/14, p. 143 – 144.

Hodgson, C.J., 1993, Mesothermal lode-gold deposits, *in* Mineral Deposits Modelling *edited by* R.V. Kirkham, W.D. Sinclair, R.I. Thorpe, and J.M. Duke: Geological Association of Canada, Special Paper 40, p. 635-678.

Hronsky, J.M.A., and Groves, D.I., 2008, The science of targeting: definition, strategies, targeting and performance measurement: Australian Journal of Earth Sciences, v. 55, p. 3-12.

Krapež, B., Barley, M.E., and Brown, S.J.A., 2008, Late Archaean synorogenic basins of the Eastern Goldfields Superterrane, Yilgarn Craton, Western Australia Part I. Kalgoorlie and Gindalbie Terranes: Precambrian Research, v. 161, p. 135–153.

McInnes, B.I.A., Gregoire, M., Binns, R.A., Herzig, P.M., and Hannington, M.D., 2001, Hydrous metasomatism of oceanic sub-arc mantle, Lihir, Papua New Guinea: petrology and geochemistry of fluid-metasomatised mantle wedge xenoliths: Earth and Planetary Science Letters, v. 188, p. 169-183.

Micklethwaite, S., 2007, The significance of linear-trends and clusters of fault-related mesothermal lode-gold mineralization: Economic Geology, v. 102, p. 1157–1164.

Miller, J., Nugus, M., and Henson, P., 2007, New structural insights into the world-class Archean Wallaby gold deposit, Laverton, Western Australia, *in* Proceedings of Geoconferences (WA) Inc. Kalgoorlie '07 Conference, 25-27 September 2007, Kalgoorlie, Western Australia *edited by* F.P. Bierlein and C.M. Knox-Robinson: Geoscience Australia, Record 2007/14, p. 209-213.

Miller, J., Blewett, R., Tunjic, J., and Connors, K., in press, The role of early formed structures on the development of the world class St Ives Goldfield, Yilgarn, Western Australia: Precambrian Research.

Neumayr, P., Walshe, J., Hagemann, S.G., Petersen, K., Roache, A., Frikken, P., Horn, L., and Halley, S., 2008b, Oxidized and reduced mineral assemblages in greenstone belt rocks of the St. Ives gold camp, Western Australia: vectors to high-grade ore bodies in Archaean gold deposits?: Mineralium Deposita, v. 43, p. 363–371.

Potma, W.A., Schaubs, P.M., Robinson, J.A., Sheldon, H.A., Roberts, P.A., Zhang, Y., Zhao, C., Ord, A., and Hobbs, B.E., 2007, *in* Proceedings of Geoconferences (WA) Inc. Kalgoorlie '07 Conference, 25-27 September 2007, Kalgoorlie, Western Australia *edited by* F.P. Bierlein and C.M. Knox-Robinson: Geoscience Australia, Record 2007/14, p. 214-217.

Robert, F., Poulsen, K.H., Cassidy, K.F., and Hodgson, C.J., 2005, Gold metallogeny of the Yilgarn and Superior cratons: Economic Geoloy, 100th Anniversary Volume, p. 1001–1033.

Smithies, R.H., and Champion, D.C., 1999, Geochemistry of felsic igneous alkaline rocks in the Eastern Goldfields, Yilgarn Craton, Western Australia: a result of lower crustal delamination? — implications for Late Archaean tectonic evolution: Journal of the Geological Society of London, v. 156, p. 561-576.

Stern, R.A., Hanson, G.N., and Shirey, S.B., 1989, Petrogenesis of mantle-derived, LILE-enriched Archean monzodiorites and trachyandesites (sanukitoids) in southwestern Superior Province: Canadian Journal of Earth Sciences, v. 26, p. 1688-1712.

Vielreicher, N.M., Groves, D.I., Snee, L.W., Fletcher, I.R., and McNaughton, N.J., 2010, Broad synchroneity of three gold mineralization styles in the Kalgoorlie Gold Field: SHRIMP, U-Pb, and $^{40}Ar/^{39}Ar$ geochronological evidence: Economic Geology, v. 105, p. 187-227.

Walshe, J.L., Neumayr, P., Petersen, K., Halley, S., Roache, A., and Young, C., 2006, Scale-integrated, architectural and geodynamic controls on alteration and geochemistry of gold systems in the Eastern Goldfields Province, Yilgarn Craton, Project M358: Minerals and Energy Research Institute of Western Australia, Report No. 256, 200p.

Weinberg, R.F., Hodkiewicz, P.H., and Groves, D.I., 2004, What controls gold distribution in Archean terranes?: Geology, v. 32, p. 545–548.

.

I don't work on anything less than fifty million ounces: the geology of the Timmins–Porcupine Archaean gold deposits (Ontario), and parallels with the Golden Mile (Kalgoorlie, Western Australia)

by

Roger Bateman[1]

Introduction

Among the lode gold deposits in Archaean rocks, the multiple deposits of the gold camps at Timmins–Porcupine (northern Ontario, Canada) and the Golden Mile (Kalgoorlie, Western Australia) are peerless gold camps. Modern and historic production in the Timmins–Porcupine camp totals 69 Moz from numerous mines and deposits that occur over a strike length of 35 km. The Kalgoorlie gold camp is more focused over 10 km, and comprises the Mt Percy open pit, Mt Charlotte underground mine and the Fimiston Superpit. Historic production from 1894 to 1989 yielded 105 Mt @ 11.5 g/t (40 M oz gold); from 1989 to 2010 84.3 Mt @ 2.5 g/t (15 M oz gold), totalling 55 Moz. These camps are of interest in their own right alone, but also for the common factors shared by these two camps. The similarity in the mapscale appearance is well known, but this is scarcely an account of processes. My work on these two deposits between 1995 and 2005 are summarized here and synthesized in an attempt ultimately to determine the important factors in the formation of ore bodies on this scale. The ideas presented here come from Bateman and Hagemann (2004), Bateman and Bierlein (2007), and Bateman et al. (2008) and references therein, plus later works cited below.

Timmins–Porcupine

New mapping and ideas from the Discover Abitibi Initiative aim to revive interest in Timmins–Porcupine. New lithogeochemical data reveal excision of stratigraphy and hence a low-angle unconformity lying between the Tisdale assemblage (tholeiites) and the Porcupine assemblage (sediments). This was the regional uplift-extension D_1 event. Subsequent D_2 was south-over-north imbrications of a set of thrust sheets, predating the unconformity at the base of the Timiskaming assemblage above Porcupine assemblage. Gold deposits were previously believed to lie in the footwall of the Porcupine-Destor deformation zone, a situation at odds with common observations for Archaean gold, but it is now seen that they lie in the hangingwall of the D_2 thrusts along the north side of the Porcupine-Destor deformation zone, and seismic data show they are rooted in it. Ankerite veining and a minor proportion of mineralization in Dome and Aunor mines are crosscut by and predate the Timiskaming unconformity. Clasts of colloform-crustiform ankerite veins in conglomerate of the Dome Formation at Dome demonstrate early hydrothermal low grade mineralization. D_3 consists of foliation and en echelon folds along the northern flank of the curvilinear trace of the Porcupine–Destor deformation zone. These can be interpreted as resulting from left-lateral strike-slip movement along this zone continuing from before to after Timiskaming sedimentation. The Timiskaming assemblage rocks lie within a jog along the Porcupine-Destor deformation zone formed as a half-graben, with the Dome Fault forming the faulted margin. Cu-Au-Ag-Mo mineralization in the Pearl Lake porphyry is post-Timiskaming assemblage (porphyries also intrude the Timiskaming assemblage) but predates main-stage quartz-gold veins in Hollinger-McIntyre, similar to Blueberry Hill near Dome. The Pearl Lake porphyry is ~2.69 Ga. The important gold-depositional phases postdate Timiskaming sedimentation, as S_2 foliation is overprinted by alteration. S_2 foliation seems not to have affected the Pamour porphyry, dated at 2.677 Ga (McDonald, 2010). S_3 foliation crosscuts early ankerite veining and alteration and some quartz veining, as at Vedron. The main-stage gold-quartz mineralization at Hollinger-McIntyre and in other deposits was late D_3, at the earliest. Quartz-carbonate-tourmaline-gold veins (Hollinger-McIntyre, Hoyle Pond, Dome, Aunor-Delnite mines) also formed within Timiskaming assemblage and adjacent Tisdale assemblage rocks. These gold deposits developed largely as oblique-slip and extensional vein arrays formed during north-south shortening and local strike-slip faulting. D_4 movement was right lateral transpression, folding S_3 foliation. The vertically extensional network of auriferous quartz veins at Pamour is late to post S_4 foliation, and was formed during D_4 north-south shortening, dip-slip fault movement. These D_4 mineralizations postdate the ~2.669 Ga Timiskaming assemblage deposition. Intense D_5

[1] Tenth Symphony Geoscience, P.O. Box 1490, West Perth, WA 6872 Australia

constrictional strain west of the inflection in trend of the Porcupine-Destor deformation zone reflects the previously dilatational (D_3) jog becoming a compressional jog during right lateral slip. D_5 constriction generated quartz ladder veins.

Diversity is manifested in both timing and in diversity in style (veining, vein mineralogy, disseminated, sulphide-rich mineralization), alteration mineralogy (massive ankerite, albite, sericite), sulphide and ore minerals (pyrite, tellurides) and metals (Au, Ag, Cu, Mo, W). Orogenic quartz-carbonate vein deposits are commonly spatially associated at the regional scale with Timiskaming-like regional unconformities and suggest an empirical relationship between large-scale greenstone quartz-carbonate gold deposits, deformation opening of these basins, and regional unconformities.

The Golden Mile

On the Golden Mile, the lodes at Fimiston, Oroya and Mt Charlotte represent distinct styles of gold mineralisation. Fimiston consists of about 1,000 lodes and hydrothermally altered wall rock. The Oroya shoot appears to be the only full-scale lode of this type, but it is also an alteration style found elsewhere. There are numerous Charlotte-style vein systems throughout the Golden Mile. These three lode types commonly have overprinting relationships because they occur over a smaller area than Timmins–Porcupine.

Fimiston-style mineralisation is structurally related to east-over-west thrusting on the D_1 (local deformation scheme) Golden Mile Fault. Regional D_1 is very probably a distinct and earlier event, involving north-south thrusting. Lodes do not crosscut this fault, but are cut by it. Small remnants of lode can be found isolated within the Golden Mile Fault. Fimiston lodes are also crosscut by an abundant set of D_2 reverse faults during east-west shortening, especially clear in the Western Lodes. D_3 structures such as Adelaide Fault, North Kalgurli Fault and Australia East Fault also crosscut and deform the lodes. Finally, D_4 faults (Drysdale and Hannan's Star Faults) offset the Fimiston lodes. Lodes were thus formed between late-D_1 between ~2.64-2.66 Ga (the age of D3) and ~2.67±5 Ga (the age of felsic mineralized dykes: Veilreicher et al., 2010). Lodes were subhorizontal at the time of formation, and were steepened in D_2 folding.

Fimiston-style mineralisation is characterised by addition of CO_2, K, Rb, Te, S and Au, V, Sb, Ba and B. Fimiston ore fluids consisted of an aqueous-carbonic mixture: salinities of <6 equiv. wt% NaCl, temperatures of 250 to 350°C, pressures of 100 to 200 MPa. Oroya fluids were similar, but with significantly higher CH_4 content. Stable isotopic compositions of the Fimiston ore fluids are compatible with seawater and/or meteoric fluids. Pyrite sulphur isotope compositions from Fimiston are complex and indicate multiple sulphur sources (e.g. igneous, syn-sedimentary and possibly seawater) and multiple depositional processes, such as phase immiscibility and fluid mixing.

The Oroya shoot was a shallowly plunging linear shoot, formed in a late D_2 dilatational jog during west-over-east reverse faulting. The D_2 shear that was involved in Oroya lode formation is also crosscut by D_3 faults. The Oroya shoot is characterised by microbreccias, abundant free gold, Au-tellurides, pyrite and V–Fe–Ti minerals ('green leader'), and Oroya fluids were broadly similar to Fimiston fluid. A regionally-determined age for D_2 is between 2.675 Ga and 2.657 Ga.

Charlotte-style gold mineralisation consists of sheeted quartz–carbonate veins controlled by D_4 right lateral-oblique faults and reactivated west-dipping D_2 reverse faults in competent rock units, particularly granophyric Unit 7 of the Golden Mile Dolerite. At Mt Percy, porphyry dykes within ultramafic rocks provided the competency contrast. Charlotte-style lodes formed at around 2.643 Ga: 2.655±13 Ga (xenotime Pb-Pb: Rasmussen et al., 2008) or 2.638±6 Ga (zircon U-Pb in lamprophyre), and ~2.63 Ga (sericite Ar-Ar) during D_4. Charlotte-style fluids contain co-existing liquid- and vapour-rich two-phase aqueous-carbonic inclusions that homogenise at temperatures of 120 to 440°C from isotopically homogeneous ore-fluids over a small temperature range. The three distinct mineralisation styles in the Golden Mile represent distinguishable phases, with protracted activity throughout orogenesis and deformation, over perhaps as much as 30.

A comparison, and distillation of common elements

The features that appear to be crucial in the formation of these very large gold deposits are summarised in the Table.

In both Timmins–Porcupine and Kalgoorlie, the gold-bearing structures formed over a protracted period of time that spanned early thrusting, the opening of the late-tectonic sedimentary basins and strike–slip deformation. Both camps are characterised by well developed early thrust faults, giving the camps their distinctive map patterns. Thrusting followed by strike–slip deformation generates an intersecting array of fractures that may tap a very large volume of rock, necessary to access the large amount of gold that was deposited. Jogs in the trend of the strike–slip faults present in both Kalgoorlie and Timmins–Porcupine may concentrate the vertical conduits into a focused zone.

Timmins–Porcupine consists of about 30 deposits dispersed over a relatively large area. This dispersal may be a function of the several D_2 thrusts present, contrasting with Kalgoorlie where there is one early thrust (Golden Mile Fault) and relatively few deposits. The listric nature of major shear zones in both camps, and crustal Re–Os isotope signatures suggest that gold and/or another critical fluid component was derived from within, or from the base of, the supracrustal sequence, or had at least an extended period of residence at that structural level. Diverse auriferous fluid types, some of which may have been early-formed and/or epizonal, allow for a diversity of gold deposits. Dilatation that allows for basin formation may also facilitate magma and fluid ingress. These fluids can exploit structures and conduits that were open and active for an extended period. Finally, a supply of

Table: Summary of features crucial to the formation of very large gold deposits

Characteristic	Timmins–Porcupine	Golden Mile	Role
Layered gabbros	Uncommon rock type, minor host of Au	Common rock type, major host of Au	Serve important rheological role where present (other rock types may serve the same role)
Porphyries, albitites, lamprophyres	Minor in volume. Albitites broadly synchronous with Au	Minor in volume, broadly synchronous with Au	No genetic role
Late-orogenic marine, fluvial sediments	Locally an important host to Au	Not present or identified within the Kalgoorlie camp	Serve important rheological role (other rock types may serve the same role)
Age of stratigraphy	~2.703 Ga to <2.655 Ga	2.700–2.716 Ga to <2.679 Ga	Largely coincidental: volcanic rocks erupted along same structures that transmitted auriferous fluids
Ultramafic rocks	Komatiites, intrusive peridotites present	Komatiites, intrusive peridotite, depleted Au in normalized PGE plot	Ultramafic rocks may be a source of Au
Stage of cratonisation	At the end of Archaean crust formation; prior to major, final deformation	Around the end of Archaean crust formation; prior to major, final deformation	Au deposited during the later stages of Archaean crust formation, deformation and cratonisation
3D structure	Mineralised structures listric to base of supracrustal rocks; no detachment recognized at base of supracrustal rocks	Mineralised structures listric to major detachment at base of supracrustal rocks	Limited depth extents of major faults controls the sources of fluid components and their conduits
Transpression	Overall left-lateral strike–slip and en-echelon folding; subsequent right-lateral strike–slip	Overall left-lateral strike–slip with right-lateral antithetic faulting. Diachronous D_2	Mineralisation in each camp spanned transpression. Diachronous deformation allows time for fluid flow, mineralisation
Timings of Au	pre-D_3 (pre ~2.679 Ga); Dome ~2.67 Ga; to D_4 (~2.66 Ga)	D_2 (~2.67-2.66 Ga) and D_4 (~2.642 Ga)	Long duration of deformation and mineralisation promotes large ore body
Basin opening, deposition of late orogenic sediments	Basins opened during D_3 strike–slip	Basins opened prior to major D_2 shortening	Extension implicit in basin opening also conducive to mineralisation
Tellurides	Minor amounts present, widespread elsewhere in Abitibi Province	Abundant at Fimiston, common in other parts of Eastern Goldfields	Te possibly has an important role in chemistry of Au-bearing fluids
Epithermal-style fluids	Minor amounts present, widespread elsewhere in Abitibi Province	Mixed seawater–hydrothermal water, oxidising fluid (anhydrite, hematite, V+3), tellurides	Early contribution from possible epithermal/igneous source common in Eastern Goldfields and Abitibi provinces
Early thrusting	Well developed stacked thrust sheets formed early	Golden Mile Fault is early thrust	Perhaps necessary role in developing extensive array of interconnected fractures and fluid conduits

gold must be sustained for the duration of conduit activity. In both provinces, this supply of gold was assured via the abundance of intrinsically gold-rich, oceanic-character source rocks that formed in fore-arc to back-arc environments. Importantly, the formation of this oceanic crust in both the Eastern Goldfields and the southern Abitibi Province preceded gold deposition at ca. 2.65 Ga by 30 to 70 million years. Therefore, one factor in the generation of the Kalgoorlie and Timmins–Porcupine camps appears to be the formation of juvenile crust. Thermal regimes driving giant hydrothermal systems are fundamental to such scenarios and can be linked to the occurrence of major lithospheric instabilities and asthenospheric upwelling. These could have provided the thermal engine for the gold-forming event in both provinces during peak periods of continental growth at ca. 2.7–2.65 Ga.

Acknowledgements

The work presented here was carried out while I was Senior Research Geologist at Kalgoorlie Consolidated Gold Mines (Kalgoorlie, Western Australia), and as postdoctoral fellow at Laurentian University (Sudbury, Ontario). John Ayer, Benoit Dubé, Phillips Thurston, Steffen Hagemann, Cam McCuaig, Cees Swager, Frank Bierlein and Kevin Cassidy all contributed to the ideas herein. Kalgoorlie Consolidated Gold Mines, Discover Abitibi Initiative and the Timmins Economic Development Corporation funded the work.

References

Bateman, RJ, and Hagemann, S, 2004, Gold mineralization through about 45 Ma of Archaean orogenesis: protracted flux of gold in the Golden Mile, Yilgarn Craton, Western Australia: Mineralium Deposita, v. 39, p. 536-559.

Bateman, RJ, and Bierlein, FP, 2007, On Kalgoorlie (Australia), Timmins–Porcupine (Canada), and factors in intense gold mineralization: Ore Geology Reviews, v. 32, p. 187-206.

Bateman, RJ, Ayer, JA, and Dubé, B, 2008, The Timmins–Porcupine gold camp, Ontario: anatomy of an Archean greenstone belt and ontogeny of gold mineralization: Economic Geology, v. 103, p. 1285-1306.

McDonald, PJ, 2010, The geology, lithogeochemistry and petrogenesis of intrusions associated with gold mineralization in the Porcupine gold camp, Timmins, Canada: MSc thesis, Laurentian University, 188p.

Rasmussen, B, Mueller, AG, and Fletcher, IR 2008, Zirconolite and xenotime U–Pb age constraints on the emplacement of the Golden Mile Dolerite sill and gold mineralization at the Mt Charlotte mine, Eastern Goldfields Province, Yilgarn Craton, Western Australia: Contributions to Mineralogy and Petrology, v. 157, p. 559-572.

Vielreicher, NM, Groves, DI, Snee, LW, Fletcher, IR, and McNaughton, NJ, 2010, Broad synchroneity of three gold mineralization styles in the Kalgoorlie gold field: SHRIMP, U-Pb, and $^{40}Ar/^{39}Ar$ geochronological evidence: Economic Geology, v. 105, p. 187-227.

RECORD 2010/20

YILGARN–SUPERIOR WORKSHOP — Abstracts

This Record is published in digital format (PDF) and is available online at <www.dmp.wa.gov.au/GSWApublications>.
Laser-printed copies can be ordered from the Information Centre for the cost of printing and binding.

Further details of geological products produced by the Geological Survey of Western Australia can be obtained by contacting:

Information Centre
Department of Mines and Petroleum
100 Plain Street
EAST PERTH WESTERN AUSTRALIA 6004
Phone: (08) 9222 3459 Fax: (08) 9222 3444
www.dmp.wa.gov.au/GSWApublications

Wyche